



Dibris



ISTITUTO ITALIANO
DI TECNOLOGIA

UNIVERSITY OF GENOVA – ISTITUTO ITALIANO DI TECNOLOGIA

PHD PROGRAM IN BIOENGINEERING AND ROBOTICS
CURRICULUM: BIONANOTECHNOLOGY

Novel Boronic Ester Cross-linkers and Biobased Vitrimers for Fibre-reinforced Composites

Davide Sangaletti

36° cycle

Tutors/Supervisors

Dr. Athanassia Athanassiou

Dr. Arkadiusz Zych

Dr. Giovanni Perotto

Tutor
Supervisor
Supervisor

Examiners

Antonio Politano

Alessandro Martucci

External examiner
External examiner

Acknowledgments

To my late grandfathers, Edilio who departed too early and Angelo who recently passed away, who greatly influenced the person I have become.

To my family, whose unwavering support has been invaluable.

To my friends, and especially to Her, who provided reassurance during the darkest moments.

My deepest gratitude to my Tutor, Dr. Athanassia Athanassiou, for the opportunity to work in the Smart Materials group, an extraordinary and multidisciplinary team from which I've gained invaluable knowledge. A special thanks to the technicians, Lara and Giorgio, for their assistance throughout these three years. Gratitude also extends to all others who, in various ways, offered their support.

I am grateful to my supervisor, Dr. Giovanni Perotto, for his guidance, precious suggestions and for being a starting point when things weren't going as planned.

Especially, I want to express my appreciation to my supervisor, Arkadiusz Zych (Arek), for introducing me to the fascinating world of vitrimers. Your profound scientific expertise and unwavering support have continually enriched me with incredible knowledge through teaching and guidance.

Declaration

I declare the contents of this dissertation, except where specific reference is made to the work of others, are original and have not been submitted in whole or in part for consideration for any other degree or qualification in this, or any other university. This dissertation is my own work and contains nothing which is the outcome of work done in collaboration with others, except as specified in the text and acknowledgements.

Davide Sangaletti,

December 2023

Table of Contents

Acknowledgments	ii
Declaration	iii
Abstract	vi
List of figures	vii
List of tables.....	x
List of equations.....	x
List of abbreviations.....	xi
Introduction.....	1
1.1. <i>Plastics, a quick overview on types and recycling</i>	1
1.2. <i>Vitrimers and the boronic ester chemistry</i>	7
1.3. <i>Fibre-reinforced composites</i>	15
1. Chapter I: ELO-DBEDT, a Boronic Ester Vitriimer from Epoxidized Linseed Oil for Recyclable Carbon-fiber Composites	19
Objectives.....	19
1.1 <i>MATERIAL, METHODS, and MEASUREMENTS</i>	20
1.1.1 Materials	20
1.1.2 Methods	20
1.1.3 Measurements	21
1.2 <i>RESULTS AND DISCUSSION</i>	22
1.2.1 Design of the vitriimer resin	22
1.2.2 Vitriimer characterization.....	23
1.2.3 Shape memory effect	26
1.2.4 Vitriimer recycling	27
1.2.5 Carbon fibre composite preparation and characterization	29
1.2.6 Composites recycling.....	30
1.3 <i>CONCLUSIONS</i>	32
1.4 <i>APPENDIX</i>	33
<i>Design of the vitriimer resin</i>	33
<i>Vitriimer recycling</i>	37
<i>Composites Recycling</i>	39
2. Chapter II: Low melting and Liquid Boronic Ester Cross-linkers for the preparation of Vitrimers.....	42
Objectives.....	42
2.1 <i>MATERIAL, METHODS and MEASUREMENTS</i>	43
2.1.1 Materials.....	43
2.1.2 Methods	43
2.1.3 Measurements.....	44
2.2 <i>RESULTS AND DISCUSSION</i>	44
2.3 <i>APPENDIX</i>	51

<i>Dithiol diboronic ester cross-linkers</i>	51
<i>Dimercapto diboronic ester cross-linker</i>	52
<i>Diamine diboronic ester cross-linkers</i>	52
<i>Dihydroxy diboronic ester cross-linkers</i>	55
<i>Dicarboxy diboronic ester cross-linkers</i>	56
3. Chapter III: Amino-Boronic Ester Vitriimer for Room-temperature Curable Biobased Recyclable Carbon-fibre Composites	57
Objectives.....	57
3.1 <i>MATERIAL, METHODS, and MEASUREMENTS</i>	58
3.1.1 Materials.....	58
3.1.2 Methods	58
3.1.3 Measurements.....	58
3.2 <i>RESULTS AND DISCUSSION</i>	60
3.2.1 Design of the vitriimer resin	60
3.2.2 Vitriimer characterization.....	62
3.2.3 Shape memory effect	65
3.2.4 Vitriimer recycling	66
3.2.5 Carbon fibre composite preparation and characterization	70
3.2.6 Composites recycling	71
3.3 <i>CONCLUSIONS</i>	73
3.4 <i>APPENDIX</i>	63
<i>Design of the vitriimer resin</i>	63
<i>Vitriimer recycling</i>	69
<i>Composites Recycling</i>	72
Conclusions and outlook	74
List of publications and patents	76
References	77

Abstract

In the last decades environmental concerns regarding petroleum-based synthetic polymers have been growing, which has facilitated the development of new strategies in the field of polymer science. Indeed, plastic materials and especially thermoset polymers, thanks to their versatile and multifunctional properties, are widely used for many applications and especially in fibres reinforced polymer composites, a market with an enormous growth the last decades. Thermoset matrices in such composites include epoxies, polyesters, vinyl esters, phenolics, cyanate esters, bismaleimides, and polyimides. However, epoxies currently are the dominant resins used for high-performance composites at low and moderate temperatures (up to 200 °C) thanks to the superior mechanical performance, lighter weight and resistance to environmental degradation in comparison to the other thermoset resins.

On the other hand, fundamental chemicals for the production of epoxy resins, like bisphenol A or epichlorohydrin, have been found toxic. Furthermore, epoxy resins derive from petroleum, contributing both to the rapid depletion of non-renewable fuel sources and to the related environmental problems. Indeed, like the other thermosets, epoxy resins show a strong permanent covalent network which preclude flow, even at high temperatures, which makes mechanical and chemical recycling challenging. As a result, most thermosets are incinerated or landfilled at the end of their lifetime.

All these issues can be potentially solved by biobased *vitrimers*, a new class of polymers which makes the thermosets meet the thermoplastics thanks to the presence of dynamic bonds which allow for easy reprocessing and recycling of covalently crosslinked polymers. Indeed, these revolutionary thermosetting polymeric material are, recyclable and malleable like thermoplastic but still maintain their outstanding properties awarded by crosslinked network structure.

During the first part of my PhD, a new vitrimer resin for carbon fibre reinforced composites, based on epoxidized linseed oil and dithiol boronic ester cross-linker was synthesized.

As a continuation of that research a series of new low melting or even liquid boronic ester cross-linkers were developed which allowed for a room temperature curing. Crosslinkers with several functional groups, like thiol, hydroxyl, carboxyl and amino group were successfully synthesized following green chemistry principles. The most promising one containing amino groups was used together with phloroglucinol triglycidyl ether, a biobased epoxy from brown algae to fabricate a new, room-temperature curable vitrimer resin.

The synthesized vitrimers were used to produce fibre-reinforced composites and tested in comparison to a commercial epoxy-based composite. Moreover, the vitrimers were found to be mechanically recyclable through techniques typically employed for thermoplastics polymer as well as chemically recyclable through hydrolysis in aqueous ethanol as a green solvent.

The chemical recycling gives the possibility, at the end of their lifetime, of recovering the components of the composite, therefore bringing environmental and economic advantages. Besides, the new materials showed also signs of biodegradability in sea water, which is important to prevent the vitrimer accumulation in the marine environment in case of an accidental release into the environment. For all these reasons, the developed vitrimers and composites can address many challenges facing conventional polymers and thermosets composites.

Key-words:

Biobased vitrimers
Covalent adaptable network
Dynamic crosslinks
Reprocessability and recyclability
Fibre-reinforced composites

List of figures

Introduction

Figure I1. World annual plastics production 1950-2023 (adaptation from nature.com)(A) and Plastics production by region in 2022 (plasticseurope.org) (B).

Figure I2. The most common plastics and their main applications.

Figure I3. Distribution of plastics demand by sectors (A) and by materials (B) (adaptation from plasticseurope.org).

Figure I4. Mismanaged plastic waste for country (A); Plastic items dominate the ocean garbage (B); Plastic mass across the world's surface oceans by mass (C) and by particle count (D) (adaptation from ourworldindata.org).

Figure I5. Bioplastics classification (A); Global production capacities of bioplastics in 2022 by materials (B) and Global production capacities of market in 2022 (adaptation from european-bioplastics.org).

Figure I6. Plastics recycling methodology (A) and thermosets recycling way (B) (adaptation from plasticseurope.org and tandfonline.com).

Figure I7. Schematic overview of the existing concepts to develop recyclable thermoset polymers (A) and Covalent adaptable networks classification (B) (adaptation from tandfonline.com).

Figure I8. Dynamic covalent chemistries used in the synthesis of biobased vitrimers (*= dissociative exchange) (adaptation from <https://doi.org/>).

Figure I9. Equilibrium between phenylboronic acid and its diols esters.⁸⁰

Figure I10. Boron hybridization changes on interaction with a Lewis base.⁹⁰

Figure I11. Boronic acid esters transesterification mechanism.⁸⁹

Figure I12. Synthetic strategies for the synthesis of boronic acid esters-based vitrimers (A); cross-linking of macromolecules with cyclic boronates containing reactive groups (B); cross-linking of diol-containing macromolecules with boronic diacids (C); cross-linking of cyclic boronates-containing macromolecules via metathesis (D); reaction between molecules with functionality > 2 and cyclic boronates containing complementary reactive groups.⁹⁰

Figure I13. Common structural formulas of cross-linkers applied for the formation of boronic acid esters based vitrimers.⁹⁰

Figure I14. The number of published papers (according to Scopus, searching for fibre-reinforced composites and vitrimers in the title of the article).¹³¹

Chapter 1

Figure 1.1 ¹H NMR spectra of DBEDT (A) and ELO (B) in CDCl₃.

Figure 1.2 Schematic representation of the ELO-DBEDT vitrimer synthesis (A), the thiol-epoxy “click” reaction (B) and network rearrangement by boronic ester exchange (C).

Figure 1.3 Typical tensile curve (A), young modulus (B) and flexural strength (C) of vitrimer and commercial epoxy; typical flexural curve (D), young modulus (E) and flexural strength (F) of vitrimer and commercial epoxy; DMTA (G) and stress relaxation curves of vitrimer and commercial epoxy (H); BOD of the ELO, vitrimer and cotton fabric as a reference (I).

Figure 1.4 Shape memory effect of the vitrimer (A) and the commercial epoxy (B)

Figure 1.5 Typical tensile curve (A), ultimate strength (B) and Young Modulus (C) of the virgin (I gen) and the reprocessed (II-V gen) vitrimer.

Figure 1.6 Mechanically recycled vitrimer (A) and unsuccessful attempt to mechanically recycle the commercial epoxy (B) under 5 ton of pressure for 10 min at 160 °C; Chemical recycling of the vitrimer by hydrolysis and dissolution in 90% v/v ethanol at 75 °C for 3 h and subsequent solvent casting to regenerate the vitrimer as a thin, transparent film (C) and unsuccessful attempt to chemically recycle commercial epoxy (D).

Figure 1.7. ¹H NMR spectra of ELO (DMSO-d₆), DBEDT (DMSO-d₆) and ELO-DBEDT vitrimer hydrolysed in aqueous DMSO-d₆. Assignment of signals corresponding to ELO reacted with thioglycerol present after the hydrolysis is omitted for clarity since they are broad and not clearly visible in the spectrum.

Figure 1.8 Fabrication of the carbon fibre-reinforced composites (A); Optical microscope images of the top surface and the cross-section of the vitrimer composite (B-C) and commercial epoxy composite (D-E); SEM images of the cross-section of the vitrimer composite (F-G) and the commercial epoxy composite (H-I); Typical flexural curve (L), flexural strength (M) and Young Modulus (N) of the vitrimer composite and the commercial epoxy composite.

Figure 1.9 Recyclability scheme of the vitrimer composite (A); digital images showing dissolution progress of the matrix in the vitrimer composite. (B); SEM images of fresh and recycled carbon fibre at different time of the process, C:0h, D:1h, E:2h and F:3h; Raman spectra of the virgin and recycled carbon fibres(G) and X-ray diffraction patterns of the virgin and recycled carbon fibres (H).

Figure appx. 1.1 Gel fraction of vitrimer at different curing times.

Figure appx. 1.2. Samples of the vitrimer (A) and the commercial epoxy (B) before (left) and after (right) the gel fraction test.

Figure appx. 1.3. DSC curves of the vitrimer and the commercial epoxy.

Figure appx. 1.4. Arrhenius plot of relaxation times of the vitrimer.

Figure appx. 1.5. Stress relaxation curves of vitrimer (A) and commercial epoxy (B).

Figure appx. 1.6. TGA curves of virgin (dark yellow) and recycled (orange and light yellow) vitrimer and commercial epoxy (green).

Figure appx. 1.7. FT-IR spectra of the virgin vitrimer and reprocessed up to 4 times.

Figure appx. 1.8. DMTA curves of virgin (I gen) and reprocessed (III-V gen) vitrimer and commercial resin.

Figure appx. 1.9. FT-IR spectra of vitrimer as synthesized and after hydrolysis, dissolution in 90% v/v EtOH and casting.

Figure appx. 1.10. Partial dissolution of the vitrimer matrix in 90% EtOH solution, where the carbon fibre in contact with the solution was separated from the resin.

Figure appx. 1.11 TGA curves of the fresh carbon fibre (black), vitrimer composite (yellow) and commercial epoxy composite (blue).

Figure appx. 1.12 Matrix and reinforcement content

Figure appx. 1.13 Unsuccessful attempt to recycle carbon fibre-reinforced commercial epoxy composite in 90% EtOH solution.

Figure appx. 1.14. Typical tensile curve (A), ultimate strength (B) and Young Modulus (C) of the virgin and recycled vitrimer composite.

Chapter 2

Figure 2.1 ^1H NMR spectra of 1,4-Butanediol diglycidyl ether before and after hydrolysis.

Figure 2.2 Curing reaction mechanism involved between epoxy and amine curing agent.

Figure 2.3 General scheme of the cross-linker synthesis.

Figure 2.4 All the synthesized cross-linkers divided by functional group

Figure 2.5 ^1H NMR spectra of meta-DGBEA using different green solvents, the NMR analysis confirmed the successful of the reactions

Figure appx. 2.1 Reaction scheme (A); ^1H NMR spectrum (B); TGA (C) and DSC (D) of meta-DBEDT.

Figure appx. 2.2 Reaction scheme (A); ^1H NMR spectrum (B); TGA (C) and DSC (D) of para-DBEDT.

Figure appx. 2.3 Reaction scheme (A); ^1H NMR spectrum (B); TGA (C) and DSC (D) of meta-MDGBE.

Figure appx. 2.4 Reaction scheme (A); ^1H NMR spectrum (B); TGA (C) of orto-DGBEA.

Figure appx. 2.5 Reaction scheme (A); ^1H NMR spectrum (B); TGA (C) and DSC (D) of meta-DGBEA.

Figure appx. 2.6 Reaction scheme (A) and ^1H NMR spectrum (B) of para-DGBEA.

Figure appx. 2.7 Reaction scheme (A); ^1H NMR spectrum (B); TGA (C) and DSC (D) of meta-BDBEA.

Figure appx. 2.8 Reaction scheme (A); ^1H NMR spectrum (B); TGA (C) and DSC (D) of meta-PTBEA.

Figure appx. 2.9 Reaction scheme (A); ^1H NMR spectrum (B); TGA (C) and DSC (D) of meta-HDGBE.

Figure appx. 2.10 Reaction scheme (A); ^1H NMR spectrum (B); TGA (C) and DSC (D) of meta-HBDBE.

Figure appx. 2.11 Reaction scheme (A); ^1H NMR spectrum (B); TGA (C) and DSC (D) of meta-CDGBE.

Figure appx. 2.12 Reaction scheme (A); ^1H NMR spectrum (B); TGA (C) and DSC (D) of meta-CBDBE.

Chapter 3

Figure 3.1 .Schematic representation of the PHTE-DGBEA vitrimer synthesis (A), the amino-epoxy “click” reaction (B) and scheme of the network rearrangement by boronic ester exchange (C).

Figure 3.2 Gel fraction of PHTE-vitrimer at different curing times during the curing (A) and post-curing treatment (B).

Figure 3.3 Rheology frequency sweep curves of PHTE-vitrimer (A) and commercial epoxy (B).

Figure 3.4 Typical flexural curve (A), young modulus (B) and flexural strength (C) of PHTE and EPP vitrimers and commercial epoxy; TGA (D) and DSC (E) curves of vitrimers and commercial epoxy; IR spectrum of the PHTE-vitrimer (F) and EPP-vitrimer before and after curing (G) DMTA curves of the PHTE-vitrimer and commercial epoxy (H); BOD of the DGBEA cross-linker, PHTE, PHTE-vitrimer and cotton fabric and poly-propylene as references (I).

Figure 3.5 Shape memory effect of the PHTE-vitrimer (A) and the commercial epoxy (B)

Figure 3.6 Typical bending curve (A), flexural strength (B) and young modulus (C) of the virgin (I gen) and the reprocessed (II-V gen) PHTE-vitrimer and bending curve (D), flexural strength (E) and young modulus (F) of the virgin and the reprocessed EPP-vitrimer

Figure 3.7 Mechanically recycled PHTE-vitrimer (A), EPP-vitrimer (B) and unsuccessful attempt to mechanically recycle the commercial epoxy (C) under 5 ton of pressure for 10 min at 100 °C; Chemical recycling of the vitrimers by hydrolysis and dissolution in 90% v/v ethanol at 60 °C for 20 minutes and subsequent solvent casting to regenerate the vitrimer as a thin, transparent film (D and I) and unsuccessful attempt to chemically recycle commercial epoxy (F).

Figure 3.8 ^1H NMR spectra of PHTE (DMSO- d_6), DGBEA (DMSO- d_6) and PHTE-DGBEA vitrimer hydrolysed in aqueous DMSO- d_6 .

Figure 3.9 Fabrication of the carbon fibre-reinforced composites (A); Optical microscope images of the top surface and the cross-section of the PHTE-vitrimer composite (B-C) and commercial epoxy composite (D-E); SEM images of the cross-section of the PHTE-vitrimer composite (F-G) and the commercial epoxy composite (H-I); Typical flexural curve (L), flexural strength (M) and Young Modulus (N) of the PHTE-vitrimer composite and the commercial epoxy composite.

Figure 3.10 Recyclability scheme of the PHTE-vitrimer composite (A); Optical (B) and SEM (C) images of recycled carbon fibre at different time of the process at 0h, 1.5h and 3h.; Raman spectra of the virgin and recycled carbon fibres (D); XRD patterns of the virgin and recycled carbon fibres (E).

Figure appx. 3.1 ^1H NMR spectra of DGBEA in CDCl₃.

Figure appx. 3.2. ¹H NMR spectra of PHTE in CDCl₃.
Figure appx. 3.3 ¹H NMR spectra of EPP in CDCl₃.
Figure appx. 3.4 Schematic representation of the EPP-DGBEA vitrimer synthesis.
Figure appx. 3.4 Schematic representation of the EPP-DGBEA vitrimer synthesis.
Figure appx. 3.6 Samples of the PHTE-vitrimer (A), EPP-vitrimer and the commercial epoxy (B) before (left) and after (right) the gel fraction test.
Figure appx. 3.7 Typical flexural curve (A), young modulus (B) and flexural strength (C) of PHTE-vitrimer and epoxy resin cured and post-cured.
Figure appx. 3.8 PHTE-vitrimer sample before (A) after the DMA measurement (B).
Figure appx. 3.9 Arrhenius plot of relaxation times of the PHTE-vitrimer.
Figure appx. 3.10 TGA curves of virgin, mechanically and chemically recycled PHTE-vitrimer (A) and EPP-vitrimer (B).
Figure appx. 3.11 FT-IR spectra of the of the virgin PHTE-vitrimer and reprocessed up to 4 times.
Figure appx. 3.12 DMTA curves of virgin (I gen) and reprocessed (III-V gen) PHTE-vitrimer and commercial resin.
Figure appx. 3.13 FT-IR spectra of vitrimer as synthesized and after chemical and mechanical recycling (A); recovered material after hydrolysis in 90% v/v EtOH and casting (chemical recycling)
Figure appx. 3.14 ¹H NMR spectra of EPP (DMSO-d₆), DGBEA (DMSO-d₆) and EPP-DGBEA vitrimer hydrolysed in aqueous DMSO-d₆.
Figure appx. 3.15 Partial dissolution of the PHTE-vitrimer matrix in 90% EtOH solution (left part) and carbon fibres in contact with the solution were separated from the resin (right part)
Figure appx. 3.16 TGA curves of the virgin carbon fibres (black), PHTE-vitrimer composite (brown) and commercial epoxy composite (aqua green).
Figure appx. 3.17 Matrix and reinforcement content
Figure appx. 3.18 Unsuccessful attempt to recycle carbon fibre-reinforced commercial epoxy composite in 90% EtOH solution.
Figure appx. 3.19 Typical bending curve (A), flexural strength (B) and young modulus (C) of the virgin and recycled PHTE-vitrimer composite

List of tables

Chapter 1

Table appx. 1.1. Gel fraction of the vitrimer at different curing times.

Table appx. 1.2. Composition, gel fraction after curing and glass transition temperature of the vitrimer resin and the commercial epoxy resin

Table appx. 1.3. Density of the vitrimer, the commercial epoxy and the composites.

Table appx. 1.4. Gel fraction of the vitrimer and the commercial epoxy.

Table appx. 1.5. Gel fraction, thermal stability and mechanical performance of the virgin and the reprocessed vitrimer.

Table appx. 1.6. Gel fraction of the virgin vitrimer and reprocessed up to 4 times.

Table appx. 1.7. Chemical Recyclability of the vitrimer, commercial epoxy, commercial epoxy composite and vitrimer composite.

Chapter 2

Table 2.1 Lists of the reagents used to synthesize the boronic ester cross-linkers.

Table 2.2 Melting point, glass transition and state of the CLs (*: degradation before melting point)

Table 2.3 Composition, curing percentage and curing temperature of the commercial epoxy pre-polymer.

Chapter 3

Table appx. 3.1 Composition, gel fraction after post-curing and glass transition temperature of the vitrimer resins and the commercial epoxy resin

Table appx. 3.2 Gel fraction of the PHTE-vitrimer (curing) at different curing times.

Table appx. 3.3 Gel fraction of the PHTE-vitrimer (post-curing) at different curing times.

Table appx. 3.4 Gel fraction of the vitrimers and the commercial epoxy.

Table appx. 3.5 Density of the PHTE-vitrimer, the commercial epoxy and the composites.

Table appx. 3.6 Gel fraction, thermal stability and mechanical performance of the virgin and the reprocessed PHTE-vitrimer.

Table appx. 3.7 Gel fraction of the virgin PHTE-vitrimer and reprocessed up to 4 times.

Table appx. 3.8 Chemical Recyclability of the PHTE-vitrimer, commercial epoxy, commercial epoxy composite and PHTE-vitrimer composite.

List of equations

Introduction

Equation 1

List of abbreviations

Abbreviation	Meaning
BADGE	bisphenol A diglycidyl ether
BOD	biochemical oxygen demand
CANs	covalent adaptable networks
CDCl ₃	deuterated chloroform
CF	carbon fibres
DBEDT (or p-DBEDT) *	DiBoronic Ester DiThiol
DCB	dynamic covalent bonds
DMSO-d ₆	deuterated DMSO
DPNs	dynamic polymer networkscovalent bonds
DSC	differential scanning calorimetry
E _a	activation energy
ELO	bpoxidized linseed oil
EPP	commercial epoxy pre-polymer (based on bisphenol A diglycidyl ether)
EtOAc	ethyl acetate
EtOH	ethanol
FT-IR	infrared spectroscopy
m-BDBEA	meta-diAmine ButaneDiol hydrolized diBoronic Ester diAmine
m-CBDDE	meta-diCarboxy ButaneDiol diBoronic Ester
m-CDGBE	meta-diCarboxy DiGlycerol diBoronic Ester
m-DBEDT	meta-diThiol DiBoronic Ester DiThiol
m-DGBEA	meta-diAmine DiGlycerol diBoronic Ester diAmine
m-HBDBE	meta- diHydroxy ButaneDiol diBoronic Ester
m-HDGBE	meta-diHydroxy DiGlycerol diBoronic Ester
m-MDGBE	meta- diMercapto DiGlycerol diBoronic Ester
m-PTBEA	meta-diAmine PentaeryThritol diBoronic Ester diAmine
M-THF	methyl tetrahydrofuran
Mt	million tons
o-DGBEA	orto-diAmine DiGlycerol diBoronic Ester diAmine
p-DBEDT *	para-diThiolDiBoronicDiBoronic Ester DiThiol
p-DGBEA	para-DiGlycerol diBoronic Ester diAmine
PBAT	polybutylene adipate terephthalate
PBS	polybutylene succinate
PCL	Polycaprolactone
PE	polyethylene
PET	polyethylene terephthalate
PGA	polyglycolic acid
PHA	polyhydroxyalkanoates
PHB	polyhydroxybutyrate
PHTE	phloroglucinol triglycidyl ether
PHU	polyhydroxyurethanes
PI	polyimines
PLA	polylactic acid
PP	polypropylene
PS	polystyrene
PU	polyurethane
PVC	polyvinyl chloride
RT	room temperature
SEM	scanning electron microscopy
T _g	glass transition temperature
TGA	thermogravimetric analysis
THF	tetrahydrofuran
T _m	melting point
TMS	tetramethylsilane
T _v	topology freezing transition temperature
XRD	x-ray diffraction

Introduction

This *Introduction* is structured in three main parts. The first regards an overview about plastic materials, focusing, in particular on the importance for the current society, the main advantages and drawbacks and the principal application fields of these materials. The second part describes the properties and the use of a new class of plastics - vitrimers that can act as a merging point between the tradition thermosets and thermoplastics. The last part talks about the world of fibre-reinforced composite materials with some examples of the combination of natural polymers and natural filler elements to obtain natural polymer composites with tuneable final properties.

I.1. Plastics, a quick overview on types and recycling

Plastics in general have gained significant technological and economic importance alongside metals and ceramics, changing completely human habits from the middle of 20th century when they gradually have paved the way for substituting the old, outdated materials. Indeed, the last century witnessed an explosive growth in plastics production, thanks to their extraordinary properties, as in fact, the name means. The term “plastic” derived from the Greek word “*plastikos*”, meaning “capable of being moulded into various forms”, moreover these materials also known with the name of “polymers” from the Greek “*poly*”, meaning “many” and “*mero*”, meaning “parts”. From the meaning of their name its clearly evident how peculiar is this class of materials. Indeed plastics are extremely malleable, allowing the possibility to create different shapes like films, fibres as well as bottles and other tree-dimensional objects.¹

The global production of plastics reached more than 400 million tons (Mt) in 2023, with an increment of ~35% in the last 10 years (Figure I1A).²

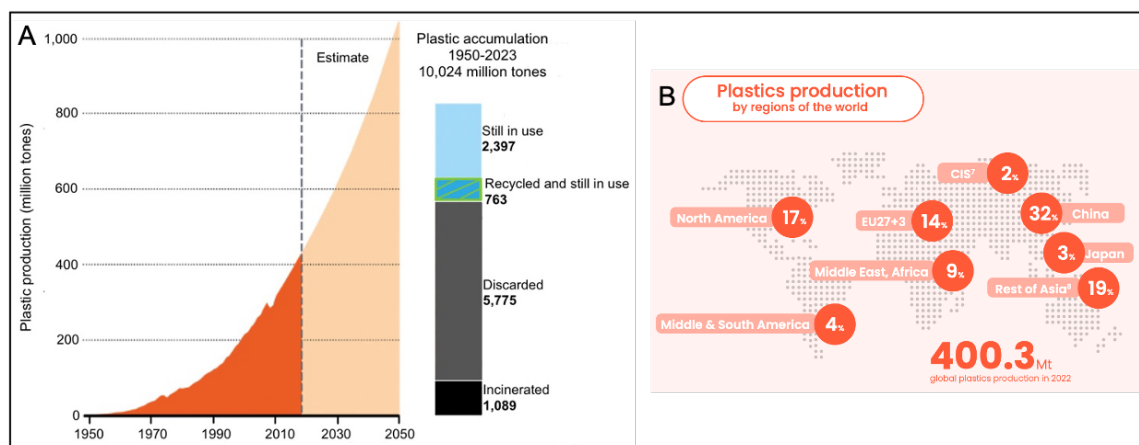


Figure I1. World annual plastics production 1950-2023 (adaptation from nature.com)(A) and Plastics production by region in 2022 (plasticseurope.org) (B).

Asia is the largest producer with an annual production of ~50% of the entire world production, followed by North America with 17% and Europe with 14%. Keeping into consideration that China alone is the largest producing country with an annual production of ~32%, while in Europe more than 75% of the plastics demand is concentrated in five countries: France, Germany, Italy, Spain, and United Kingdom. From an economic perspective, plastics are an “industry” which employs over 1.5 million people in around 50000 companies with an estimated annual turnover of more than 400 billion euros, considering just Europe (Figure I1B).³

Plastics, from the chemical point of view, are materials with high molecular weight, *i.e.*, they are composed of very large molecules (macromolecules), in fact, as already mentioned, the terms plastic and polymer are often used synonymously. But more in details, the term *polymer* is applicable to all materials with a macromolecular structure, whereas the term *plastics* only describes polymers that are modified with additives to meet the requirements of industrial processing technologies.⁴

These materials can be classified in different ways, for example can be organized by the origin of the raw materials and type of process, here we have: natural polymers derived by living organism such as natural polyesters (polyhydroxyalkanoates (PHA) and polyhydroxybutyrate (PHB)), artificial polymers which are obtained by modification of natural polymer like chitosan and cellulose esters, synthetic polymers produced from natural resources like polylactic acid (PLA), synthetic polymers generally obtained by chemical process starting from the petroleum (polyolefins, polystyrene, polyesters, polyurethanes and polyamides) and finally inorganic polymers with a skeletal structure that does not include carbon atoms in the backbone, but atoms like silicon and phosphorous (polysilanes, polysiloxanes and polyphosphazenes).

The last classification can be done considering the mechanical properties; therefore, polymers can be divided into thermoplastics characterized by linear or branched chains, interacting with each other by non-covalent forces, therefore never cross-linked, indeed they can be heated until fluidification (as in the case of amorphous polymers) or melting (as in the case of semi-crystalline polymers) and can be subjected to reversible thermal transformation (re-moulded), and therefore they are recyclable. Examples include polyolefins, polyesters and polyamines.

On the other hand, thermosets are obtained by irreversible hardening (curing) of viscous liquid pre-polymer (resin), in which the chains are connected together through covalent bonds, therefore they cannot be fluidified or melted and if heated they undergo irreversible degradation, which means they are non-recyclable. This class of polymers dominates the world of high-performed material.

Another noteworthy classification is made by considering the lifecycle, in particular plastics can be divided in recyclable polymers which are soluble in solvents and/or can be reversibly fluidified/melted, for examples the polyolefins (codified by the European commission decision number 97/129(CE)).⁵ Non-recyclable polymers which are insoluble in solvents and/or cannot be reversibly moulded/melted such as thermosets polymers like epoxy resins and phenolic resin. Biodegradable polymers in which the skeleton degrades under the activity of microorganism (polycaprolactone, cellulose derivatives, polylactic acid (PLA) and polyglycolic acid (PGA)), finally compostable polymers which can be transformed into compost as fertilizer in agriculture, like starch derived polymers.

The market is, instead, dominated by the so-called “big six plastics” group, *i.e.*, polyethylene (PE), polypropylene (PP), polyvinyl chloride (PVC), polyurethanes (PU), polyethylene terephthalate (PET) and polystyrene (PS), since most of the commodities are made of these materials. (**Figure I2**).





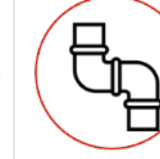

Polyethylene (PE)	Polypropylene (PP)	Polystyrene (PS)	Polyethylene terephthalate (PET)	Polyvinyl chloride (PVC)	Polyurethane (PU)
					
Bags Storage containers	Bottle caps Ropes	Single use disposable cutlery Storage containers	Drink bottles Textile fibres	Pipe Storage containers	Panels Automotive

Figure 12. The most common plastics and their main applications.

Plastics have multitude of beneficial properties including lightweight, since they have low density, chemical and environmental inertia, low thermal and electric conductivity, and especially easy processing and low costs, thanks to which they are widely used in many applications. However, the most driving sector is the packaging market as shown in **Figure 13**, with a predominate use of the “big six plastics” among all the plastic materials.³

Nevertheless, approximately 12% of the global plastic production volume, i.e., approximately 44 million tons, are thermosets; they predominantly include epoxies, polyurethanes, silicones, phenolics and polyesters. Moreover, it is worth pointing out that the global thermosetting plastics market is projected to grow in the next few years.

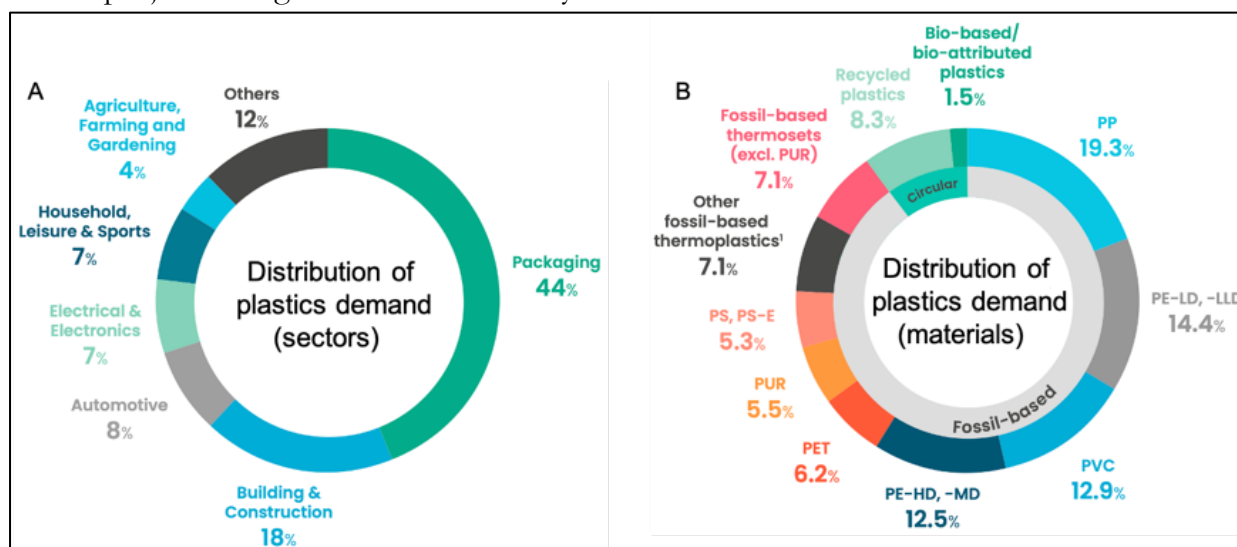


Figure 13. Distribution of plastics demand by sectors (A) and by materials (B) (adaptation from plasticseurope.org).

To give numbers, the average lifetime of a disposable single-use plastic is 15 minutes, instead for packaging materials it is 6 months and, generally, the average lifetime for a plastic material is 10 years, while they take more than 300 years to start decomposing in environmental conditions. According to these data the necessity of a more sustainable and circular approach is clearly evident.⁶

Indeed, the problem has risen because, as mentioned before, most of the plastics are derived from fossil feedstock including toxic and poorly biodegradable monomers and additives, which consumes non-renewable resources, in addition to the huge and uncontrolled production.⁷

To sum up, the high amount of waste generated is undoubtedly the worst consequence related to the use of petroleum-based plastics. Additionally, there is also the mismanagement of the

plastic waste that has to be taken into consideration. Indeed, **Figure 11A** shows a global analysis of all mass-produced plastics ever made (thermoplastics and thermosets) out of which only 7.6% has been recycled, 10.8% has been incinerated, and 57% has been accumulated in landfills.³ At this point, a question arises spontaneously:

Where do poorly managed plastic materials end up?

The answer is: in the environment and especially in the oceans, but plastic will only enter rivers and the ocean if it's poorly managed. To give some numbers the amount of plastic entering the oceans annually is a staggering figure, indeed an estimated 8 million tons of plastic enter the oceans every year. Moreover around 90% of seabirds have plastic in their stomachs) and half of marine turtles have eaten plastic and it's estimated that by 2050, there could be more plastic in the ocean than fish (by weight).⁸⁻¹⁰

In fact, in rich countries, nearly all the plastic waste is incinerated, recycled, or sent to well-managed landfills. It's not left open to the surrounding environment. On the other hand, low-to-middle income countries tend to have poorer waste management infrastructure, therefore waste can be dumped outside of landfills, and landfills that do exist are often open, leaking waste to the surrounding environment. Mismanaged waste is the sum of materials which are either littered or inadequately disposed. Subsequently formed plastic debris have significant harmful effects on the marine environment because of their persistence and effects on wildlife and potentially humans, not only because marine species are known to ingest big plastic residues, but also because many of them have been affected by plastic debris (microplastics)¹¹⁻¹⁴ (**Figure 14**).

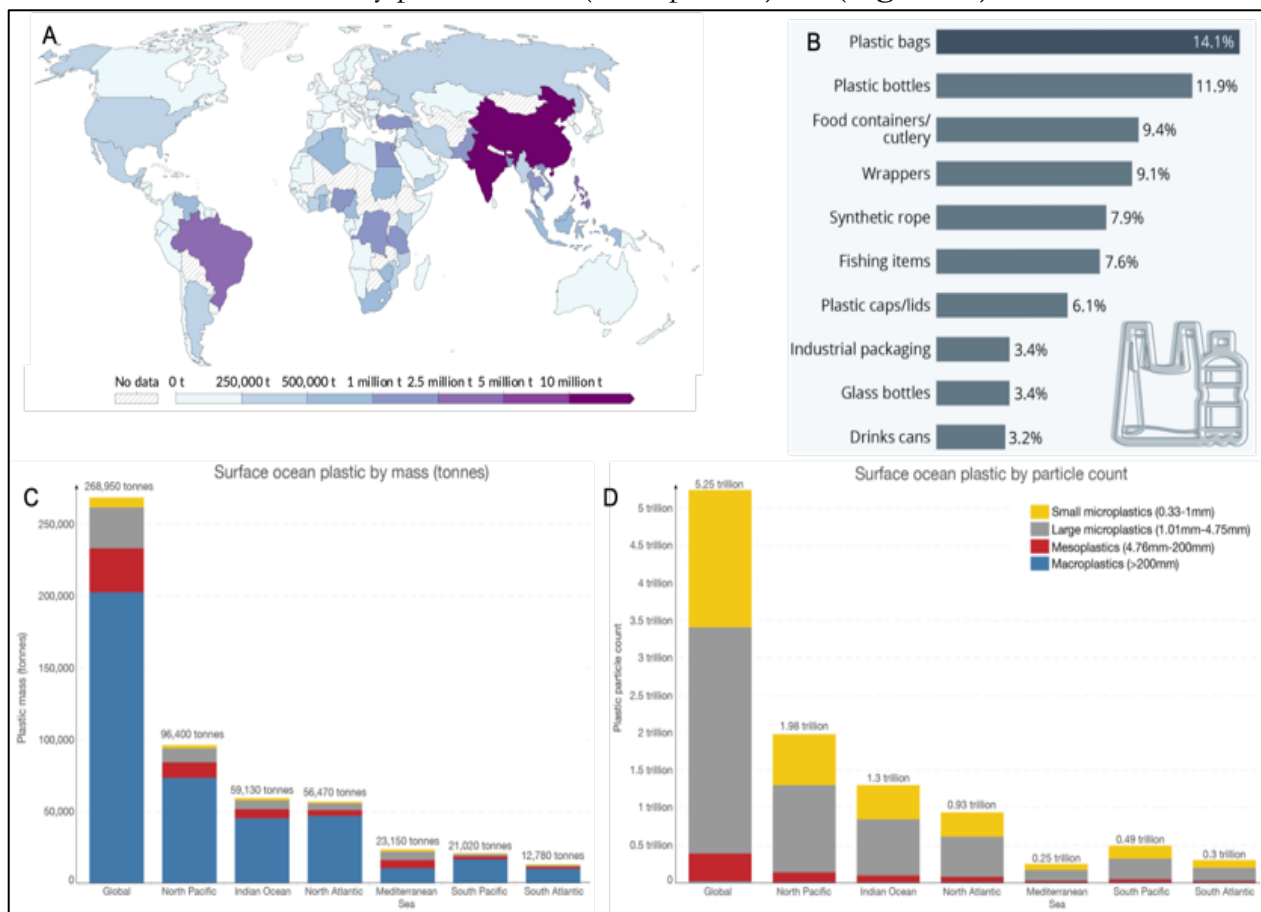


Figure 14. Mismanaged plastic waste for country (A); Plastic items dominate the ocean garbage (B); Plastic mass across the world's surface oceans by mass (C) and by particle count (D) (adaptation from ourworldindata.org).

To overcome petroleum-based synthetic polymers' drawbacks, the production of bioplastics with similar properties to the conventional ones is considered a sustainable and realistic alternative, and indeed it is an emerging reality, especially in the last 10 years.

Bioplastics gather together three categories, the bio-based, but non-biodegradable materials which are chemically and physically identical to their fossil-based counterparts, but made from bio-based resources (are also called drop-in materials), such as the bio-PET, bio-PE and polyethylene furanoate (PEF). The ones fossil-based, but biodegradable like the polybutylene adipate terephthalate (PBAT) or Polycaprolactone (PCL) and the ones bio-based and biodegradable, like the PHA and polybutylene succinate (PBS) as show in **Figure I5A**.

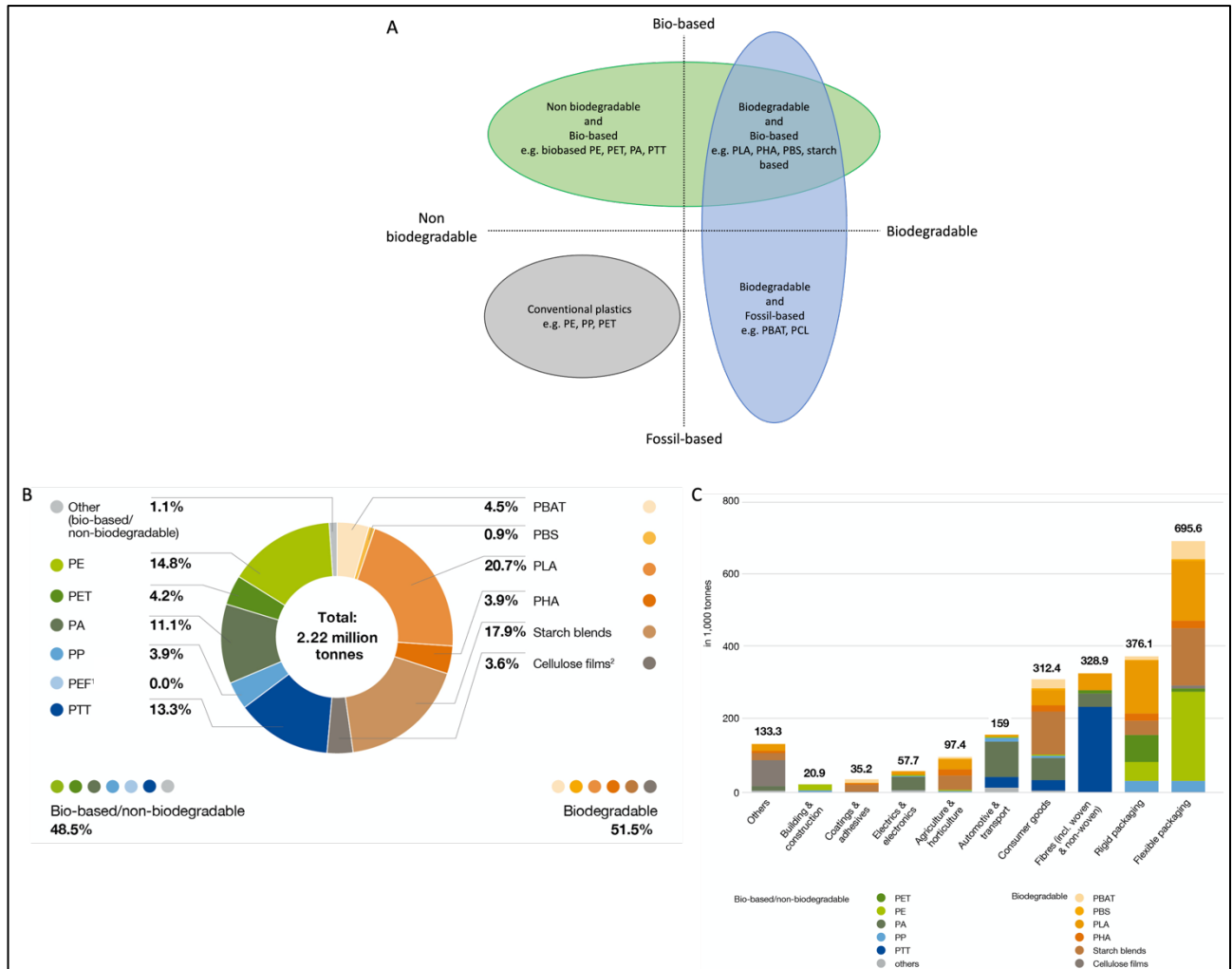


Figure I5. Bioplastics classification (A); Global production capacities of bioplastics in 2022 by materials (B) and Global production capacities of market in 2022 (adaptation from european-bioplastics.org).

Currently, bioplastics still represent around one percent of the entire annual plastic production, as shown in **Figure I3B** and biodegradable plastics altogether account for more than 51 percent (over 1.1 million tonnes) of the global bioplastics production capacities. Moreover, the production of biodegradable plastics is expected to increase to over 3.5 million tonnes in 2027 due to a strong development of polymers, such PLA and PHA. Instead, biobased, but non-biodegradable plastics all together make up for more than 48 percent (almost 1.1 million tonnes) of the global bioplastics production capacities and their relative share is predicted to further decrease to about 44 percent in 2027. Bioplastics are used in an increasing number of markets,

but packaging remains the largest market segment for bioplastics with 48 percent (almost 1.1 million tonnes) of the total bioplastics market in 2022 (**Figure I5B and C**).¹⁵

Nonetheless, to be biodegradable or recyclable is not enough to solve the big issue about the plastics end-of-life, indeed, efficient waste management is a key point. Plastics can be recycled through a mechanical process (also called primary and secondary recycling, in particular the first one is done on the recycle material after their life time, the second, instead, is referred to the recycling of virgin scraps) in which the materials are shredded, melted and extruded into pellets. Or through a chemical process (tertiary recycling), divided into different methods, in which polymers are reduced to their chemical building-blocks (feedstock and monomers), which then can again be polymerised into fresh plastics.¹⁶

In theory, this allows for near infinite recycling as impurities, additives, dyes and chemical defects are completely removed with each cycle. In practice, chemical recycling is far less common than mechanical recycling, because technologies do not yet exist to reliably depolymerise all polymers on an industrial scale and, also, because the equipment and operating costs are much higher in comparison to mechanical recycling.¹⁷⁻¹⁹

Thermal recovery or quaternary recycling, involves processing at high temperatures, can be mainly classified as combustion or incineration, for only energy recovery and fluidized-bed combustion to principally recover reinforcement fibres from polymer composites, and anaerobic combustion, i.e., pyrolysis, to recover simpler molecules used as feedstock for new chemical processing. Thermal recovery is often the waste management method of last resort, a position previously held by landfill because it interrupts the recycling circle, but also because burning has long been associated with the release of harmful substances (**Figure I6**).^{3, 20-23}

The mechanical and chemical recycling are extensively used for thermoplastics polymers, and especially polyolefins and polyesters. On the contrary, thermosets polymers, due to their strong covalent network cannot be properly mechanically recycled since they cannot fluidify, therefore they can be only grinded and used as fillers. They cannot be chemically recycled as well due to their cross-linked. Indeed, they are generally disposed in landfills or incinerated.²⁴are s

For what concern Europe, in 2021 the total amount of plastics produced was 57.2 Mt, the post-consumer plastics waste collected was 29.5 Mt, 15 Mt were mixed plastics and 14.5 Mt were separated plastics. Out of the mixed plastics 5% went to recycling, 57% to the energy recovering facilities and 38% to landfills. Instead, the separated plastics were recycled in 65%, the 27% went for energy recovery and 8% ended up in landfills.²⁵

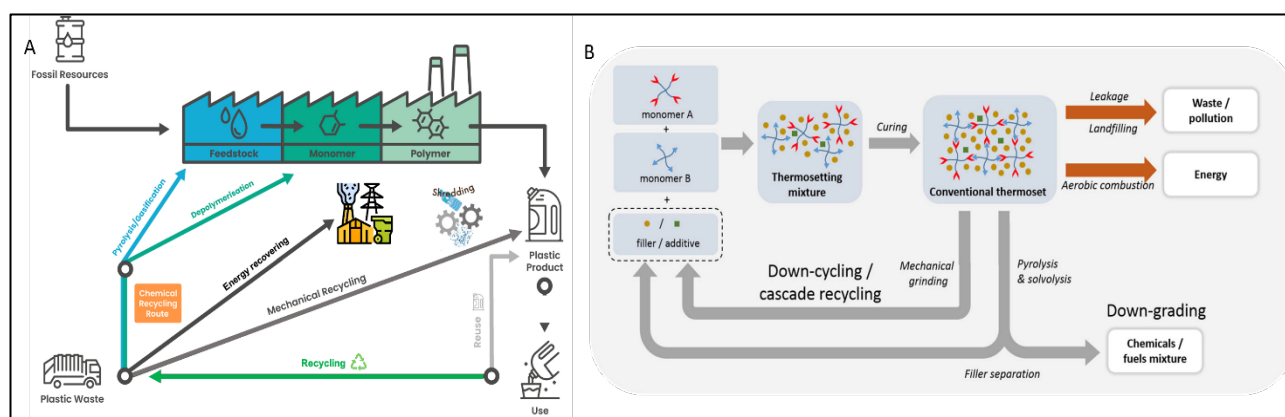


Figure I6. Plastics recycling methodology (A) and thermosets recycling way (B) (adaptation from plasticseurope.org and tandfonline.com).

I.2. Vitrimers and the boronic ester chemistry

As pointed out in the previous paragraph, the use of biodegradable polymers from renewable resources represents a realistic and sustainable alternative to the use of petroleum-based synthetic polymers, but mainly focuses on thermoplastics. Despite the fact that extracted natural polymers can achieve encouraging mechanical performance, generally it is still lower with respect to their synthetic counterparts. On the other side, in the recent years, researchers have developed a new approach to overcome the difficulty of recycling thermosets. By modifying the matrix with “special connections” it is possible to make these materials much easier to break down while retaining their mechanical properties.

The strategy is based on the introduction of degradable or dynamic structures which allow to de-crosslink and re-crosslink thermosets by means of exchange reactions of cleavable bonds. The dynamic bonds are stimuli responsive, therefore they could be used to activate structural changes. Nowadays current research projects are focusing both on the study of natural resources and on their functionalization for the development of novel materials with tuneable properties, in particular on the synthesis of polymer networks with high performance and recyclability.

The aforementioned molecular debonding can be obtained by stimuli-triggered degradation or by introducing dynamic covalent bonds in the networks. Stimuli-triggered degradation is performed by incorporation of labile bonds to the conventional cross-linked resin. Depending on the amount and location of the cleavable linkages within the polymer structure the material can be degraded into different product. Total degradation of the matrix leads to lower molecular weight organic substances, depolymerization of the polymer backbone yields monomers or oligomers, and decrosslinking of a crosslinked, linear polymer results in a thermoplastic linear polymer. Even though stimuli-triggered degradation can yield an improved thermoset recyclability, the original polymer architecture is irreversibly destroyed and, as a consequence, the recycled polymer needs to be resynthesized or be used in lower performance applications. This drawback can be overcome using dynamic covalent networks which function via either associative or dissociative mechanisms (**Figure I7A**). Indeed, both mechanisms lead to a cross-linked structure with properties similar to the original thermoset which, yet allow a reprocessing and recycling through methods typically employed for thermoplastics polymers.

The dynamic covalent bonds (DCB) open the path to the covalent adaptable networks (CANs) The dynamic bonds are not only cleavable, but also reversible, implying that the materials can be repeatedly broken, remoulded and reformed under an external stimulus.

To give a short background, the earliest evidences of the dynamic thermosets came from stress relaxation experiments at high temperature performed between the '40s and '50s on polysulfide and silicone rubbers.²⁶⁻²⁸ The decay of stress as a function of time was attributed to the rearrangement (scission/re-storing) of the crosslinks catalysed by non-reacted residual impurities. As often happens in research, for many years these results were essentially overlooked, until their importance for the reprocessability and, especially, self-healing ability of crosslinked polymers was understood. Indeed, in 2002, Wudl reported a furan/maleimide polymer network, whose thermal reversibility enabled a remarkable self-healing ability.²⁹ Few years later, in 2005 Bowman designed for the first time a thermoset with photo-induced stress relaxation and introduced the concept CAN.^{30,31} More recently, in 2011 Lieber's group extended the realm of associative CANs by adding a suitable transesterification catalyst to epoxy/acid or epoxy/anhydride polyester-based networks. This thermally triggered catalytic transesterification reaction resulted in permanent polyester/polyol networks that show a gradual viscosity decrease upon heating, a typical and distinctive feature of vitreous silica, which has never been observed in organic polymer materials. Hence, the authors introduced the name *vitrimers* for those materials.³²

To synthesize CANs two strategies can be adopted, in fact, they are classified in associative and dissociative CANs, as shown in **Figure I7B**. The first group makes use of a dissociative cross-link exchange mechanism through which chemical bonds are firstly broken and then reformed in another position. Upon heating, the cross-linking reaction becomes reversible, leading to an increased rate of bond breaking/reforming and also to a net bond dissociation. Thus, such materials can achieve very fast topology rearrangements (stress relaxation and flow) because of a decrease in connectivity. This temporary loss of cross-links typically results in a sudden viscosity drop and the material becomes soluble, similarly to a thermoplastic polymer. Upon cooling, the cross-links are formed again, usually to the same extent as in the starting material, thus preserving or re-installing the desirable thermosetting properties. In this way, these dynamic cross-links allow for thermal (re-)processing of polymeric networks.^{31, 33}

The second group makes use of associative bond exchanges between polymer chains, in which the original cross-link is only broken when a new covalent bond to another position has been formed.

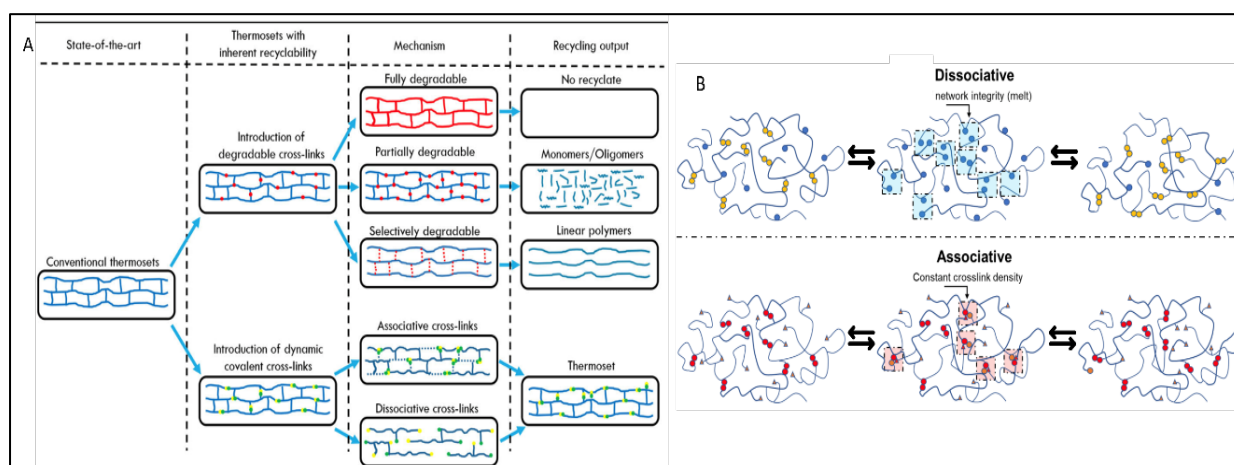


Figure I7. Schematic overview of the existing concepts to develop recyclable thermoset polymers (A) and Covalent adaptable networks classification (B) (adaptation from [tandfonline.com](https://www.tandfonline.com)).

Differently, here, a rise in temperature increases solely the kinetics of the bond exchange, without affecting the crosslinking degree. Thus, the material gradually reduces its viscosity and flows when heated over a certain temperature without losing its insolubility.³² Indeed, the material does not depolymerise upon heating, but is characterized by a fixed cross-link density. Covalent bonds are only broken when new ones are formed, therefore, the cross-link density can be considered approximately constant.³³⁻³⁹

In the dissociative rearrangement, a polymer chain is first subjected to cleavage, generating a temporarily de-crosslinked intermediate state where chain ends are reactive, and thus, has higher energy. In the second step, the chain ends can reform the crosslink, completing the rearrangement. When the rearrangement has the associative mechanism, the two polymer chains are first associated to form a reactive (higher energy) intermediate. A subsequent fragmentation, involving another crosslink, completes the rearrangement. Overall, energy profiles of both mechanisms show an endothermic, higher energy intermediate, characterized by a different degree of connectivity.³⁶ The rearrangement can be activated only if the energy barrier (ΔG^\ddagger) between reactant/products and the intermediate is overcome. The activation energies reported in for selected dynamic covalent chemistries provides a good estimation of the enthalpic component of this energy barrier.

Indeed, the activation energy (E_a) values of reversible covalent bonds (~ 15 to 156 kJ/mol) are lower than the bond energy of typical irreversible carbon-carbon bonds (~ 376 kJ/mol) and thus,

they are labile bonds. However, the chemical reactivity of the dynamic polymer networks DPNs is not only related to bond exchange rate, but also strongly influenced by other factors like network architecture, presence of additives, solvents or impurities.⁴⁰⁻⁴⁸

As mentioned before, in 2011 the field was enriched by the introduction of the vitrimers, which are classified as the associative CANs and owing to their unique properties, are considered a new family of plastic materials.

Indeed, the great interest in these novel polymers and in their outstanding properties is highlighted by the rapid growth of this field within polymer science. In fact, the number of vitrimer-related publications and citations has been increasing, before 2014 sporadic articles were published, instead, from 2014 to nowadays there was an increase of more than 98%; from 1 article in 2014 to almost 200 in 2022.⁴⁹

The term vitrimer reflects the similarity of some of the properties of these organic networks with vitreous silica. These materials are characterized by a permanent network and upon heating the network can be modified thanks to the exchange reactions, while maintaining a constant number of crosslinks, leading to a transition from (visco)elastic solid to viscoelastic liquid. This property allows vitrimer networks to flow when heated, giving the possibility to reshape the materials, without losing their integrity. In particular, this behaviour is possible since these polymers are characterized, not only by the glass-transition temperature, but also by another temperature, defined as topology freezing transition, T_v , above which the material can flow following the Arrhenius trend (like the silica-based glass). Therefore, this feature enables the vitrimers to behave like a thermoset below the T_v and as a reprocessable and reshapable viscoelastic fluid above T_v .^{50, 51}

In essence, this temperature represents a critical point at which the molecular architecture or topology of a material becomes 'frozen' or kinetically trapped, impacting its structural rearrangement.

At higher temperatures, the molecular constituents within a CAN have increased mobility, facilitating bond exchange and molecular rearrangements. However, as the temperature decreases, molecular motion slows down. The topology freezing temperature signifies the point at which the molecular rearrangement or dynamic bond exchange within the material becomes significantly hindered due to reduced molecular mobility. At this temperature, the network 'freezes' in a particular configuration, preserving its topology.

Below the topology freezing temperature, the material's structure becomes kinetically trapped, preventing further reconfiguration or healing. This phenomenon defines a temperature range wherein the material's topology remains relatively fixed despite its dynamic nature.^{52, 53}

In summary, understanding the topology freezing temperature is crucial in designing CANs for specific applications. It influences the operational temperature range, durability, and the material's ability to maintain desired properties. Controlling this temperature range can be pivotal in optimizing the material's performance. The advantages of vitrimers are:

Dynamic Adaptability: vitrimers exhibit dynamic properties, allowing them to undergo controlled rearrangements when subjected to external stimuli. This feature enables reshaping, self-healing, and recyclability, offering versatility in applications.

Self-Healing Capability: one of the most notable advantages is their ability to autonomously heal when damaged. The reversible covalent bonds within the network allow for the material to mend cracks or breaks, extending the lifespan of products made from vitrimers.

Recyclability and Sustainability: vitrimers can be reprocessed multiple times without significant degradation in properties. This feature aligns with the growing need for sustainable materials, reducing waste in various industries.

Tailorable Properties: their chemistry allows for fine-tuning of properties such as flexibility, strength, and thermal characteristics, making vitrimers adaptable to specific application requirements.

Durability: vitrimers often exhibit robust mechanical properties, making them suitable for applications requiring resilience and long-term durability.

The disadvantages or limitations of vitrimers are:

Limited Temperature Range: Vitrimers may have a limited operating temperature range due to their topology freezing temperature. Below this point, their dynamic behaviour decreases significantly, restricting their functionality.

Processing Challenges: despite the dynamic nature of vitrimers, processing such as moulding and shaping can present challenges due to high viscosity of those materials.

Chemical Stability: some vitrimers may be susceptible to certain chemical environments or specific solvents, limiting their use in certain applications where chemical resistance is critical.

Long-term Stability and Aging: understanding the long-term stability and aging behaviour of vitrimers remains an ongoing area of research. Predicting their performance over extended periods, especially in harsh conditions, is crucial for practical applications.

Complex Synthesis: while vitrimer synthesis methods continue to evolve, achieving precise control over the network's dynamics while maintaining mechanical strength can be challenging and often requires sophisticated chemistry.³³

A wide number of chemistries which can induce this remarkable thermal behaviour have been explored, especially to synthesize biobased vitrimers (**Figure I8**). Currently, the major parts of the developed systems are based on transesterification (**Figure I8a**). To activate the exchange reaction, free OH groups are required within the network, and the presence of a catalyst and relatively high temperature are typically needed.

Vinylogous urethane exchange, first introduced by Du Prez and co-workers⁵⁴, has also been used several times in biobased vitrimers (**Figure I8b**). The exchange involves free amine groups and proceeds via two different pathways, depending on the temperature.⁵⁵ Transesterification of boronic esters was first reported by Guan and co-workers (**Figure I8c**).⁵⁶ Later, Röttger et al. showed that the exchange reaction could also proceed in the absence of free diols, by metathesis, thus increasing the stability of these systems and opening a wider range of applications.³⁵

In some cases, the line between dissociative and associative mechanisms is difficult to draw. Some exchange reactions were first presented as associative before additional experiments finally showed a dissociative pathway. In addition, some exchange reactions can involve different mechanisms, dissociative or associative, that can coexist depending on environmental conditions. This is the case for instance in PU, where the exchange can involve urethane reversion (dissociative) and transcarbamoylation (associative)⁵⁷⁻⁵⁹, polyhydroxyurethanes (PHU), with reversible cyclic carbonate aminolysis (dissociative) and transcarbamoylation (associative)⁶⁰⁻⁶², or polyimines (PI), with imine hydrolysis (dissociative) as well as transimination and metathesis (associative) (**Figure I8d-f**).⁶³⁻⁶⁷

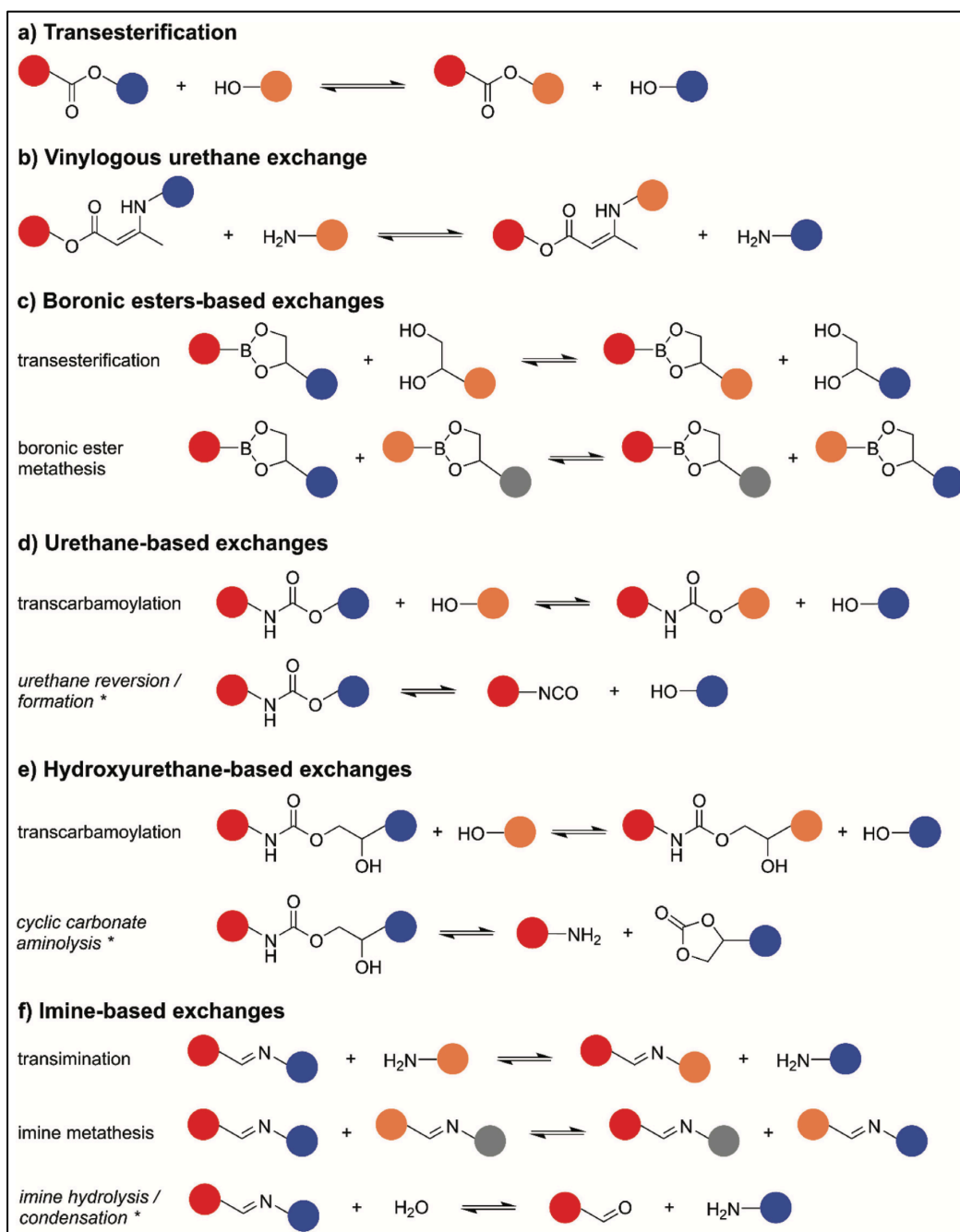
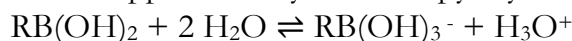


Figure 18. Dynamic covalent chemistries used in the synthesis of biobased vitrimers (*= dissociative exchange) (adaptation from <https://doi.org/>).

This thesis is focused, among all the chemistries, on the boronic ester metathesis. Boronic acids represent trivalent organoboron compounds formulated as $\text{RB}(\text{OH})_2$, where R denotes an organic substituent. The boron atom adopts sp^2 hybridization and retains an unoccupied p orbital. Consequently, boronic acids act as mild Lewis acids, diverging from conventional Brønsted acids in water; instead, they facilitate water ionization, generating hydronium ions through an 'indirect' proton transfer (**Equation 1**). The pK_a values of aryl boronic acids vary from 8.9 for phenylboronic acid to approximately 4.0 for 3-pyridylboronic acid.



Equation 1

Similar to carboxylic acids, boronic acids establish esters with alcohols. Acyclic boronic esters exhibit hydrolytic vulnerability. However, they readily form more enduring cyclic esters, notably

five- and six-membered structures with 1,2- and 1,3-diols, respectively.⁶⁸ Saturated cyclic boronic esters are termed dioxaborolanes for the five-membered and dioxaborinanes for the six-membered rings. The capacity of boronic acids to generate stable cyclic esters with diols has captivated researchers since the late 1950s.⁶⁹ Given that diol groups are inherent in saccharides, the interaction of boronic acids with diols has been harnessed for sensor development and in separation systems for carbohydrates and glycoproteins.⁷⁰⁻⁷² Additionally, boronic esters serve as protective agents in organic chemistry.⁷³ The dynamic nature of boronic ester connections, evident in their high transesterification rates, has intrigued polymer materials scientists for constructing dynamically interconnected networks, in bulk, organic solvents, or aqueous media, to create hydrogels. Boronic acid-based hydrogels are extensively studied for biomedical uses owing to their self-repair abilities and responsiveness to stimuli.⁷⁴⁻⁷⁹

Consideration of the thermodynamics and kinetics of boronic acid esterification involves numerous factors. The boronic acid can exist in either trigonal sp^2 or sp^3 hybridization, with the tetrahedral hybridization favouring ester formation (**Figure I14**).⁸⁰ The apparent equilibrium constant of esterification relies on factors like the acid and diol pK_a values, structural elements such as conformational rigidity, stereochemical hindrance, etc.⁸¹

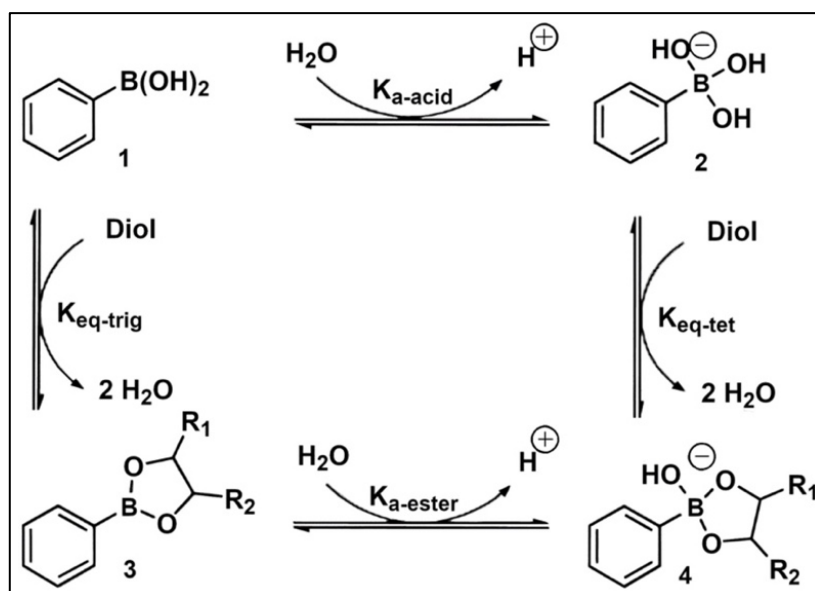


Figure 19. Equilibrium between phenylboronic acid and its diols esters.⁸⁰

The equilibrium between trigonal and tetrahedral states holds significance in aqueous systems, particularly during pH fluctuations. In the case of bulk vitrimers, regarded as anhydrous, the boron atom's hybridization in ester cross-links typically remains trigonal. In this state, boron atoms act as Lewis acids, known to interact with nitrogen donors through coordinative or dative $N \rightarrow B$ bonds. The equilibrium constant for complex formation through this interaction can reach up to 10^6 M^{-1} , allowing for the formation of supramolecular constructs.⁸²⁻⁸⁶ Crucially, upon complex formation, the geometry of the boron atom and surrounding bonds transitions to a tetrahedral state (**Figure I10**), enhancing the stability of boronate esters.⁸⁷ Nitrogen donors like amines, pyridines, amides, and imidazoles can be introduced as additives or integrated into the structure of an acid or a diol⁸⁸, offering flexibility in designing systems that leverage these interactions. Additionally, the positioning of a carbonyl group adjacent to the boron center, such as in the case of 2-acrylamidephenylboronic acid⁵⁶, facilitates boronate ester formation due to the interaction between boron and oxygen.⁸⁹

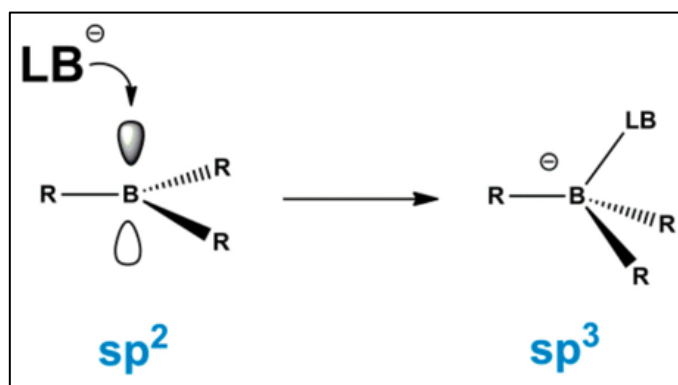


Figure I10. Boron hybridization changes on interaction with a Lewis base.⁹⁰

The rearrangement of boronate cross-links might be governed by two reactions: transesterification with free diol groups in the system or metathesis.⁸⁹ Wulff's investigation highlighted that the proton transfer step (**Figure I14**) determines the rate of ester transesterification.⁹¹ Hence, an appropriately positioned basic group, like an amine group, can significantly expedite the transesterification rate, unrelated to dative bond formation. Moreover, the reaction rate is influenced by the structural characteristics of the acid and diols participating in the reaction.⁶⁸

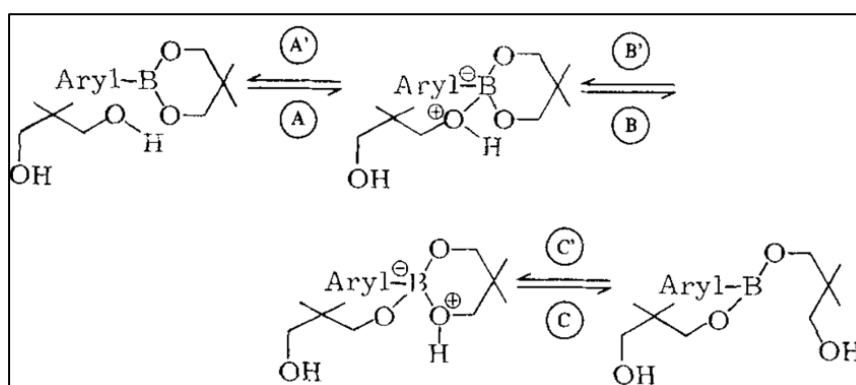


Figure I11. Boronic acid esters transesterification mechanism.⁸⁹

The second, more commonly employed rearrangement reaction in boronate-based vitrimers involves boronate esters' metathesis. Rotger et al. first confirmed this reaction by demonstrating the equilibration of a mixture of two boronate esters, 4-ethyl-2-phenyl-1,3,2-dioxaborolane (B1-D2) and 4-methyl-2-(3,5-dimethylphenyl)-1,3,2-dioxaborolane (B2-D1), forming four esters: B1-D1, B1-D2, B2-D1, and B2-D2.³⁵ The kinetics of the exchange reaction followed a second-order model, assuming a single metathesis rate. The determined activation energy (E_a) was ~ 15.9 kJ/mol. For six-membered esters, the reaction proceeds more slowly, with Yang et al. determining an E_a of 23.6 kJ/mol for model small molecules.⁹¹ A significantly higher E_a (62.9 kJ/mol) was observed for the intramolecularly stabilized diethanolamine ester with an N-B dative bond. Additionally, it was noted that the ester metathesis reaction accelerates in the presence of catalytic amounts of free alcohols and diols. The inclusion of 1 mol % excess neopentyl glycol reduced the E_a of metathesis from 23.6 to 6.9 kJ/mol.^{91, 92} The precise mechanism of the reaction remains undisclosed. Winne and Leibler proposed that the exchange mechanism might involve multiple steps, initiated by the formation of a zwitterionic adduct, allowing for the facile exchange of alkoxide residues between the two boron centers.³⁶

The resurgence of polymer networks built upon boronic acid esters is closely linked to the rise of CANs and vitrimers, where the labile nature of boron ester bonds becomes exploitable. Recent

investigations on boronate-based networks highlight two predominant trends. The initial trend involves vitrimer synthesis from low-molecular-weight resins wherein one constituent feature cyclic boronate groups. The resin components cross-link due to the interaction between reactive groups in the resin constituents (**Figure I12**), such as thiol and vinyl groups or isocyanate and hydroxyl groups. Tailoring the properties of the synthesized vitrimer involves altering the molecular weight of the components, for instance, using telechelic oligomers, modifying the functionality of the components, and introducing inactive components lacking boronic acid esters. The second prevalent approach revolves around macromolecule cross-linking, including commercial polymers, using a low-molecular-weight cross-linking agent containing the dioxaborolane group. This is achieved directly, without necessitating modifications to the macromolecular structure, or by incorporating additional functional groups into the polymer structure to facilitate interaction with the cross-linking agent. Beyond these primary strategies, a vitrimer can be formed via a reaction between two sets of macromolecules containing complementary groups that interact, generating dynamic boronate cross-links.

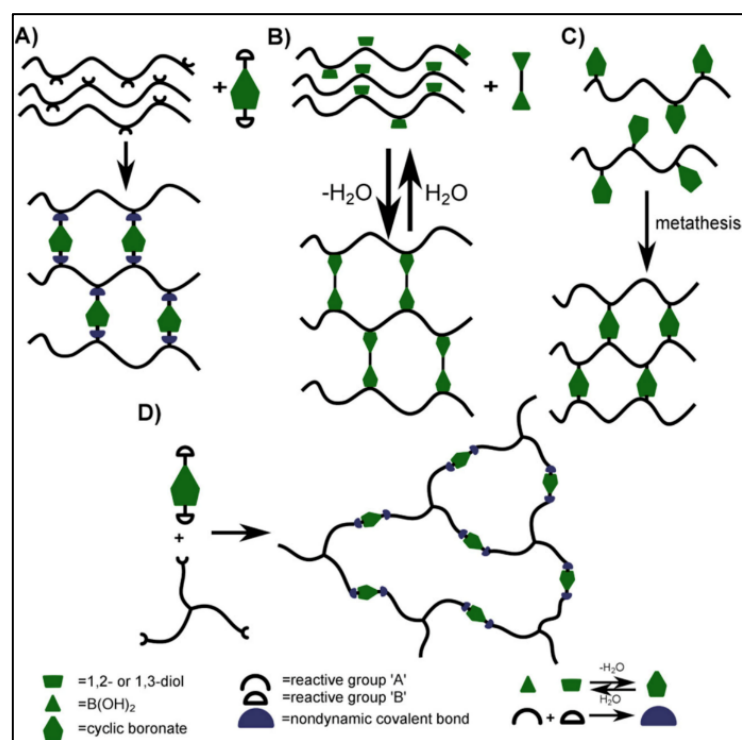


Figure I12. Synthetic strategies for the synthesis of boronic acid esters-based vitrimers (A); cross-linking of macromolecules with cyclic boronates containing reactive groups (B); cross-linking of diol-containing macromolecules with boronic diacids (C); cross-linking of cyclic boronates-containing macromolecules via metathesis (D); reaction between molecules with functionality > 2 and cyclic boronates containing complementary reactive groups.⁹⁰

A variety of cross-linkers containing boronic acid or boronate groups can be employed depending on the resin/polymer composition. These may include derivatives of phenylboronic acid or benzene-1,4-diboronic acid (**Figure I13**). Commonly used are esters of these acids, which react with the resin through boronate metathesis or alternative reactions, such as thiol addition, hydroxyl addition to isocyanate, etc. These reactions leverage additional functional groups present in the boronate cross-linker and other vitrimer components. Opting for boronates over direct condensation proves advantageous as it eliminates the necessity of water removal.

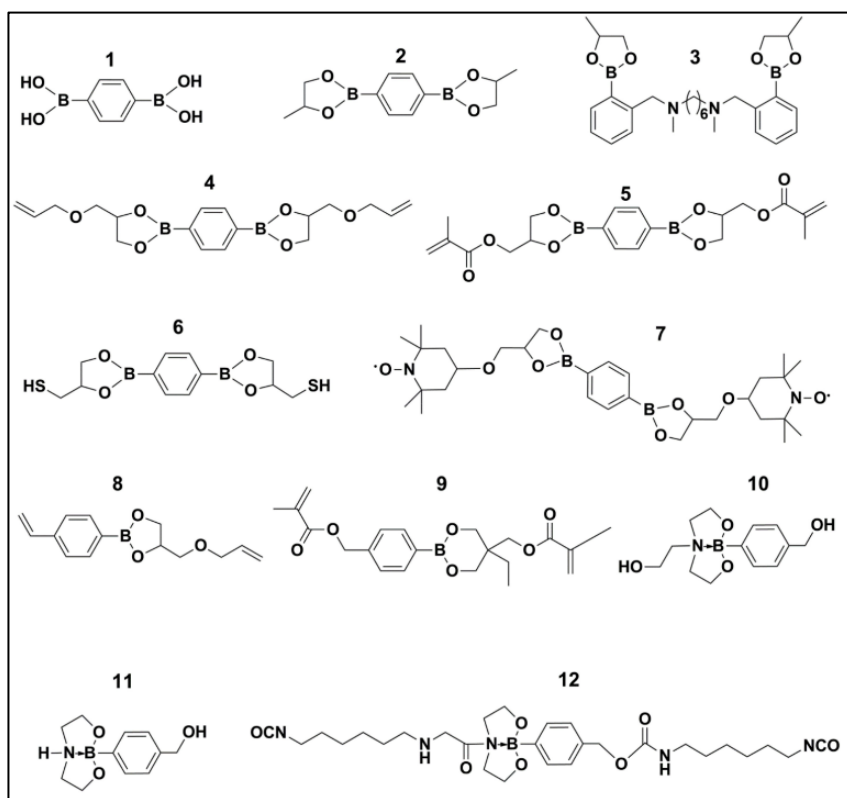


Figure I13. Common structural formulas of cross-linkers applied for the formation of boronic acid esters based vitrimers.⁹⁰

In literature boronic ester vitrimers are mainly focused on diboronic ester dithiol dynamic cross-linker (DBEDT).^{47, 48, 93, 94} However, only few examples are biobased. Other authors have also prepared vitrimer using directly boronic acid as cross-linker such as Wang et al.⁹⁵ did or other boronic esters molecules such as Xie et al. did.⁹⁶

In addition, many epoxy derivatives synthesized by natural molecules such as epoxidized plant oils^{47, 48, 97, 98}, isosorbide^{99, 100}, lignin derivatives^{101, 102}, itaconic acid¹⁰³, vanillin¹⁰⁴ and other epoxy natural molecules^{105, 106} have been used for the preparation of epoxy vitrimers and thermosets.^{107, 108} In particular researchers focus on them, because it is of great importance to design green, biobased and reprocessable alternatives to conventional thermosets, that can biodegrade after their use. Especially since epoxy polymers are generally prepared starting from petrol-derived epoxy compounds, as an example bisphenol A diglycidyl ether (BADGE), which is classified as unsafe because it is an endocrine disruptor.¹⁰⁹

I.3. Fibre-reinforced composites

Fibre-reinforced polymer composites encompass polymer matrices fortified with fibrous reinforcement. The matrix can potentially consist of any polymer adept at transferring loads amid the fibres; both primary classes of polymers (thermoset and thermoplastic) are extensively utilized.

Common thermoset matrices in such composites include epoxies, polyesters, vinyl esters, phenolics, cyanate esters (CE), bismaleimides (BMI), and polyimides. However, epoxies currently are the dominant resins used for high-performance composites at low and moderate temperatures (up to 200 °C). Even though the polyesters and vinyl esters can be used at approximately the same temperatures as epoxies, they show lower mechanical performances.¹¹⁰⁻¹¹⁵

Phenolics are used in applications requiring very high temperatures since they offer outstanding smoke and fire resistance. Cyanate esters are a relatively new class of resins that were produced to compete with both epoxies and BMI and offer lower moisture absorption and better electrical

properties although these benefits come at a higher cost. Polyimides and BMI are the thermoset polymers which can work at the higher temperature range (300–350 °C). BMI resins can be processed at the same conditions as epoxies, but polyimides are much more difficult to process than epoxies or BMI. Moreover, both polyimides and BMI exhibit higher moisture absorption and lower toughness values than CEs and epoxies. In conclusion, epoxies are the most used thermosets for high-performance composites when the service temperatures are below 200 °C, due to the superior mechanical performance, lighter weight and resistance to environmental degradation in comparison to the other thermoset resins.¹¹⁶

On the other hand, essential prerequisites include fibre adhesion and the intrinsic mechanical characteristics of rigidity, potency, and resilience. Historically, reinforcements (fibres) have comprised carbon, glass, or aramid (such as Kevlar®). Carbon fibres have been used for decades in the industry thanks to their high stiffness, tensile strength, chemical resistance, high strength to weight ratio, etc. Nevertheless, they are relatively expensive compared to glass fibres and therefore mainly used for high performance and structural applications. Indeed, for almost a century, glass fibres have been widely used to manufacture composite parts for applications in energy (wind turbines) or transports (boats). According to the JEC Observer, they represent more than 90% of the reinforcement fibre world market.¹¹⁷ Although they exhibit weaker mechanical performance in comparison to carbon fibres, there are still commonly used for structural applications because of their much more affordable cost. They also exhibit superior insulating features and high chemical resistance but with drawbacks to be considered such as low tensile modulus, relatively high density and low fatigue resistance compared to carbon fibres.¹¹⁸

Instead, aramid reinforcements, possess remarkable tensile strength, making them highly resistant to breaking or stretching under load. Indeed, they are known for their flexibility and ability to withstand cyclic loading without undergoing significant fatigue, contributing to their durability over prolonged usage, making them suitable for applications requiring toughness and protection against sudden forces or impacts. On the other hand, aramid reinforcements may experience degradation when exposed to ultraviolet (UV) radiation, leading to a reduction in their mechanical properties. Moreover, they tend to be relatively expensive compared to some other reinforcing materials, which can impact the overall cost of manufacturing composite structures.

While mineral fibres like basalt have also found application, recently sustainable fibres derived from plants, including hemp, flax and jute have recently gained considerable attention.¹¹⁹⁻¹²¹ FRPs typically serve as semi-structural or load-bearing materials, commonly applied in high-performance scenarios. High-performance FRPs fall into the category of 'advanced composites,' recognized for their high fibre volume fraction (>50%) and continuous fibres, though short fibre FRPs are prevalent in less demanding, semi-structural uses. Moreover, several researchers have lately showcased the potential of highly aligned short fibres to rival the mechanical performance of traditional continuous fibre composites.^{32, 33, 38, 122, 123}

High-performance FRPs and advanced composites play a vital role as structural materials, boasting exceedingly high specific stiffness and strength.¹²⁴ Consequently, FRPs are ideal for weight-sensitive applications. Beyond strength and stiffness, their versatility in terms of design elements (fibre type, orientation, matrix composition, etc.) provides an additional advantage in tailoring them to specific applications. The aerospace industry has been a key catalyst in the advancement and integration of FRPs. In modern passenger aircraft, FRPs find extensive use, exemplified by the Airbus A350, reportedly comprising >52% carbon fiber.¹²⁴ While the automotive industry traditionally limited composite usage to (low-production) high-performance sports cars justified by higher material costs,^{54, 125, 126} recent years have witnessed a substantial shift driven largely by emissions-reduction regulations from the EU, US, and others. Currently, FRPs serve also diverse purposes in marine structures, sports equipment, and energy applications,

particularly in wind turbines, where the demand for higher blade sizes necessitates the use of materials with an exceptionally high stiffness-to-weight ratio, hence the prevalent use of high-performance CFRP.

However, despite recent achievements and indications of substantial growth, FRPs are not devoid of drawbacks.¹²⁷ Chief among these is the frequently mentioned low toughness (brittleness) of composites, compounded by inadequate transverse (out-of-plane) mechanical properties stemming from their laminated structure, making them prone to damage and premature failure. Additionally, aside from being often expensive and complex to manufacture, FRPs face challenges related to repair and especially to recycling.

Indeed, the extensive utilization of thermoset matrices poses a significant hurdle for closed material cycles because, after regular use, they are either transformed into thermal energy, deposited in landfills, or their genuine recycling demands a considerable amount of energy. Consequently, researchers are exploring alternative material concepts that exhibit extended lifespans via self-restoration or recycling/reprocessing.¹²⁸

Building upon the aforementioned context, vitrimers stand as a distinct category of network materials with dynamic covalent bonds. Thus, on macroscopic timescales, the network connectivity remains intact during bond exchange in vitrimers, a remarkable characteristic that enables unique functionalities.^{29, 129}

The evolution of vitrimers has expanded the traditional classification of polymer materials (often categorized as either thermoplastic or thermoset), where vitrimers exhibit thermoset polymer-like mechanical properties/durability alongside thermoplastic-like malleability/processability simultaneously.¹³⁰ In essence, vitrimers amalgamate the benefits of both thermoset and thermoplastic polymers. Given the substantial volume of non-recyclable waste from thermoset polymer-based products, the promise of the vitrimer concept is exceedingly appealing, aligning with the growing need to create polymers with efficient recyclability, while mitigating CO₂ emissions and reducing petroleum resource consumption. The data in **Figure I14** indeed distinctly illustrates the rapid increase in publications on fibre-reinforced vitrimer composites over the past couple of years.

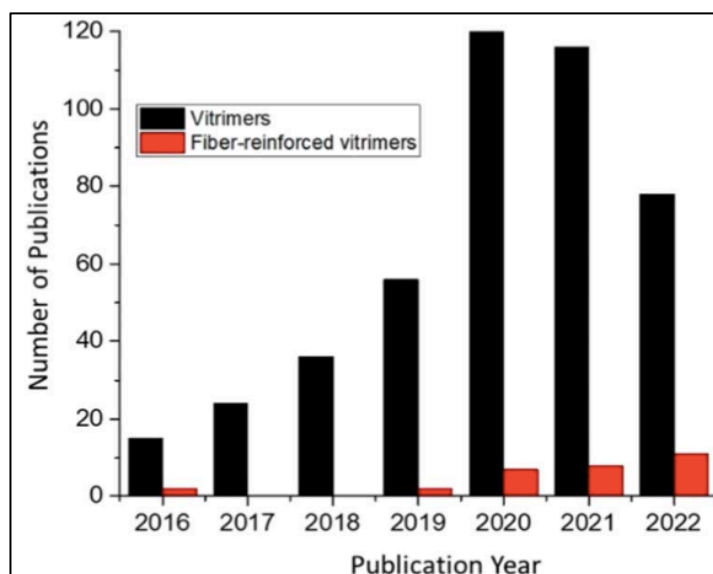


Figure I14. The number of published papers (according to Scopus, searching for fibre-reinforced composites and vitrimers in the title of the article).¹³¹

Thanks to a variety of bond-exchange chemistries, the group of adaptable covalent networks (ACNs) takes a courageous stride in bridging the divergence between thermoplastics and

thermosets. Drawing from their dynamic essence, numerous interchangeable chemical processes have been utilized in fabricating vitrimeric materials, with the most prevalent methods encompassing transesterification, transcarbamoylation, disulfide exchange, trans-amination of vinylous urethanes, transalkylation of triazolium salts, and amine imine exchange (commonly referred to as Schiff Chemistry).

However, there are only few examples in the literature of biobased alternatives. Liu et al.¹³² synthesized a biobased vitrimer resin for recyclable carbon fibre composites employing transesterification reactions using itaconic acid-based epoxy, glycerol and maleic anhydride. Even though, in this case, no catalyst was required for mechanical recycling of the resin, a long-time of 2 h and a high temperature of 190 °C had to be used for compression moulding. Moreover, a strong base (1 M NaOH aqueous solution) was used to degrade the vitrimer resin and recover the carbon fibre reinforcement from the composite. The vitrimer resin was not recovered most likely because of the presence of NaOH. Another vitrimer resin from tung oil was published by Li¹³³ and co-workers which presents similar drawbacks in addition to Zn catalyst used for transesterification. Generally, different authors are still using toxic compounds for the synthesis of the resin, such as catalyst, or acids and bases for the recycling. The large use of these chemicals could be problematic both for the mechanical properties of the final material and for the recycling since these chemicals are hard to separate from the vitrimer.

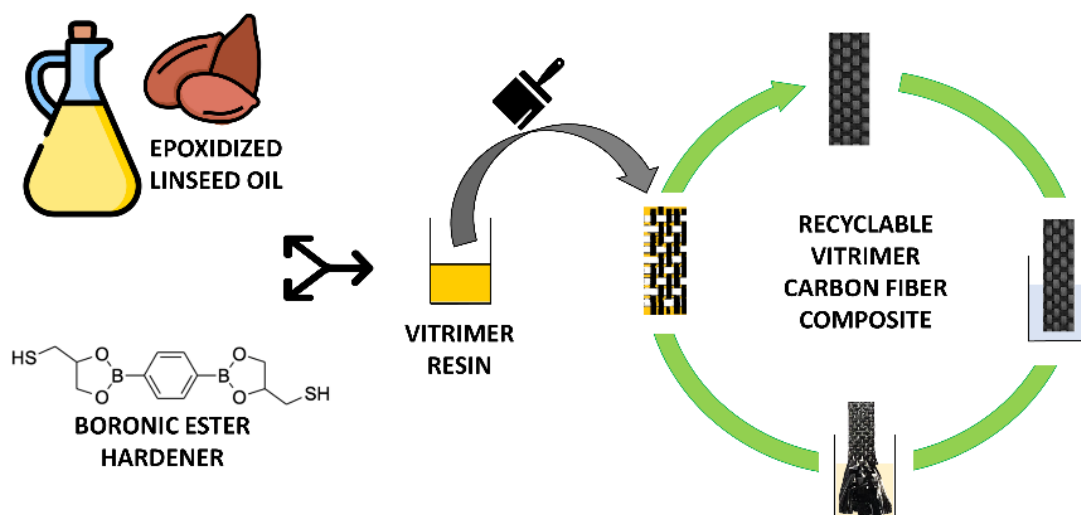
This thesis presents new vitrimer resins that can compete with commercial epoxy resins. To the best of knowledge, this is the first report on biobased vitrimer resin for carbon fibre-reinforced composites based on boronic esters.

1. Chapter I: ELO-DBEDT, a Boronic Ester Vitrimer from Epoxidized Linseed Oil for Recyclable Carbon-fiber Composites

Objectives

In this chapter the development of a new biobased vitrimer, synthesized from a vegetable oil and a boronic ester cross-linker is presented.

Using the vitrimer as a matrix, carbon fibre-reinforced composites, with mechanical performance similar to the ones prepared with a conventional epoxy resin, were obtained. Moreover, the composites could be conveniently recycled under mild conditions by reversible hydrolysis of the boronic ester crosslinks in 90% ethanol and subsequent solvent evaporation, regenerating both the carbon fibre reinforcement and the vitrimer matrix.



1.1 MATERIAL, METHODS, and MEASUREMENTS

1.1.1 Materials

Epoxidized linseed oil (ELO) under the trade name Lankroflex™ L with an average molecular weight of around 1150 g/mol and average number of epoxy groups per molecule of 5.6 (calculated based on the $^1\text{H NMR}$, **Figure 1.1**) was kindly provided by Valtris Specialty Chemicals (United Kingdom). C-Systems 10 10 CFS epoxy resin was purchased from Cecchi, Italy. 1-thioglycerol (97%), benzene-1,4-diboronic acid (95%), ethanol (EtOH, 96%), ethyl acetate (EtOAc), deuterated chloroform (CDCl_3) and deuterated DMSO (DMSO-d_6) were purchased from Merck. All materials were used as received unless otherwise stated. Environmentally friendly synthesis of [2,2'-(1,4-Phenylene)-bis[4-mercaptan-1,3,2-dioxaborolane](DiBoronic Ester DiThiol, DBEDT): Benzene-1,4-diboronic acid (20.00 g, 120 mmol) and thioglycerol (25.96 g, 240 mmol) were dissolved in ethanol (400 mL) and stirred for 24 hours at room temperature (RT). Subsequently ethanol was removed under reduced pressure to obtain the target compound as a white solid (37,40 g, 99%) (**Figure 1.1**).⁴⁸

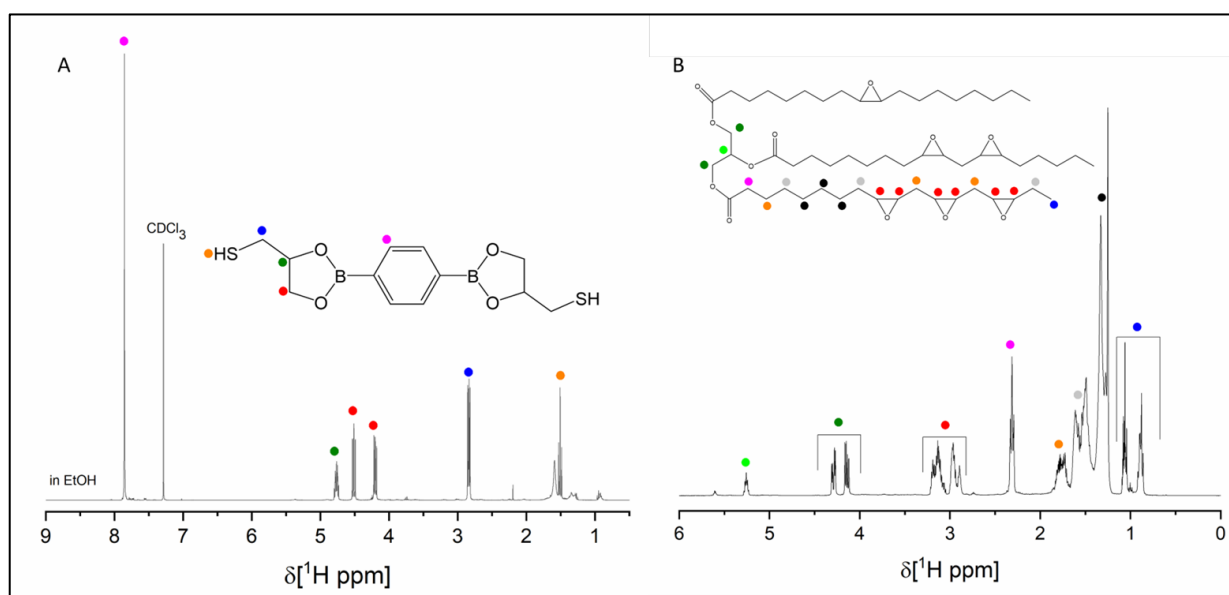


Figure 1.1 $^1\text{H NMR}$ spectra of DBEDT (A) and ELO (B) in CDCl_3 .

1.1.2 Methods

Typical procedure for ELO crosslinking: desired amount of ELO and a DBEDT (epoxide to thiol ratio of 1:1) were placed in a glass vial with a magnetic stirrer. The vial was closed and heated to 140 °C while stirring until the mixture became homogenous (around 15 min) after which it was poured into a Teflon mould and cured in an oven at 140 °C for 24 h.

Typical procedure for commercial epoxy resin crosslinking: desired amount of bisphenol A diglycidyl ether (BADGE) based pre-polymer and polyamine hardener (pre-polymer to hardener mass ratio of 2:1) were placed in an aluminium cap until the mixture became homogenous (around 2 min) after which it was poured into a Teflon mould and cured at RT for 24 h (**Figure 1.8A**).

Typical procedure for the fabrication of the composites: carbon fibre-reinforced composites were prepared by hand layup. Three carbon fibre layers with dimensions of 10 × 10 cm² were impregnated with 30 g of the commercial epoxy resin or the vitrimer resin using a spatula. The impregnated layers were overlapped, placed between two metal sheets with 9 kg

weigh on top to remove an excess resin and cured for 24 hours at RT, in case of the commercial epoxy resin, and at 140 °C in case of the vitrimer resin (**Figure 1.8A**).

1.1.3 Measurements

Infrared spectra were obtained with a single-reflection attenuated total reflection (ATR) accessory (MIRacle ATR, PIKE Technologies) coupled to a Fourier Transform Infrared (FTIR) spectrometer (Bruker Vertex 70V). All spectra were recorded under vacuum in the 4000–500 cm^{-1} range with a resolution of 4 cm^{-1} , accumulating 64 scans.

Raman spectra were recorded using a Horiba Jobin-Yvon μ Raman LabRaman HR800 spectrometer operating with a He-Ne laser source (632.8 nm). A 50 \times objective was used with a slit aperture of 200 μm .

^1H NMR analysis was carried out at room temperature using 5 mm tubes on an Avance III 400 MHz spectrometer, Bruker, equipped with a Broad Band Inverse probe (BBI). Chemical shifts are reported in ppm and were determined by reference to tetramethylsilane (TMS).

Gel fraction was determined to confirm the successful crosslinking. A small piece (\sim 200 mg) of a material was weighed and placed in a vial to which around 10 mL of ethyl acetate were added. The vial was closed and left for 24 h. Then the ethyl acetate was removed and the remaining undissolved part of the material was washed with ethyl acetate, dried under vacuum at 60 °C for 24 h, and weighed again. Gel fraction was calculated from the mass ratio of the polymer after and before exposing it to ethyl acetate.

Density was evaluated by cutting rectangular pieces for each sample, the vitrimer, commercial epoxy samples and their carbon fibre composites, measuring all the dimensions and weigh in on an analytical balance to measure their mass.

Tensile test was performed using a dual column Instron 3365 universal testing machine equipped with 2 KN load cell and pneumatic clamps. Dumbbell-shaped samples ISO 527-2 type 5A with a thickness of around 1 mm were cut out directly from cured matrices and composites.

Bending test was performed using a dual column Instron 3365 universal testing machine equipped with 2 KN load cell and a three-point bend fixture with a 10 mm anvil. Dumbbell-shaped samples ISO 527-2 type 5A with a thickness of 1 mm were cut out directly from matrices and composites.

Reprocessability tests were performed by compression moulding under 5 ton of pressure for 10 min at 160 °C using Carver 3853 CE press. The obtained sheets were cut into dog-bones and underwent the tensile test. After the first cycle, all the tested dog-bones and the residual pieces of the vitrimer went through compression moulding again, then were cut into dog-bones and were tested at the tensile tester again. This procedure was repeated for four times. At least five measurements were conducted for each sample and results were averaged to obtain a mean value. Both Young's modulus and elongation at break values were calculated using the built-in software of the tensile tester.

Recyclability of the vitrimer was evaluated by hydrolysis and dissolution of around 200 mg of vitrimer in 90% v/v EtOH overnight at 75 °C and subsequent film casting to regenerate the original vitrimer.

X-ray diffraction (XRD) was carried out on a Malvern-PANalytical 3rd generation Empyrean X-ray powder diffractometer. The instrument was equipped with a 1.8 kW $\text{CuK}\alpha$ ceramic X-ray tube operating at 45 kV and 40 mA, iCore and dCore automated modules and Pixcel 3D area detector. The diffraction patterns were collected in air at room temperature, in reflection parallel beam (PB) geometry and 2D acquisition mode, using a zero-diffraction silicon sample holder.

Differential scanning calorimetry (DSC) was performed using Discovery DSC 250, TA Instruments. The measurements were carried out at a heating and cooling rate of 10 °C/min

from 0°C to 200°C, with nitrogen as cell purge gas (50 ml/min). Glass transition temperatures were deduced from the second heating.

Thermogravimetric analysis (TGA) was performed on TGA Q 500, TA Instruments analyser under nitrogen atmosphere (flux: 50 ml/min) from 30 to 800 °C at a heating rate of 10 °C/min.

Optical microscopy images were taken with Leica DFC 420 optical microscope with a 20x magnification.

Scanning electron microscopy (SEM) analysis was conducted by JEOL JSM-6490LA scanning electron microscope (SEM), with an acceleration voltage of 10 kV with a 150x magnification.

DMTA/stress relaxation was performed using a DMTA TA Q800 in temperature sweep mode. Samples were tested in temperature sweeps from -50 to 150 °C with a heating rate of 2 °C min⁻¹. Experiments were performed in a single frequency oscillation mode with a frequency of 1 Hz and a displacement amplitude of 0.1% in auto tension offset control.

Biodegradability was assessed by measuring the biochemical oxygen demand (BOD) with OxiTop- IDS system. It was determined by monitoring the oxygen consumption in a closed bottle filled with 432 mL of seawater, as the single carbon source, and 200 mg of each sample. In particular, the seawater was chosen in order to mimic real environmental conditions, indeed it contains microorganisms and nutrients needed for their growth. Samples were tested in duplicate and the experiments were conducted at RT inside dark glass bottles hermetically closed with the OxiTop measuring head. Sodium hydroxide was used as a CO₂ scavenger to sequester carbon dioxide produced during biodegradation, and biotic consumption of the oxygen present in the free volume of the system was measured as a function of the decrease in pressure. Raw data of oxygen consumption (mg O₂/L) were corrected by subtracting the mean values of the blanks, obtained by measuring the oxygen consumption of the seawater in the absence of any test material. After this subtraction, values were normalized on the mass of the individual samples and referred to 100 mg of the material (mg O₂/100 mg).

1.2 RESULTS AND DISCUSSION

1.2.1 Design of the vitrimer resin

Following green chemistry principles, a solvent- and catalyst-free, vitrimer resin that at the end of its lifecycle does not generate any wastes or by-products was designed and developed. ELO was selected as a suitable vegetable oil for the synthesis of the vitrimer, since it has 5,6 epoxy groups per molecule that can participate in the crosslinking reaction with a diboronic ester dithiol (**Table appx. 1.2**). ELO was crosslinked through a thiol-epoxy click reaction between the epoxy groups and DBEDT in bulk (**Figure 1.2A**), by simply mixing the oil and a stoichiometric amount of the crosslinker with respect to the epoxy groups at 140 °C (**Figure 1.2B and Table appx. 1.2**). The synthesis did not require a solvent, because DBEDT is a white solid with a relatively low melting temperature of around 100 °C, which allows easy homogenization with the oil at a temperature above its melting point. Satisfyingly, after curing for 24 h at 140 °C, a transparent, yellowish, rigid material was obtained, shown in **Figure 1.2A**.

Commercial epoxy resin based on BADGE and a polyamine hardener was used as a reference to the vegetable oil based vitrimer resin. It was cured for 24 h at room temperature according to manufacturer's specification after which a rigid, transparent, greenish materials was obtained.

The difference between the vitrimer resin and the commercial epoxy resin is that the first contains dynamic crosslinks, capable of exchange reactions, enabling network rearrangements, whereas the second shows a permanent cross-linked network. At service temperatures, the

vitriimer behaves like a permanently crosslinked polymer, but at elevated temperatures the exchange reactions within its network speed up, making flow possible, while maintaining a constant number of chemical bonds and crosslinks (**Figure 1.2C**).

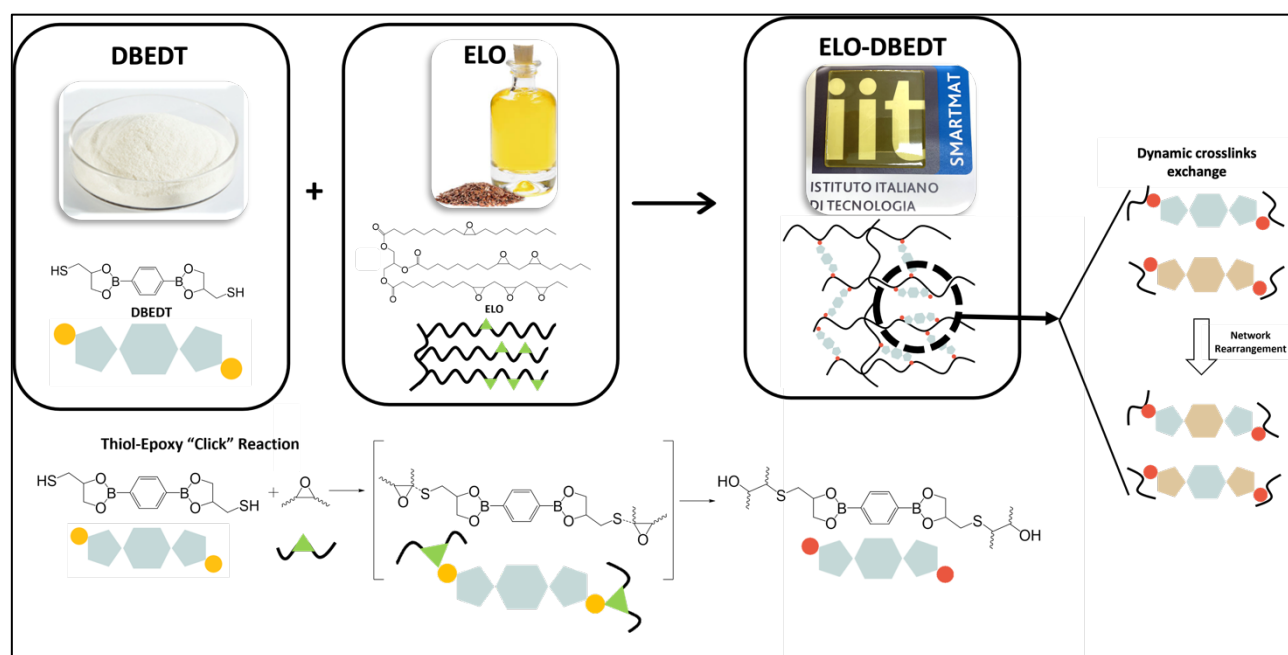


Figure 1.2 Schematic representation of the ELO-DBEDT vitriimer synthesis (A), the thiol-epoxy “click” reaction (B) and network rearrangement by boronic ester exchange (C).

Curing kinetics of the vitriimer resin at 140 °C was studied by measuring gel fraction at different time points and revealed that the plateau was reached after 15 hours indicating completion of the crosslinking reaction. However, the material was kept in the oven at 140 °C, for 24 h to ensure full curing (**Table appx. 1.1** and **Figure appx. 1.1**). The vitriimer precursors, ELO and DBEDT, as well as both components of the commercial epoxy resin, separately show high solubility in ethyl acetate, instead once cross-linked both the vitriimer (**Figure appx. 1.2A**) and the commercial epoxy (**Figure appx. 1.2A B**) were not soluble in ethyl acetate with high gel fractions of 88% and 100% respectively (**Table appx. 1.2** and **Table appx. 1.4**) proving a successful curing. The lower gel fraction of the vitriimer with respect to the commercial epoxy thermoset is most likely caused by the partial hydrolysis of boronic esters with traces of water present in the solvent.⁴⁸

1.2.2 Vitriimer characterization

Mechanical and thermomechanical performance

Materials were tested both in tension and bending in order to evaluate tensile and flexural mechanical properties. The typical stress strain curve (**Figure 1.3A**) in tension shows that the vitriimer has an average elastic modulus of 426 MPa, an average elongation at break of around 35%, and an ultimate strength of 23 MPa (**Figure 1.3B and 2C**). A tensile test was also conducted on the commercial epoxy (thermoset), to make a comparison in terms of mechanical properties. The commercial thermoset presents an average young modulus of 972 MPa, an average elongation at break of 9% and an ultimate strength of 54 MPa (**Figure 1.3B and 2C**). The thermoset shows more than double elastic modulus and ultimate strength, however, the vitriimer presents much higher elongation at break. Keeping in mind that the vitriimer is derived from a renewable vegetable oil, its obtained mechanical performance is very competitive.

In comparison, the flexural test resulted in significantly higher values both for the vitrimer and the epoxy resin. The vitrimer has an average flexural modulus of 846 MPa and a flexural strength of 27 MPa while the epoxy resin shows an average flexural modulus of 3.6 GPa and a flexural strength of 99 MPa (**Figure 1.3D, 2E and 2F**).

Both tension and bending testing apply tensile stresses to the samples which causes yielding and/or fracture, but the difference is the nature of the stresses. During a tensile test, the maximum tensile stresses are experienced throughout the entire volume of the specimen. In contrast, during bending the maximum tensile stresses are concentrated in a small region at the top surface above the neutral axis. Accordingly, for similar-sized test pieces, the tensile sample sees the maximum stresses throughout its entire gauge length, i.e., over a much larger volume than the corresponding bend sample. In brittle materials, which are highly sensitive to the defect population, this is reflected in strength and fracture properties measured in tensile tests being likely lower than the corresponding properties measured in bending, since there is a higher statistical probability of finding a larger defect in the first case.¹³⁴

Modulus obtained at RT from the DMTA measurements was found around 850 MPa for the vitrimer (**Figure 1.3G**) and around 3.5 GPa for the commercial epoxy, which is in a good agreement with the results obtained from the bending test. The glass transition temperature of the vitrimer was about 49 °C and for the commercial epoxy around 60 °C (**Figure appx. 1.3**). Moreover, for both materials a rubbery modulus was observed after the glass transition typical for covalently crosslinked materials^{135, 136} (**Figure 1.3G**).

Common polymers like thermoplastics and thermosets have characteristic transition temperatures such as glass transition temperature (T_g) and melting point (T_m), which provide an indication on the service and processing temperature windows. Vitrimers possess another characteristic transition temperature, called topology freezing transition temperature (T_v), which is also extremely important. Indeed, it indicates the upper temperature limit for use and lower temperature limit for reprocessability. Above T_v , exchangeable reactions happen fast and a vitrimer is able to be reprocessed and recycled, below T_v exchangeable reactions are slow and a vitrimer is similar to the traditional thermoset.¹³⁷ The T_v of the vitrimer presented in this work is -55 °C and is only theoretical since it is much lower than the glass transition temperature ($T_g = 49$ °C). This means that even though the boronic ester exchange reactions could occur at temperature below the T_g , they are frozen due to restricted chain mobility. Above the T_g , segmental motion is slowly initiated while the exchange reactions are already fast, therefore the network rearrangement is controlled by the segmental motion and that is reflected by a rapid viscosity decrease. Increasing the temperature, the exchange reactions dominate the network rearrangements and the viscosity decreases even lower, following the Arrhenius law (**Figure appx. 1.4**).^{48, 138, 139}

Furthermore, as it is clearly shown in **Figure 1.3H** the relaxation rate is increased with temperature, therefore in good agreement with the Arrhenius law, because the relaxation process is essentially controlled by the boronic ester exchange, process that is accelerated at a higher temperature (**Figure appx. 1.4**). Indeed, the vitrimer rapidly relaxes stress at all tested temperatures (100-140 °C) (**Figure appx. 1.5**), for example the characteristic relaxation time τ^* at 100 °C is 109 s. In addition, the activation energy (E_a) of the vitrimer is 39.5 KJ/mol and it is in a good agreement with the previously reported values. Indeed, in a previous work based on ESOA vitrimer synthesized using the same cross-linker, it showed an E_a of 29 KJ/mol.⁴⁸ Additionally Chen et al.¹⁴⁰ and Breuillac et al.⁹⁴ synthesized vitrimers with E_a from 7.7 to 13.8 KJ/mol and 32.5 and 38.9 KJ/mol using again the same boronic ester chemistry. On the contrary, the commercial epoxy presents a relaxation modulus fairly constant since it does not relax any stress due to the permanent crosslinked network which does not allow any rearrangements.

TGA confirmed that the vitrimer does not decompose to volatile compounds up to around 300 °C, which is another evidence about its stability. Instead, the commercial epoxy starts to lose mass at 150 °C (**Figure appx. 1.6**), that might be due to the evaporation of some additives present inside the resin that do not participate in the crosslinking. The DSC measurements show that the vitrimer presents a T_g of 49 °C, a bit lower than the commercial epoxy that has a T_g of 63 °C (**Figure appx. 1.3**), confirming the results obtained from the DMA measurements. Moreover, the evaluation of the density of both materials resulted in a value of around 1.15 g/cm³ for the vitrimer, and around 1.13 g/cm³ for the commercial epoxy (**Table appx. 1.3**).

Biodegradability

The vitrimer starts to biodegrade after just 3 days in seawater and within a month, the BOD reaches values of 11 mg O₂/100 mg material. This slight initial delay in the biodegradation of the vitrimer can be ascribed to the presence of boronic ester cross-links that need to undergo hydrolysis first before the biodegradation becomes possible. To compare the biodegradability of the material with a reference we report the biodegradability curve of a cotton fabric (in grey) which, reached 12.5mg O₂/100 mg material after 30 days, therefore the vitrimer biodegrades almost as fast as the cotton fabric. The ELO and the vitrimer show different rate of biodegradability, which could be explained by the fact that the vitrimer is a solid and crosslinked material therefore it requires more time to be degraded (**Figure 1.3.I**). To the best of the knowledge, this is one of the first studies about biodegradability of vitrimers and the developed vitrimer itself is one of the first examples of biodegradable vitrimers.

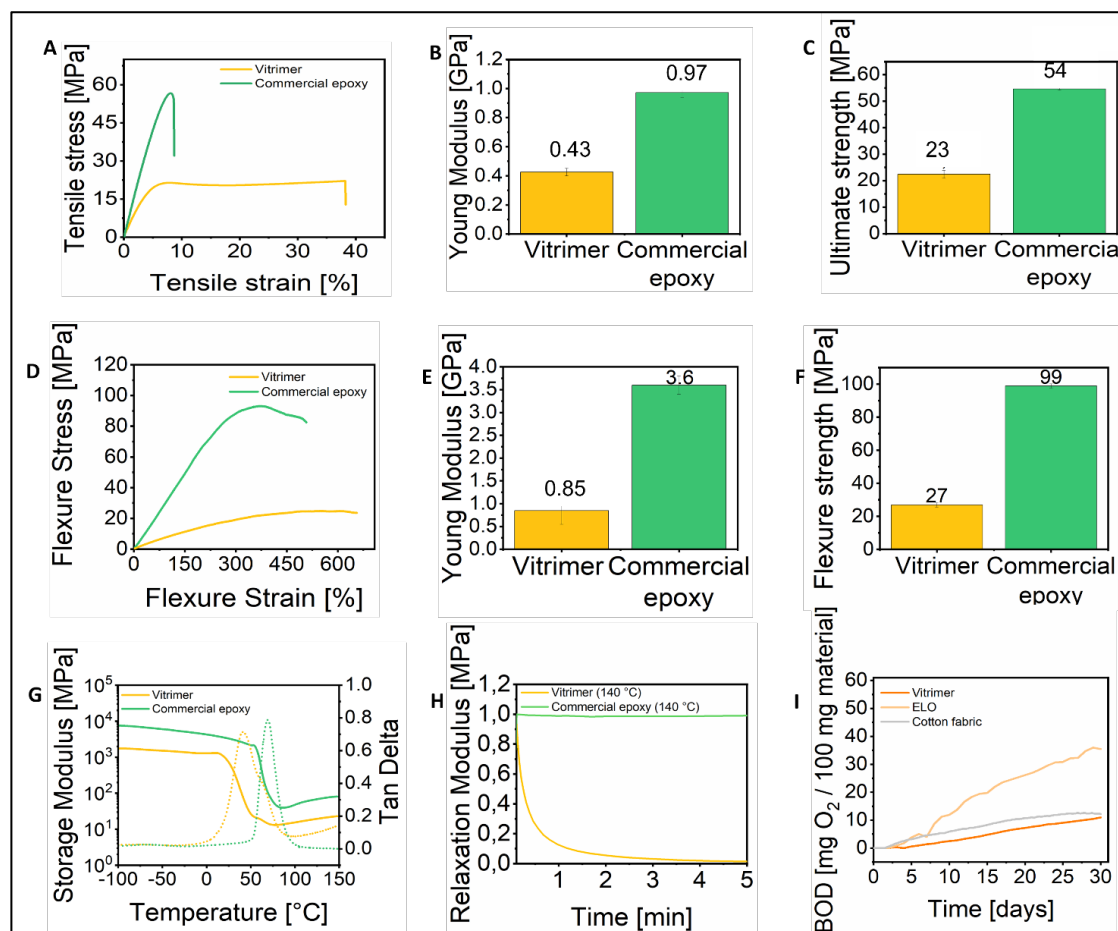


Figure 1.3 Typical tensile curve (A), young modulus (B) and flexural strength (C) of vitrimer and commercial epoxy; typical flexural curve (D), young modulus (E) and flexural strength (F) of vitrimer and commercial epoxy; DMTA (G) and stress relaxation curves of vitrimer and commercial epoxy (H); BOD of the ELO, vitrimer and cotton fabric as a reference (I).

1.2.3 Shape memory effect

The presence of the dynamic boronic ester network is responsible for the vitrimer shape memory behaviour and gives a possibility to change both temporary and permanent shapes of the material. To enable reshaping of the vitrimer, it has to be heated above its glass transition temperature to make it soft. When a low temperature and heating time is used (90 °C for 60 s), the vitrimer does not have enough time to relax all the stress induced by putting it into a new shape (from flat shape - permanent shape n°1 into a helix - temporary shape n°1). This new shape is only temporary since it is maintained by cooling the vitrimer below its T_g immediately after the reshaping (**Figure 1.4A1-A3**). The original flat shape can be recovered by reheating it to 90 °C for 5 min thanks to the remaining stress (**Figure 1.4A4**).¹⁴¹ The shape change was reversible and could be repeated several times using different permanent shapes. Since the commercial epoxy is not able to relax stress due to the presence of the static covalent network it also shows the shape memory effect as the vitrimer however, it can just change the temporary shape. (**Figure 1.4B**).

Indeed, the difference between a vitrimer and a conventional epoxy is that given enough energy and time the vitrimer can fully relax the stress induced by the reshaping and therefore it is possible to also change its permanent shape (given during the curing process). Increasing the temperature to 120 °C and the heating time to 15 min, the permanent shape could be changed from flat to spiral (permanent shape n°2). This new permanent shape could be restored after giving the sample a different temporary shape (“U” shape – temporary shape n°2) by heating it at 90 °C for 60 s (**Figure 1.4A4-A8**).

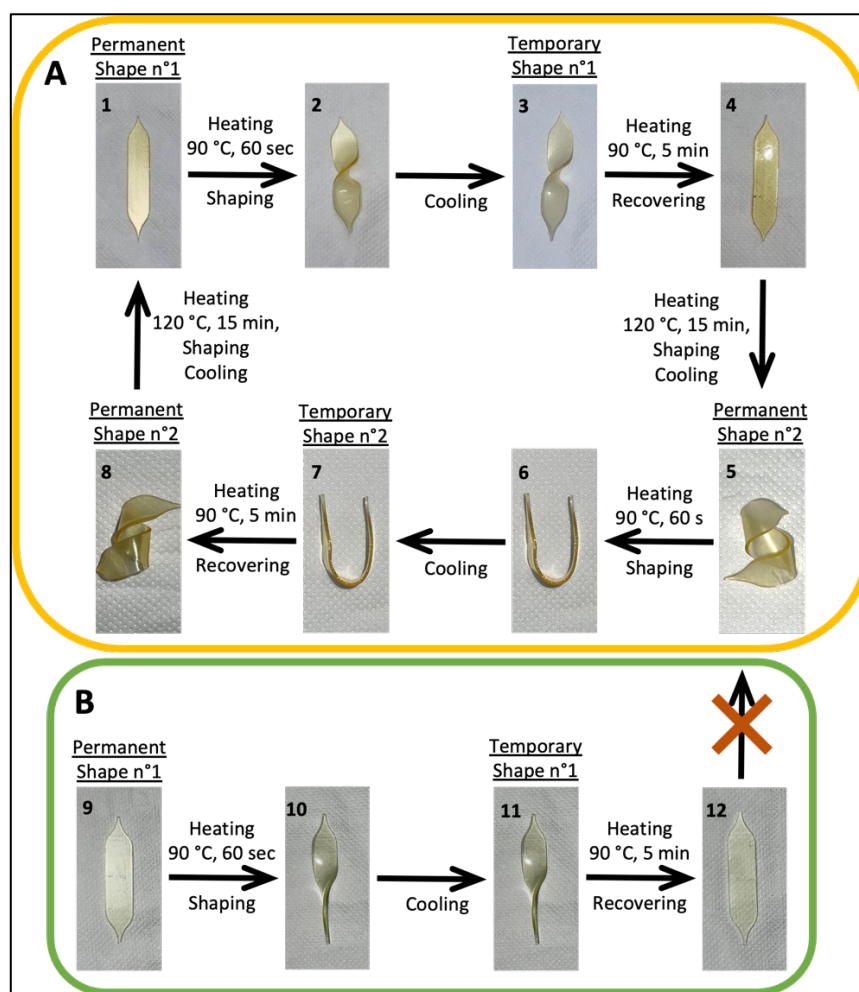


Figure 1.4 Shape memory effect of the vitrimer (A) and the commercial epoxy (B)

1.2.4 Vitriimer recycling

Commonly, recycling of polymeric materials can be divided into two main categories: mechanical, and chemical. Mechanical recycling allows obtaining polymers through mechanical processes. Thermoplastic polymers can be ground and then reworked using typical melting techniques such as, injection or compression moulding. On the other hand, thermoset materials can be ground into small particles and used only as fillers, a process that cannot be considered recycling, since the material is not reprocessable anymore after the curing, but downcycling. Chemical recycling allows the recovery of the chemicals for new synthesis of virgin polymers, mixtures of monomers or low molecular weight gases for energy recovery, but it is mainly limited to condensation polymers. This proposal for the new dynamic thermoset vitriimer resin offers the possibility to overcome all these issues and allows for both mechanical and chemical recycling, as described below.¹⁴²⁻¹⁴⁵

Mechanical recycling

The vitriimer could be recycled mechanically and could be processed using techniques typically employed for thermoplastic materials. In particular, a two-step process was used, consisting of grinding the matrix and subsequent compression moulding of the pieces to obtain a “second generation” material (**Figure 1.6A**).

The reprocessability of the vitriimer was evaluated by compression moulding followed by characterization after each processing cycle (analytically described in the experimental part), like tensile tests, DMA, gel fraction, and FT-IR. The vitriimer could be easily processed by compression moulding at 160 °C for 10 min under 3 tons of pressure, into transparent sheets. After the initial tensile testing of the virgin material, it was ground and compression moulded, up to four times. After each reprocessing step, tensile test, gel fraction and FT-IR were performed to prove that the material did not deteriorate. Even after reprocessing the vitriimer four times, no significant changes in mechanical performance (**Figure 1.5**), crosslink density (**Table appx. 1.5** and **Table appx. 1.6**) or chemical structure (**Figure appx. 1.7**) were observed, demonstrating the reprocessability, dynamic nature and robustness of the developed vegetable oil based boronic ester vitriimer.

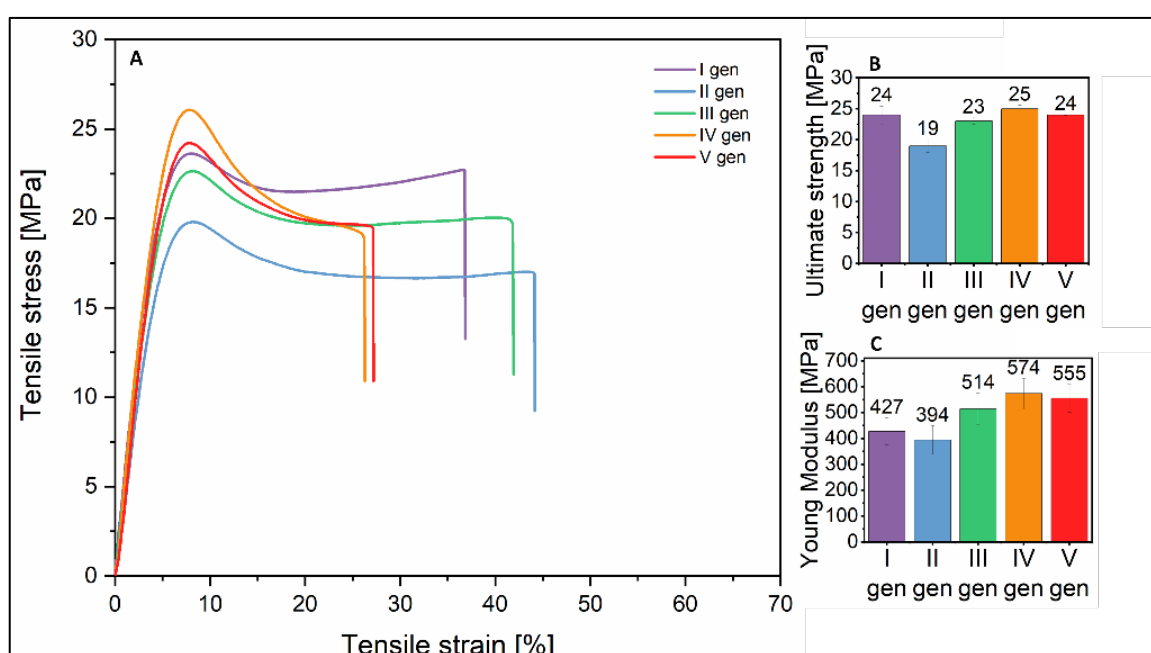


Figure 1.5 Typical tensile curve (A), ultimate strength (B) and Young Modulus (C) of the virgin (I gen) and the reprocessed (II-V gen) vitriimer.

As expected, it was not possible to reprocess the commercial epoxy since it is a thermoset. When the material was subjected to compression moulding it just broke to small pieces that did not fuse together under the tested conditions. (**Figure 1.6B**).

DMTA measurements on the four times recycled vitrimer showed that the modulus remained constant presenting the same values of around 850 MPa both for the virgin and reprocessed materials (**Figure appx. 1.8**). Therefore, it is possible to conclude that the material keeps the thermomechanical properties fairly constant for at least 4 reprocessing cycles.

TGA confirmed that the recycled vitrimer does not decompose to volatile compounds up to around 300 °C, indeed there is no difference in the TGA analysis between the virgin vitrimer and the recycled vitrimer (chemically and mechanically) (**Figure appx. 1.6**) which is another evidence about the stability of the vitrimer.

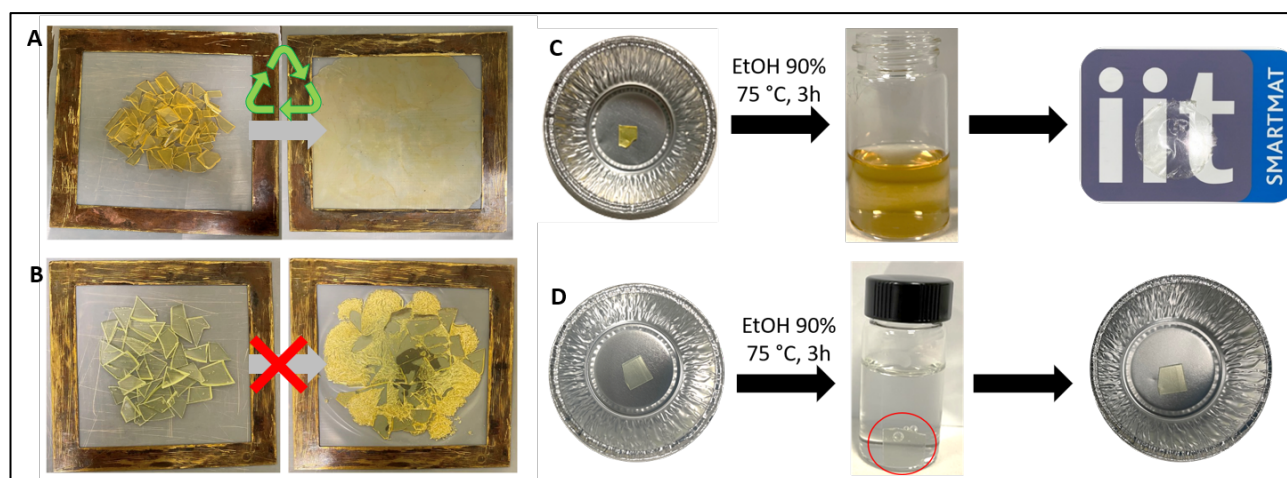


Figure 1.6 Mechanically recycled vitrimer (A) and unsuccessful attempt to mechanically recycle the commercial epoxy (B) under 5 ton of pressure for 10 min at 160 °C; Chemical recycling of the vitrimer by hydrolysis and dissolution in 90% v/v ethanol at 75 °C for 3 h and subsequent solvent casting to regenerate the vitrimer as a thin, transparent film (C) and unsuccessful attempt to chemically recycle commercial epoxy (D).

Chemical recycling

Similarly to conventional epoxy matrix, the vitrimer resin showed good resistance to different organic solvents such as tetrahydrofuran (THF), isopropanol and acetone. However, since signs of hydrolysis have been observed during the gel fraction test of the boronic ester vitrimer, we further exploited it to fully hydrolyse and dissolve the material in 90% v/v ethanol as a green solvent, recovering it for recycling purposes.^{146, 147} The dissolution of the vitrimer took place at RT but proceeded quite slowly. By heating the mixture to 75 °C the dissolution was accelerated and after 3h it was completely concluded. Heating the material above the T_g had an additional benefit of making it softer and much easier to dissolve. It was possible to dissolve 1 g of material in 25 ml of the solvent and FT-IR measurements confirmed that it was possible to fully recover the solid material by a simple casting of the hydrolysed solution (**Figure 1.6** and **Figure appx. 1.9**). In addition, it was possible to record a ^1H NMR of the vitrimer dissolved in aqueous DMSO- d_6 which confirmed that indeed the hydrolysis of boronic esters is responsible for the dissolution of the vitrimer as free benzene diboronic acid and free hydroxyl groups of thioglycerol were detected (**Figure 1.7**). Moreover, no free thiol groups of DBEDT crosslinker and no epoxy groups of ELO were visible, which confirms successful crosslinking through the thiol-epoxy reaction. On the other hand, for the commercial epoxy the chemical recycling was not possible since it did not dissolve in 90% v/v ethanol (**Figure 1.6D**).

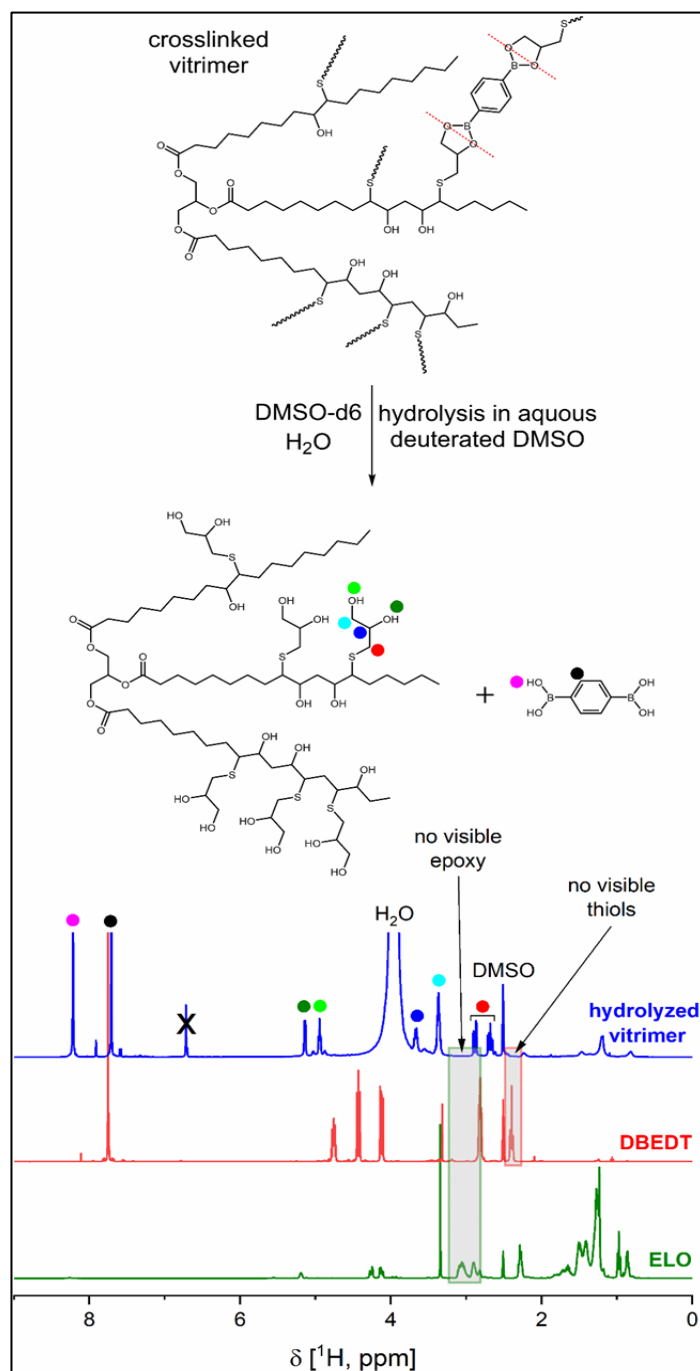


Figure 1.7. ^1H NMR spectra of ELO (DMSO- d_6), DBEDT (DMSO- d_6) and ELO-DBEDT vitrimer hydrolysed in aqueous DMSO- d_6 . Assignment of signals corresponding to ELO reacted with thioglycerol present after the hydrolysis is omitted for clarity since they are broad and not clearly visible in the spectrum.

Employing this method, a boronic ester vitrimer used as a matrix in a composite can be easily separated, purified, regenerated and reused, a process that normally is not possible for traditional thermosets, like epoxy resins.

1.2.5 Carbon fibre composite preparation and characterization

The carbon fibre composites with three carbon fibre layers were prepared by hand layup as described in the experimental section. Only flexural properties of the composites were evaluated since in tension test specimens were slipping out of the clamps. The vitrimer composites presented an average elastic modulus of 20 GPa and a flexure strength of 220 MPa while the commercial epoxy composite had an average elastic modulus of 23 GPa and a flexural strength

of 280 MPa (**Figure 1.8L, M and N**). Young's moduli for both the composites are pretty similar since the reinforcement carries the greatest part of the load, and the function of the resin is to keep the composite together. Thanks to that, using a vegetable oil based vitrimer resin, it was possible to fabricate a carbon fibre composite with very similar mechanical performance to the composite fabricated with the commercial epoxy resin.

In order to evaluate the impregnation capability of the vitrimer and the commercial epoxy resin as well as the quality of the fabricated composites, SEM and optical microscopy were employed. Images of the top and inner layers (**Figure 1.8B and D**) and of the cross-section (**Figure 1.8C and E**) revealed an excellent interfacial bonding between the carbon fibres and the matrices. Indeed, both resins (vitrimer and commercial epoxy resin) wet the carbon fibres very well, ensuring a good impregnation and adhesion between the layers and, as a consequence high flexural strength for both composites. Moreover, no exfoliation or slippage between the carbon fibre and the matrix was observed for both composites after the flexural test since the polymer matrix adhered tightly onto the surface of carbon fibre, as shown by the SEM images of the fracture surface (**Figure 1.8F-I**). The TGA analysis showed that for the commercial epoxy composite the percentage of the matrix (epoxy resin) was 60% and for the reinforcement (carbon fibres) was 40%, instead for the vitrimer composite the percentage of the matrix (vitrimer) was 40% and for the reinforcement (carbon fibres) was 60%, (**Figure appx. 1.10 and Figure appx. 1.11 and Figure appx. 1.12**). In addition, since the densities of both the matrices (vitrimer and commercial epoxy) are quite close, the densities of both the composites are pretty similar too (**Table appx. 1.3**).

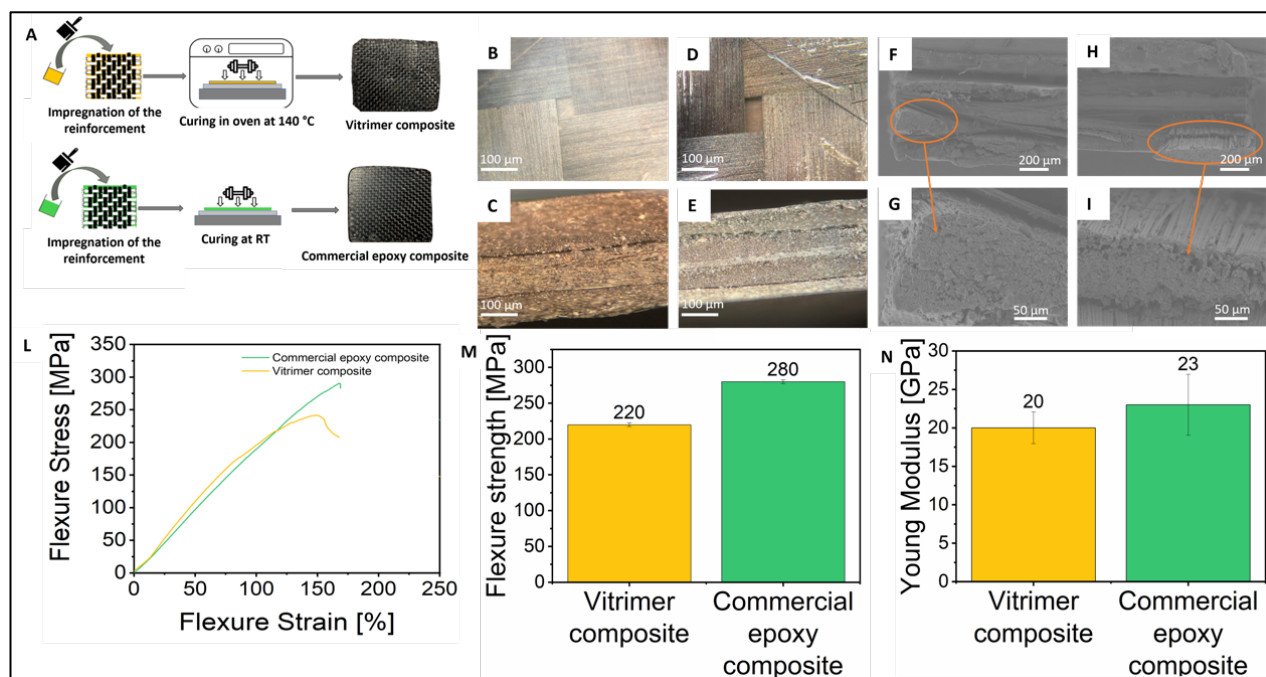


Figure 1.8 Fabrication of the carbon fibre-reinforced composites (A); Optical microscope images of the top surface and the cross-section of the vitrimer composite (B-C) and commercial epoxy composite (D-E); SEM images of the cross-section of the vitrimer composite (F-G) and the commercial epoxy composite (H-I); Typical flexural curve (L), flexure strength (M) and Young Modulus (N) of the vitrimer composite and the commercial epoxy composite.

1.2.6 Composites recycling

Recycling carbon fibres (CF) from the composites without compromising their chemical structure, mechanical properties and micro morphology is a current challenge.¹⁴⁸ Therefore, a recyclability attempt was conducted on both the epoxy and vitrimer composites (**Figure 1.9A**).

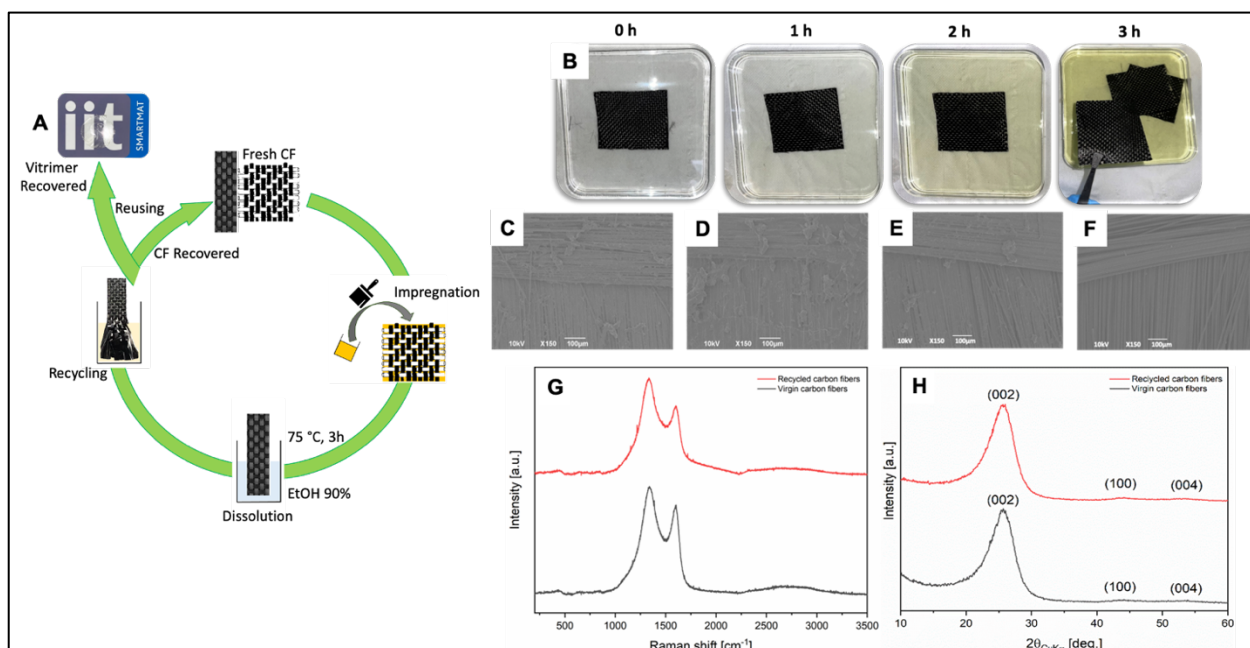


Figure 1.9 Recyclability scheme of the vitrimer composite (A); digital images showing dissolution progress of the matrix in the vitrimer composite. (B); SEM images of fresh and recycled carbon fibre at different time of the process, C:0h, D:1h, E:2h and F:3h; Raman spectra of the virgin and recycled carbon fibres(G) and X-ray diffraction patterns of the virgin and recycled carbon fibres (H).

As mentioned before, the commercial epoxy did not dissolve in EtOH 90% v/v due to its thermosetting nature and therefore it was not possible to recycle the composite and recover the carbon fibres. (**Figure appx. 1.13**).

Thanks to the hydrolysis of the boronic ester crosslinks and subsequent dissolution of the vitrimer resin it was possible to efficiently recycle the vitrimer composite under very mild conditions. The vitrimer composite was placed in EtOH 90% v/v solution at 75 °C and just after 3 h the carbon fibre layers could be easily separated, washed with fresh EtOH 90% v/v to remove any vitrimer residues and dried under ambient conditions. The vitrimer itself could be regenerated as well by simple evaporation of the solvent. Using this recycling method more than 99% of the carbon fibre and vitrimer matrix were recovered (**Table appx. 1.7**).

After the chemical recycling of the vitrimer composite the carbon fibres were recovered and the surface morphology and mechanical properties were further determined by SEM and the bending test. The SEM analysis showed that the morphology of the recovered carbon fibres was indistinguishable from the pristine ones, illustrating the effectiveness of the recycling process. Besides, it was notable that the recycled carbon fibres did not have any vitrimer residues attached (**Figure 1.9C-D**). Moreover, the recycled carbon fibres were analysed by XRD and Raman spectroscopy and the results showed no change in comparison to the new carbon fibres (**Figure 1.9G and H**).

Subsequently, a new composite was prepared reusing the recovered reinforcements using a new vitrimer resin and tested under flexion. The flexural stress-strain curves (**Figure appx. 1.14**) of the pristine vitrimer composite and the recycled vitrimer composite were almost the same, indicating that carbon fibres in the vitrimer composite could be recycled without destroying the fibres' structure and compromising their mechanical properties. The recycling of CF without sacrificing performance characteristics will bring huge economic benefits considering their high cost.

1.3 CONCLUSIONS

An environmentally friendly synthesis of a biobased vitrimer by thiol-epoxy coupling between epoxidized linseed oil (ELO) and dynamic cross-linker DBEDT in a solvent- and catalyst-free process following green chemistry principles was presented. The tensile and bending test on the vitrimer showed satisfying results in comparison to a commercial epoxy resin, taking into account that the vitrimer is made of a vegetable oil. Moreover, it was demonstrated that the vitrimer exhibits a shape memory effect and thanks to its dynamic nature not only a temporary shape could be changed and recovered like for a conventional thermoset but also, thanks to the dynamic boronic ester bonds, a new permanent shape could be programmed by using higher temperature and longer reshaping time.

The vitrimer showed an excellent mechanical recyclability using techniques typically employed for thermoplastics and could be chemically recycled as well by hydrolysis in ethanol and subsequent solvent casting to regenerate the original material under mild conditions. Moreover, the vitrimer was found to be biodegradable in sea water preventing any possible waste accumulation, in case it accidentally ends up in the marine environment.

Carbon fibre composites fabricated with the vitrimer resin had a very similar mechanical performance and density to the ones made with commercial epoxy resin. When the vitrimer was employed as a matrix in the carbon fibre composite, it was possible to fully recover the reinforcement layers, which is especially important for carbon fibres since they have high costs.

Therefore, the developed composite made of carbon fibres and sustainable biobased vitrimer can solve most problems regarding traditional thermoset composites, since it is made from renewable resources, allows for the recovery of the reinforcement under mild condition and can be repaired, reused and recycled multiple times, keeping the same mechanical performance.

1.4 APPENDIX

Design of the vitrimer resin

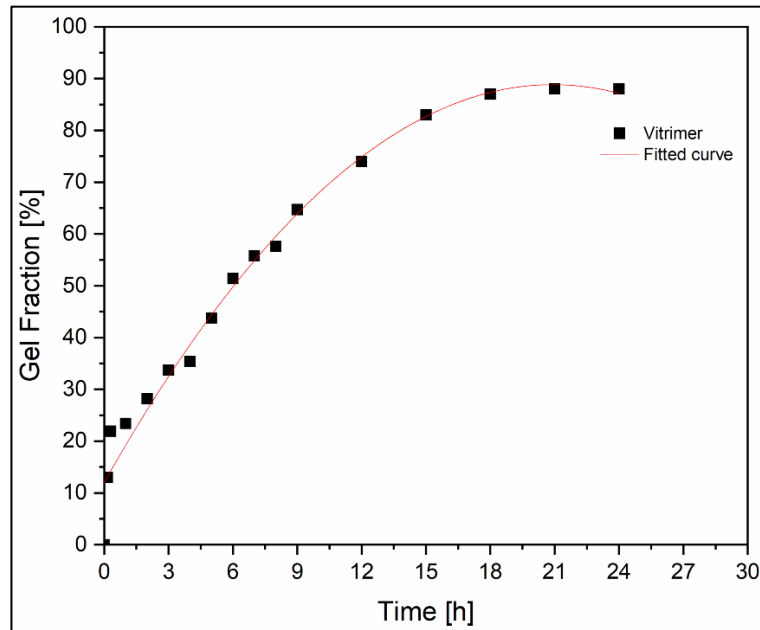


Figure appx. 1.1 Gel fraction of vitrimer at different curing times.

Table appx. 1.1. Gel fraction of the vitrimer at different curing times.

Material (vitrimer)	Before [mg]	After [mg]	Gel fraction [%]
1 h	201,3	47,10	23,4
2 h	200,0	56,60	28,3
3 h	205,3	69,40	33,8
4 h	200,0	70,80	35,4
5 h	202,2	88,50	43,8
6h	205,8	105,9	51,5
7h	201,2	112,3	55,8
8h	201,6	115,3	57,2
9h	209,2	135,3	64,7
12h	199,7	147,8	74,0
15h	201,4	167,1	83,0
18h	199,6	173,7	87,0
21h	202,4	178,1	88,0

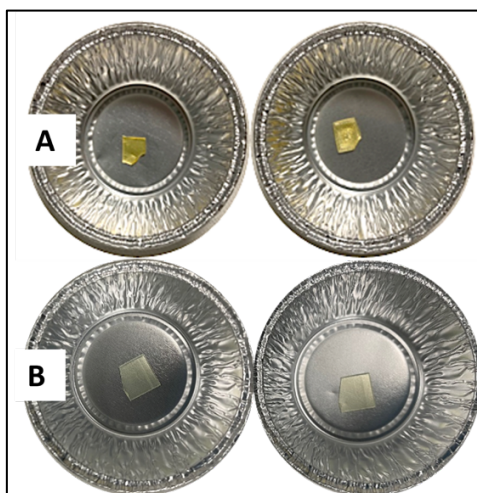


Figure appx. 1.2. Samples of the vitrimer (A) and the commercial epoxy (B) before (left) and after (right) the gel fraction test.

Table appx. 1.4. Gel fraction of the vitrimer and the commercial epoxy.

Material	Before [mg]	After [mg]	Gel fraction [%]
vitrimer	200,6	176,5	88,0
Thermoset Commercial epoxy	201,3	200,5	99,6

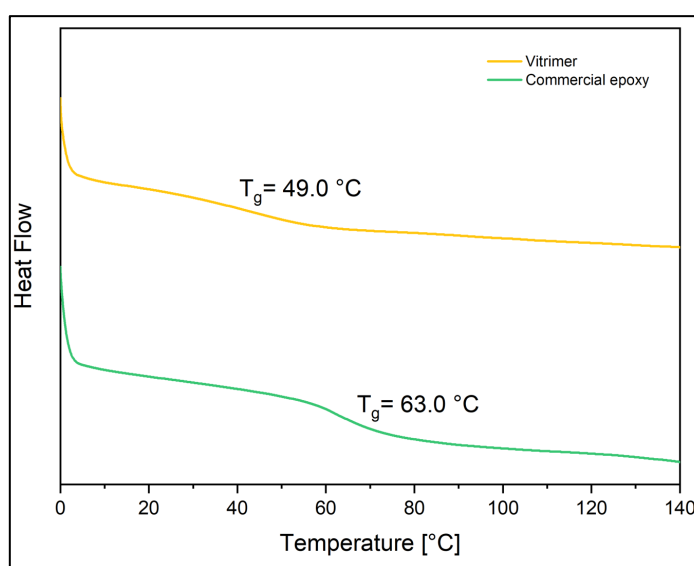


Figure appx. 1.3. DSC curves of the vitrimer and the commercial epoxy.

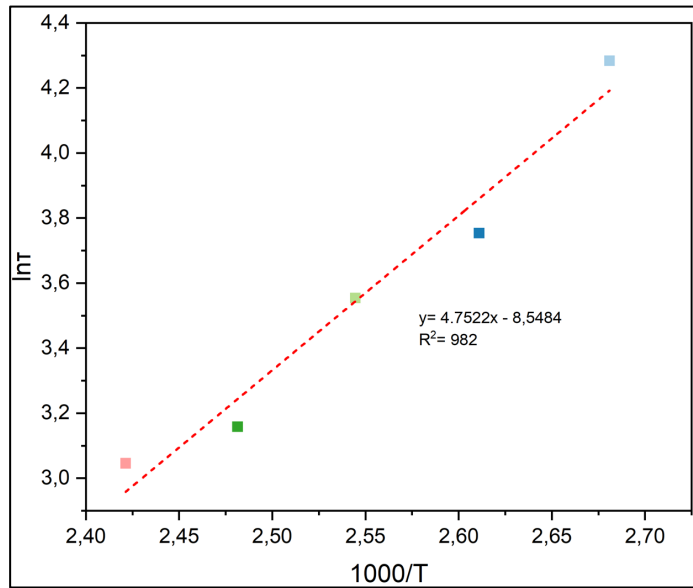


Figure appx. 1.4. Arrhenius plot of relaxation times of the vitrimer.

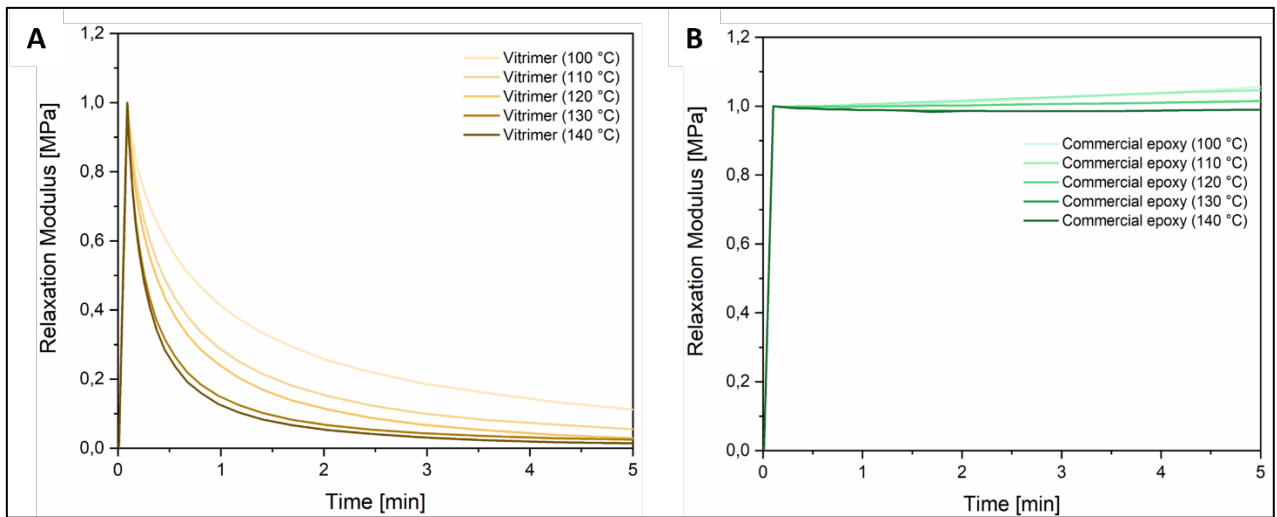


Figure appx. 1.5. Stress relaxation curves of vitrimer (A) and commercial epoxy (B).

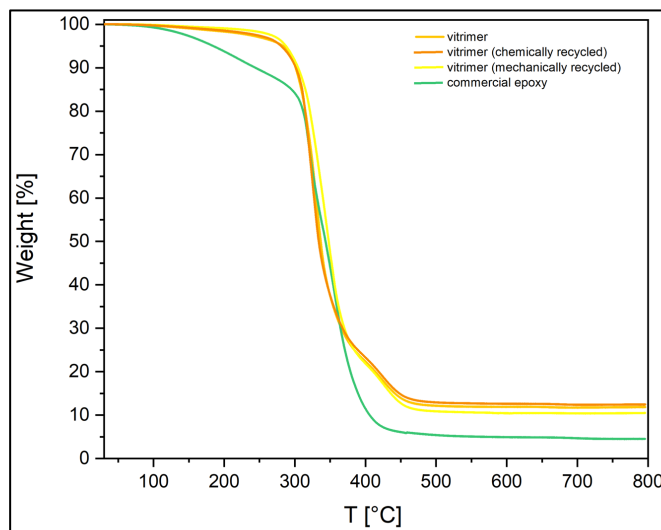


Figure appx. 1.6. TGA curves of virgin (dark yellow) and recycled (orange and light yellow) vitrimer and commercial epoxy (green).

Vitrimer recycling

Reprocessability (mechanically recycling)

Table appx. 1.5. Gel fraction, thermal stability and mechanical performance of the virgin and the reprocessed vitrimer.

Material (vitrimer)	Gel Fraction [%]	T_g (DSC) [°C]	Young Modulus (Tensile test) [MPa]
I Gen (Virgin Material)	88	49,0	426
II Gen	85	49,0	394
III Gen	87	49,0	514
IV Gen	88	49,0	574
V Gen	88	49,0	555

Table appx. 1.6. Gel fraction of the virgin vitrimer and reprocessed up to 4 times.

Material (vitrimer)	Before [mg]	After [mg]	Gel fraction [%]
I Gen (Virgin Material)	200,6	176,5	88,0
II Gen	203,9	173,3	85,0
III Gen	198,7	172,9	87,0
IV Gen	203,4	178,9	88,0
V Gen	204,3	179,7	88,0

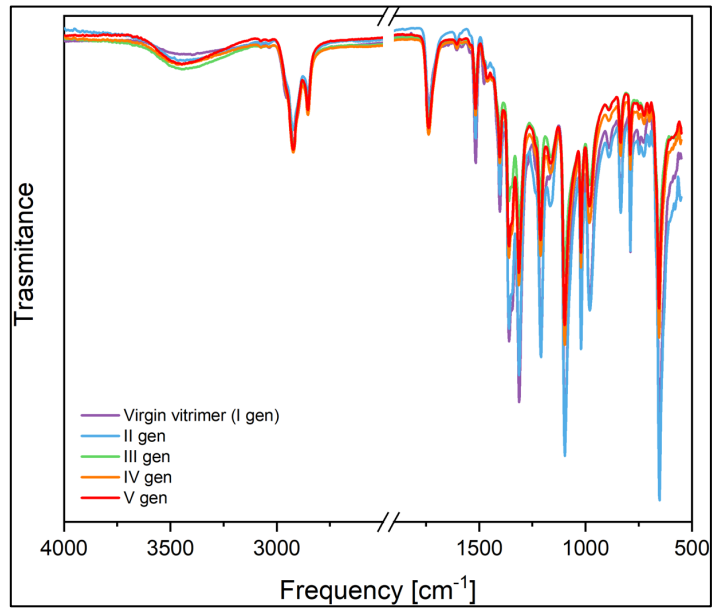


Figure appx. 1.7. FT-IR spectra of the of the virgin vitrimer and reprocessed up to 4 times.

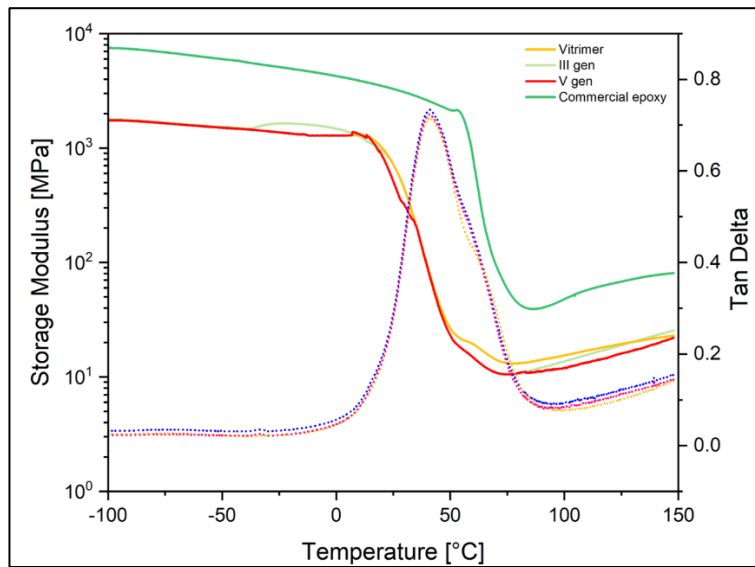


Figure appx. 1.8. DMTA curves of virgin (I gen) and reprocessed (III-V gen) vitrimer and commercial resin.

Recycling (chemical recycling)

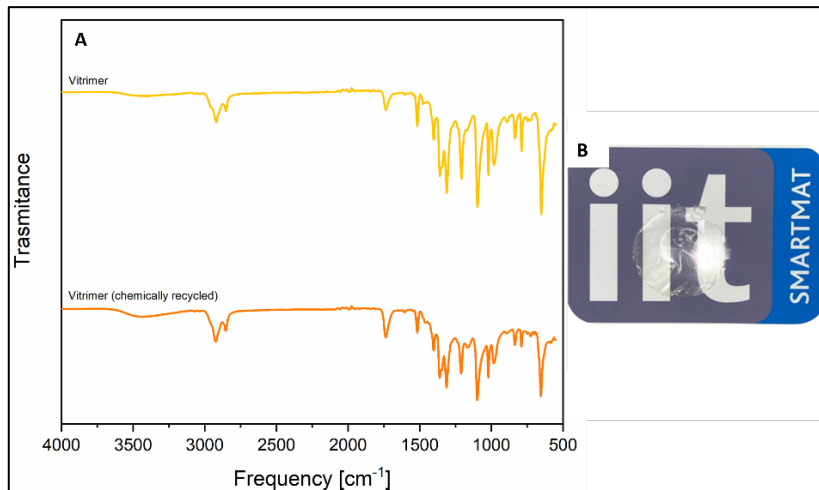


Figure appx. 1.9. FT-IR spectra of vitrimer as synthesized and after hydrolysis, dissolution in 90% v/v EtOH and casting.

Composites Recycling

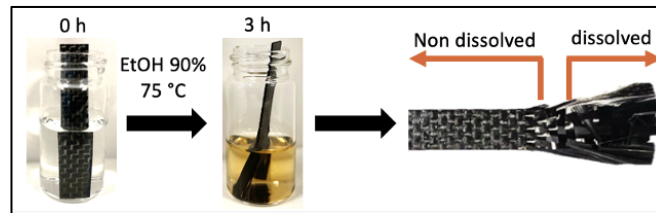


Figure appx. 1.10. Partial dissolution of the vitrimer matrix in 90% EtOH solution, where the carbon fibre in contact with the solution was separated from the resin.

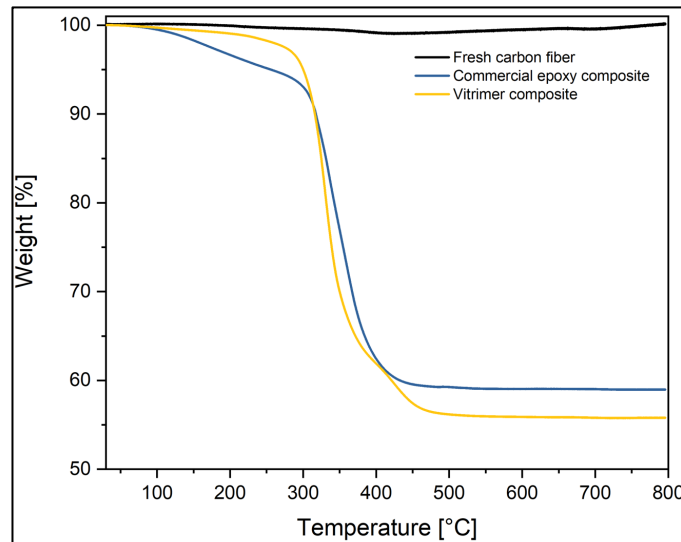


Figure appx. 1.11 TGA curves of the fresh carbon fibre (black), vitrimer composite (yellow) and commercial epoxy composite (blue).

Reinforcement: 100%
 Vitrimer residue: 15%
 Vitrimer Composite residue: 50%
 Epoxy residue: 5%
 Epoxy composite residue: 60%

x = content of the matrix
 $(1 - x)$ = content of the reinforcement

Epoxy composite: $0,6 = x \cdot 0,05 + (1 - x) \cdot 1 \rightarrow 0,6 = 0,05x - 1x + 1 \rightarrow 0,95x = 0,4 \rightarrow x \sim 0,4 \rightarrow 40\%$ matrix

Vitrimer composite $0,5 = x \cdot 0,15 + (1 - x) \cdot 1 \rightarrow 0,5 = 0,15x - 1x + 1 \rightarrow 0,85x = 0,5 \rightarrow x \sim 0,6 \rightarrow 60\%$ matrix

Figure appx. 1.12 Matrix and reinforcement content

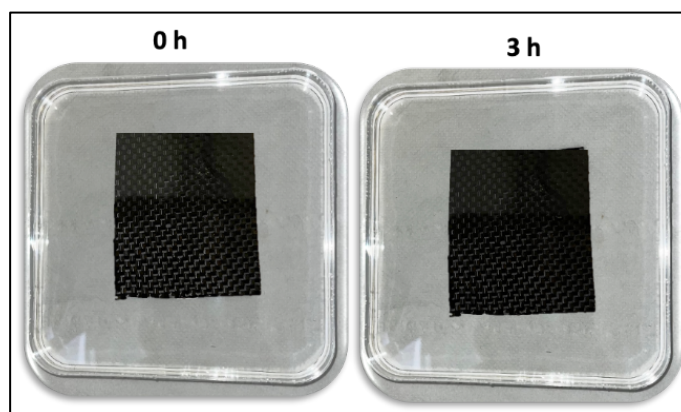


Figure appx. 1.13 Unsuccessful attempt to recycle carbon fibre-reinforced commercial epoxy composite in 90% EtOH solution.

Table appx. 1.7. Chemical Recyclability of the vitrimer, commercial epoxy, commercial epoxy composite and vitrimer composite.

Material (vitrimer)	Material Recycled [%]	Material dissolved [%]	Material undissolved [%]
Vitrimer matrix	99,20	100	-
Commercial epoxy matrix	-	-	98,5
Commercial epoxy composite	-	-	99,4
Vitrimer composite	99,09	40% (vitrimer matrix)	60% (CF)

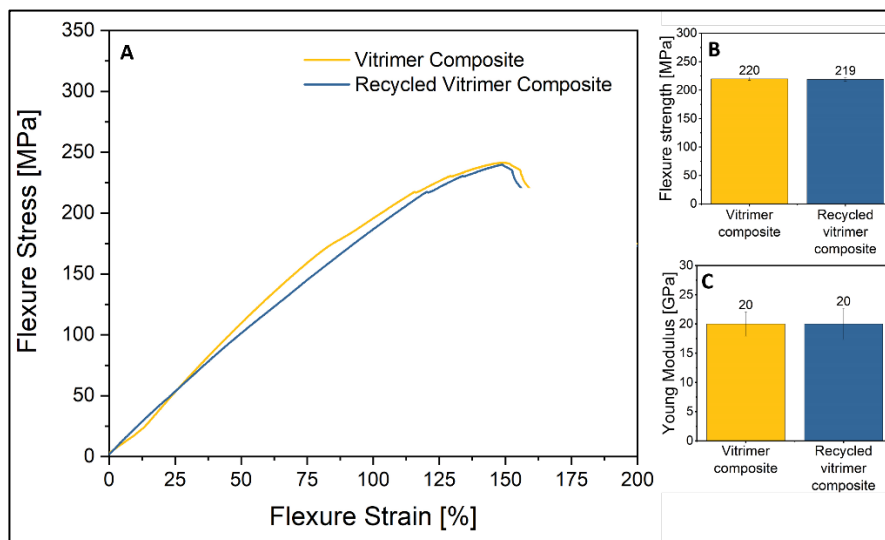
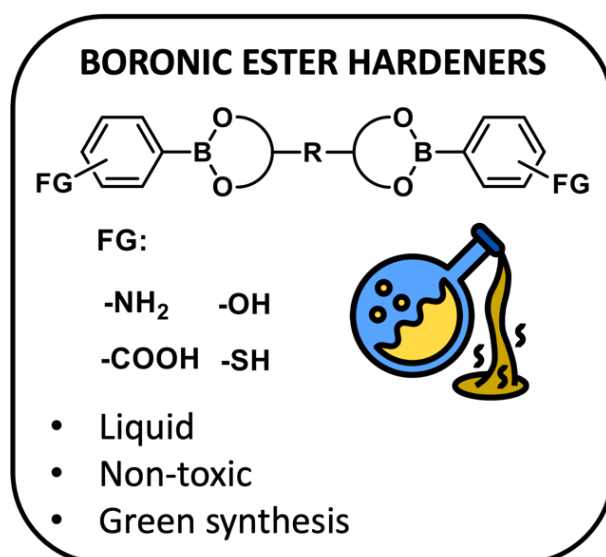


Figure appx. 1.14. Typical tensile curve (A), ultimate strength (B) and Young Modulus (C) of the virgin and recycled vitrimer composite.

2. Chapter II: Low melting and Liquid Boronic Ester Cross-linkers for the preparation of Vitrimers

Objectives

Currently, existing boronic ester cross-linkers are solid at room temperature, posing challenges in their use. Introducing liquid cross-linkers would offer significant advantages in the synthesis of boronic ester vitrimers, indeed reactions between liquids are easier compared to involving a liquid and a solid. To address these drawbacks, the chapter outlines a strategy for synthesizing liquid boronic ester cross-linkers with versatile reactive functional groups.



2.1 MATERIAL, METHODS and MEASUREMENTS

2.1.1 Materials

1,3-phenyldiboronic acid (1,3-PBA) (97%), 1,4-phenyldiboronic acid (1,4-PBA) (97%), 2-aminophenyl boronic acid (o-ABA) (97%), 3-aminophenyl boronic acid (m-ABA) (95%), 4-aminophenyl boronic acid (p-ABA) (95%), 3-carboxybenzeneboronic acid (m-CBA) (97%), 3-hydroxybenzeneboronic acid (m-HBA) (97%), 3-mercaptopbenzeneboronic acid (m-MBA) (98%) were purchased from FluoroChem.

Diglycerol was kindly provided by Spiga Nord SPA (Italy). 2-methyltetrahydrofuran (M-THF), acetone, anisole, ethanol (EtOH, 96%), ethyl acetate (EtOAc), deuterated chloroform (CDCl₃) and deuterated dimethyl sulfoxide (DMSO-d₆), pentaerythritol and thioglycerol were purchased from Merck. All materials were used as received unless otherwise stated.

2.1.2 Methods

Procedure for the hydrolysis of the 1,4-Butanediol diglycidyl ether: Desired amount of 1,4-Butanediol diglycidyl ether and water were placed in a glass flask with a magnetic stirrer at 95 °C. The flask was closed and stirred until the mixture became homogenous (few minutes), the reaction time required 24 hours. Subsequently the water was removed under reduced pressure to obtain the target compound. The successful reaction was confirmed by the ¹H NMR analysis (**Figure 2.1**).

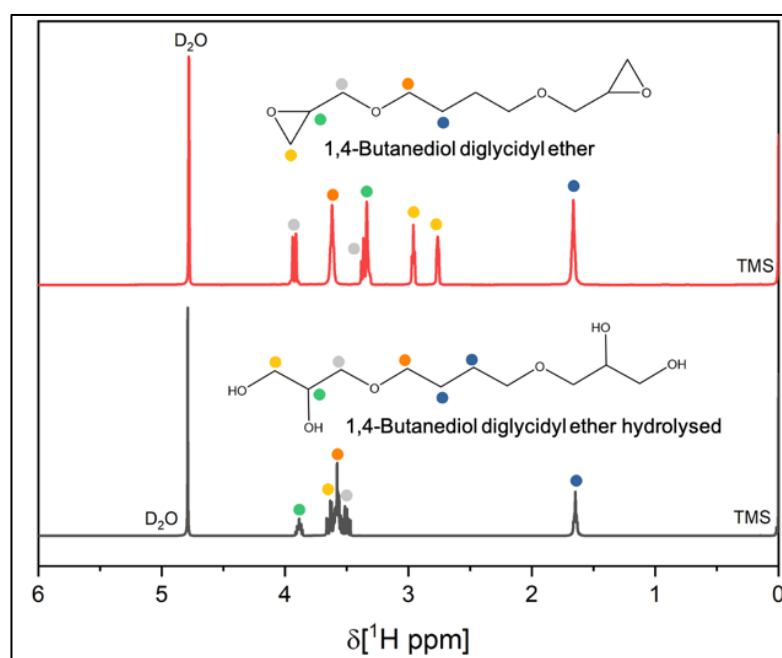


Figure 2.1 ¹H NMR spectra of 1,4-Butanediol diglycidyl ether before and after hydrolysis.

Procedure for the CLs synthesis: Desired amount of a molecule with -OH groups (component A) and a boronic acid (component B) were placed in a glass flask with a magnetic stirrer at room temperature (Errore. L'origine riferimento non è stata trovata.). The flask was closed and stirred until the mixture became homogenous (around 5 min), the reaction time required 24 hours. Subsequently the solvent was removed under reduced pressure to obtain the target compound (**Figure 2.3** and from **Figure appx. 2.1** to **Figure appx. 2.12**).

The p-DBEDT cross-linker has already been used in literature many times and it is mentioned just as a comparative example.

Table 2.1 List of the reagents used to synthesize the boronic ester cross-linkers.

Component A	Component B
Thioglycerol	1,3-phenyldiboronic acid
Diglycerol	1,4-phenyldiboronic acid
Pentaerythritol	2-aminophenyl boronic acid
1,4-Butanediol diglycidyl ether hydrolysed (BDGE hydrolysed)	3-aminophenyl boronic acid
-	4-aminophenyl boronic acid
-	3-carboxybenzeneboronic acid
-	3-hydroxybenzeneboronic acid
-	3-mercaptobenzeneboronic acid
-	3-mercaptobenzeneboronic acid

2.1.3 Measurements

¹H NMR analysis was carried out at room temperature using 5 mm tubes on an Avance III 400 MHz spectrometer, Bruker, equipped with a Broad Band Inverse probe (BBI). Chemical shifts are reported in ppm and were determined by reference to tetramethylsilane (TMS).

Thermogravimetric analysis (TGA) was performed on TGA Q 500, TA Instruments analyser under nitrogen atmosphere (flux: 50 ml/min) from 30 °C to 800 °C at a heating rate of 10 °C/min.

Differential scanning calorimetry (DSC) was performed using Discovery DSC 250, TA Instruments. The analysis on the cross-linker were carried out at a heating and cooling rate of 10 °C/min from -50°C to 150°C and the measurements on the vitrimer were carried out at a heating and cooling rate of 10 °C/min from 0°C to 200°C with nitrogen as cell purge gas (50 ml/min). Glass transition temperatures were deduced from the second heating.

2.2 RESULTS AND DISCUSSION

As the aim of this thesis was the development of new polymers which can replace the epoxy thermoset matrices, dynamic boronic ester vitrimers can be great candidates since their production follows the same procedure as the synthetic epoxy resins. Generally, epoxy resins are bicomponent systems, based on BADGE pre-polymer and polyamine hardener. In order to form an epoxy thermoset, it is necessary to mix stoichiometrically the two components, that are both viscous liquids at room temperature, before mixing and curing (**Figure 2.2**). The dynamic boronic vitrimers, instead, are characterized by an epoxy-based molecule that will be cross-linked with a dynamic boronic hardener.

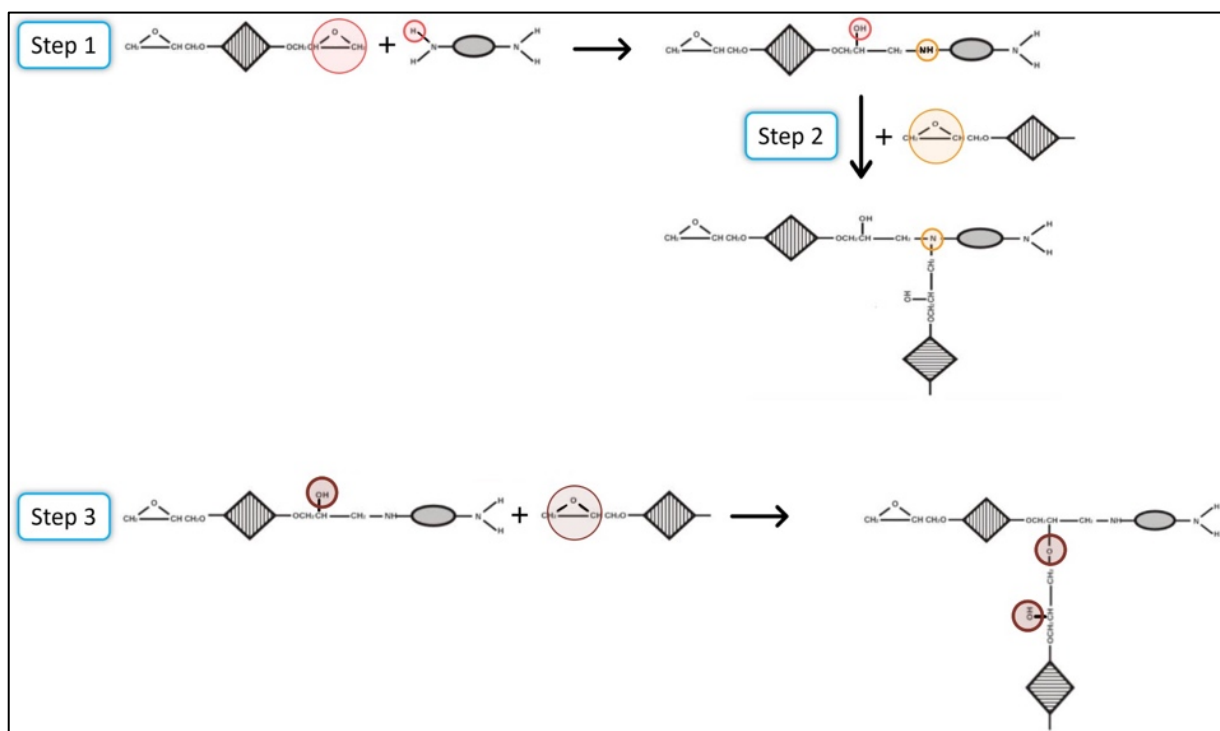


Figure 2.2 Curing reaction mechanism involved between epoxy and amine curing agent.

The aim of the research was to produce liquid boronic ester cross-linkers that act as the epoxy hardener, indeed, to the best of the knowledge, the existing boronic ester cross-linkers are all solids at RT. Liquid cross-linkers would bring huge benefits in the synthesis of the boronic ester vitrimers since it will be easier to make a reaction between two liquids in comparison to when a liquid and a solid is used and will enable curing at room temperature.

One of the most used boronic ester cross-linkers is the para-DBEDT, which was also used in the previous chapter. The DBEDT hardener had two main drawbacks, it was solid, therefore the synthesis of the vitrimer was done warming up the reaction until the melting point. Secondly it was characterized by the thiol groups and to produce the hardener it was necessary to use thioglycerol, a toxic compound with a very unpleasant smell. Therefore, the strategy for the synthesis of liquid boronic ester cross-linkers with versatile reactive, functional groups was designed.

In a conventional strategy, phenyl diboronic acid and a glycerol with a functional group are used like in the case of DBEDT, which produces a rigid molecule with a relatively high melting point of around 100 °C. Moving the boronic ester groups to the meta position, (m-DBEDT) again a solid material was obtained that degraded before the melting temperature could be reached (> 120 °C, **Figure appx. 2.1**, **Figure appx. 2.2** and **Table 2.2**). Instead, using two molecules of a phenyl mono-boronic acid connected with a bis-diol (tetraol) allows to control the melting point of the boronic ester crosslinker by simply varying the structure of the tetraol. Moreover, versatile, reactive, functional groups can be introduced into the boronic ester crosslinker by using a phenyl mono-boronic acid bearing an additional functional group in the aromatic ring like amino, hydroxy, thiol or carboxylic acid (**Figure 2.3**).

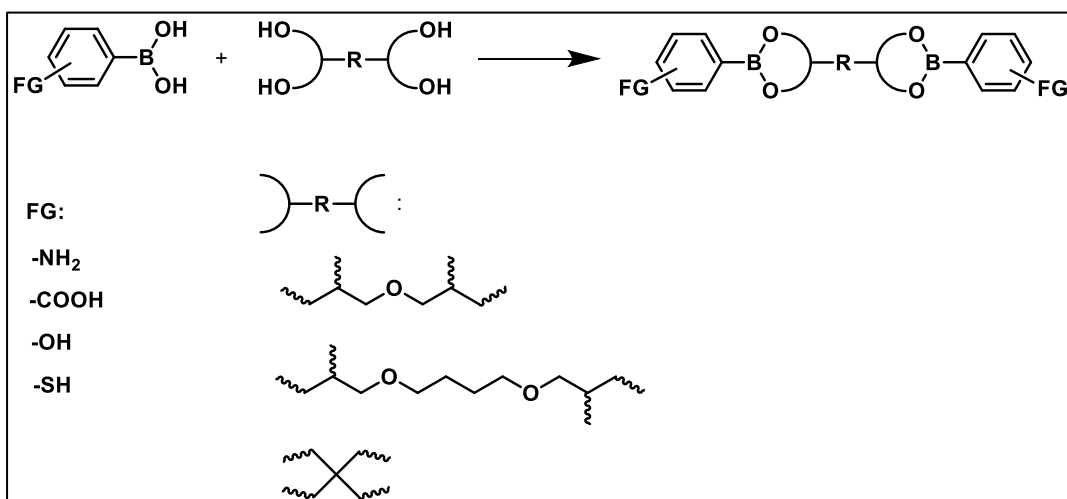


Figure 2.3 General scheme of the cross-linker synthesis.

Using a thiol-functionalized boronic acid and a flexible diol (diglycerol) a mixture of unidentified products was obtained (**Figure appx. 2.3**). Subsequently phenyl boronic acids bearing an amine in the ortho, meta and para positions were tested. Despite the facts that the o-DGBEA (**Figure appx. 2.4**) was a liquid cross-linker it starts to degrade at a very low temperature of around 50 °C. Satisfyingly, the m-DGBEA (**Figure appx. 2.5**) was a viscous liquid with a T_g of stable up to around 200 °C. Instead for the p-DGBEA (**Figure appx. 2.6**) the reaction was not successful and a mixture of unidentified products was obtained. Since the meta-aminophenyl boronic acid allowed to obtain a liquid crosslinker, stable at relatively high temperatures it was used to test the influence of different tetraols on the melting point of the product. When a hydrolysed butanediol diglycidyl ether was used as a liquid, flexible tetraol, also a liquid crosslinker with a T_g of 0 °C was obtained (m-BDBEA, **Figure appx. 2.7**). However, changing the tetraol to the solid pentaerythritol with a high melting point of 260 °C led to a solid product with a melting point > 130 °C (m-PTBEA, **Figure appx. 2.8**). After that this concept was extended also to other functional groups like hydroxyl and carboxyl. Both the hydroxyl functionalized cross-linkers (m-HDGBE and m-HBDBE, **Figure appx. 2.9** and **Figure appx. 2.10**) were successfully obtained as viscous liquids and similarly to the amino-functionalized crosslinkers, hydrolysed butanediol diglycidyl ether produced the material with a lower T_g (-9 °C) than when the diglycerol was used ($T_g = 9$ °C). On the other hand, the counterparts with the carboxyl groups (m-CDGBE and m-CBDBE, **Figure appx. 2.11** and **Figure appx. 2.12**) were white solids with high melting points (> 150 °C), and the degradation occurred before the melting during the DSC measurements.

Looking at the structures of different crosslinkers it can be concluded that the structure of the tetraol significantly affects the melting point and the crystallization ability. In general, flexible, liquid tetraols like diglycerol and hydrolysed butanediol diglycidyl ether allow to obtain liquid products in contrast to pentaerythritol. In flexible molecular chains or structures, the individual molecules are more mobile and have greater freedom of movement. This mobility often interferes with the ability of molecules to arrange themselves into an ordered, crystalline structure. Instead, these molecules might favor an amorphous or less ordered arrangement.¹⁴⁹ The kind of reactive, functional groups in the phenyl ring of the boronic acid plays also an important role. Cross-linkers with amino and hydroxy groups were liquid while the molecules containing carboxylic acid groups were solid probably do too much stronger hydrogen bonding between carboxylic acid groups in comparison to amino or hydroxyl groups. A similar trend is also visible when looking at the melting points of butanediamine ($T_m = 27.5$ °C), butanediol ($T_m = 20.1$ °C) and butane dicarboxylic acid (adipic acid, $T_m = 152.1$ °C).^{149, 150} The position of the amino functional

group in the aromatic ring of the crosslinker did not significantly influenced the melting temperature however it determined the thermal stability of the product and if the clean product could be obtained in the first place.

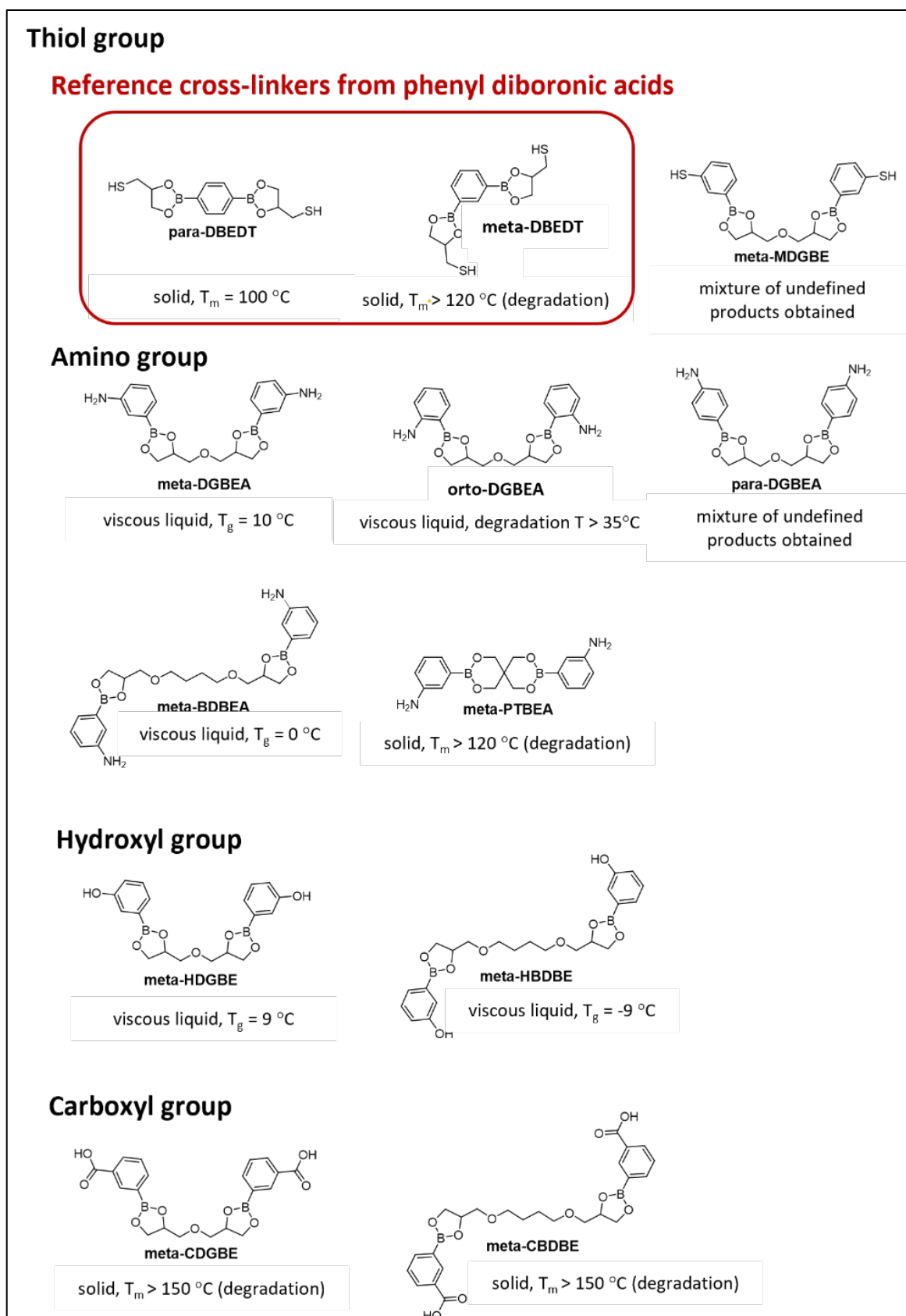
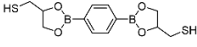
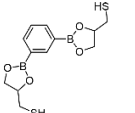
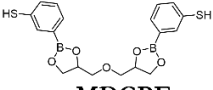
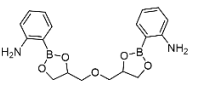
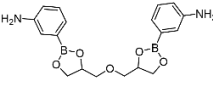
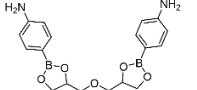
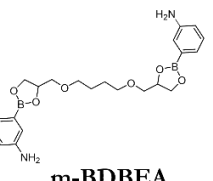
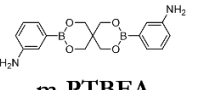
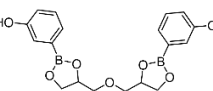
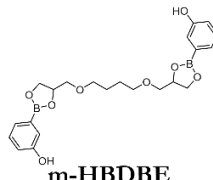
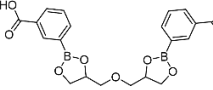
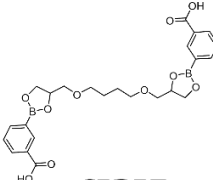


Figure 2.4 All the synthesized cross-linkers divided by functional groups.

Table 2.2 Melting point, glass transition and state of the CLs (*: degradation before melting point)

Sample	State	T _g [°C]	T _m [°C]
 p-DBEDT	solid	-	100
 m-DBEDT	solid	-	*
 m-MDGBE	Reaction not working	-	53
 o-DGBEA	viscous liquid (Not stable degradation at 35°C)	-	-
 m-DGBEA	viscous liquid	10	-
 p-DGBEA	Reaction not working	-	-
 m-BDBEA	viscous liquid	0	-
 m-PTBEA	solid	-	*
 m-HDGBE	viscous liquid	9	-
 m-HDBDE	viscous liquid	-9	-
 m-CDGBE	solid	-	*
 m-CDBDE	solid	-	*

The synthesis of the CLs was done in ethanol, but on the m-DGBEA was performed also using other green solvents, such as acetone, ethyl acetate, methyl tetrahydrofuran (M-THF) and anisole (**Figure 2.5**).

This choice was made because the traditional organic solvents despite their effectiveness, rise today many concerns as they are associated with adverse effects, both on the health and safety of workers and environment. Indeed, the most important intention of green chemistry is to decrease the use of solvents or substituting them with less toxic ones.

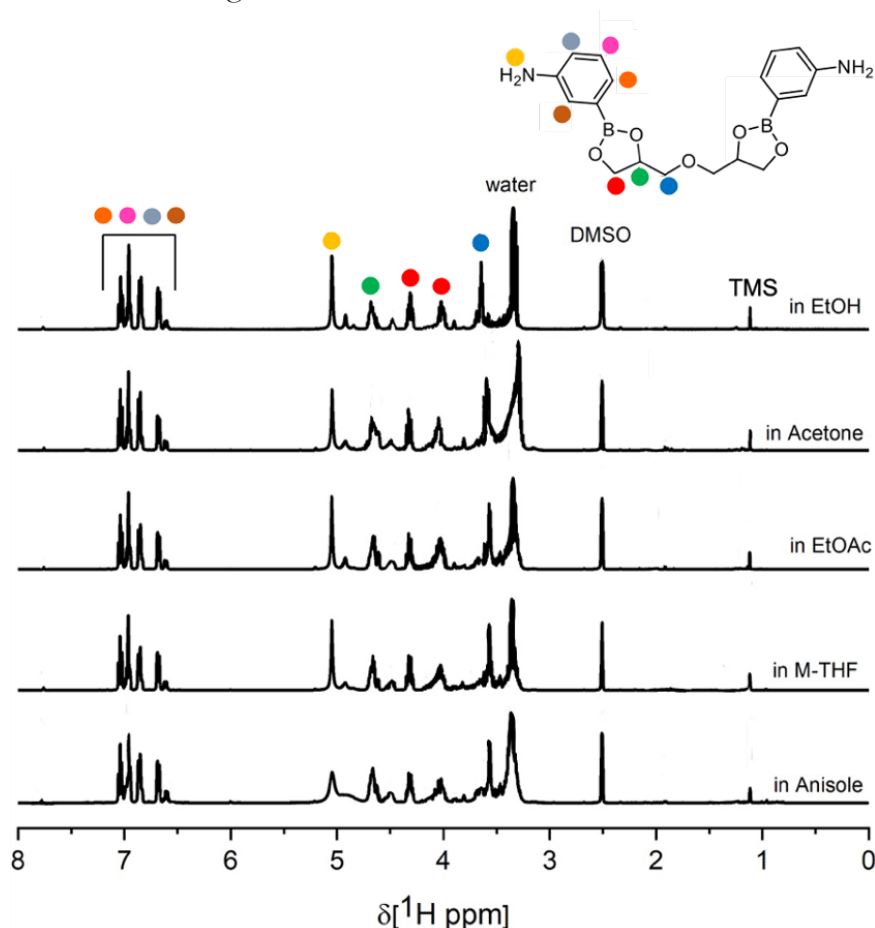


Figure 2.5 ^1H NMR spectra of meta-DGBEA using different green solvents, the NMR analysis confirmed the successful of the reactions

In summary, only the m-DGBEA, m-BDBEA, m-HDGBE and m-HBDBE were viscous liquids at RT (**Table 2.2**), therefore they were tested to prove their effectiveness as epoxy resin cross-linkers. Indeed, it was possible to cross-link a commercial epoxy pre-polymer (EPP) based on a mixture of bisphenol A diglycidyl ether and 1,4-butanediol diglycidyl ether used in the field of the epoxy resin as shown in **Table 2.3**. More in details, the most promising cross-linker among these CLs was the m-DGBEA since it was possible to prepare cross-linked materials which cure at RT, without needing a solvent or a catalyst, like for the commercial epoxy resins.

Therefore, it was used to produce new biobased amino-boronic ester vitrimers as show in the next chapter which was compared to the one produced trough the reaction between the EPP, as mentioned few lines above, and to a commercial epoxy resin.

Table 2.3 Composition, curing percentage and curing temperature of the commercial epoxy pre-polymer.

Component A (epoxy compound) [g]	Component B (cross-linker) [g]	Curing Temperature [°C]	Gel Fraction (curing) [%]	Gel Fraction (post- curing) [%]
EPP 5,51	Example 4 6,49	RT Post-curing at 60°C	80	95
EPP 4,98	Example 5 7.02	RT Post-curing at 60°C	48	66
EPP 5.50	Example 10 6,50	120	87	-
EPP 4,97	Example 11 7,03	120	66	-

2.3 APPENDIX

Dithiol diboronic ester cross-linkers

m-DBEDT

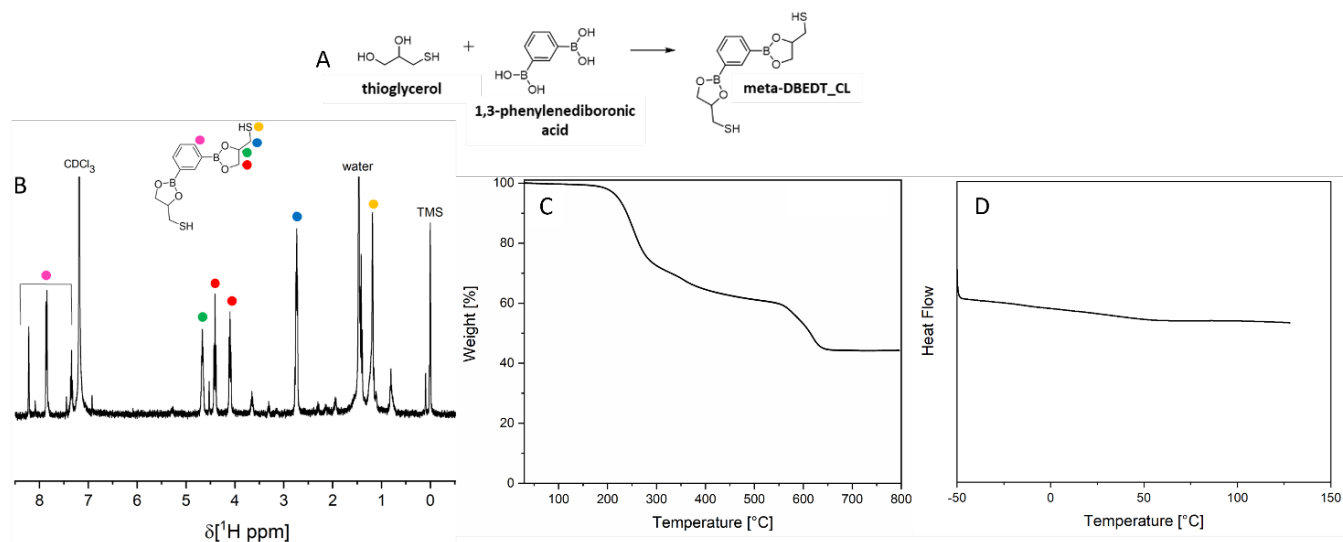


Figure appx. 2.1 Reaction scheme (A); ¹H NMR spectrum (B); TGA (C) and DSC (D) of meta-DBEDT.

p-DBEDT

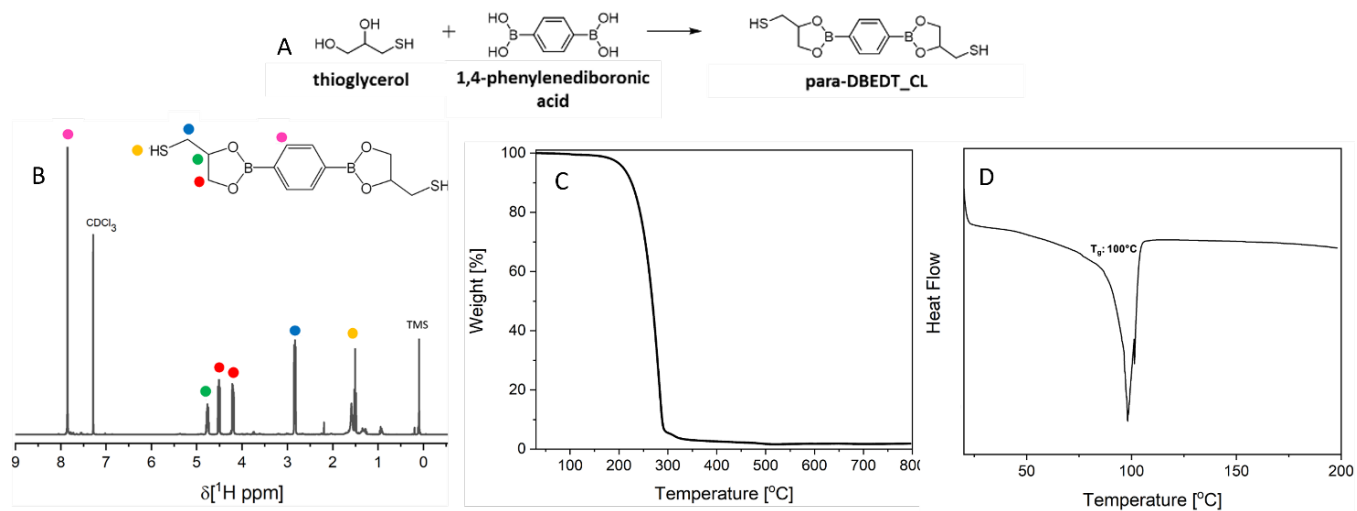


Figure appx. 2.2 Reaction scheme (A); ¹H NMR spectrum (B); TGA (C) and DSC (D) of para-DBEDT.

Dimercapto diboronic ester cross-linker

m-MDGBE

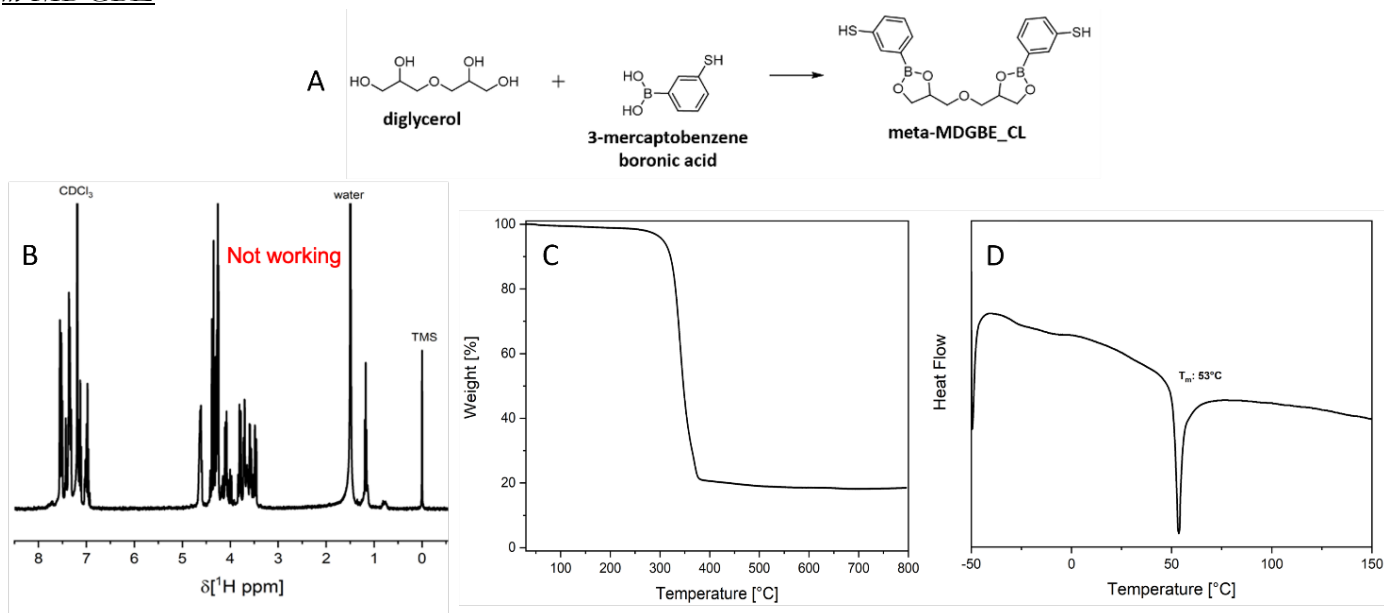


Figure appx. 2.3 Reaction scheme (A); ¹H NMR spectrum (B); TGA (C) and DSC (D) of meta-MDGBE.

Diamine diboronic ester cross-linkers

o-DGBEA

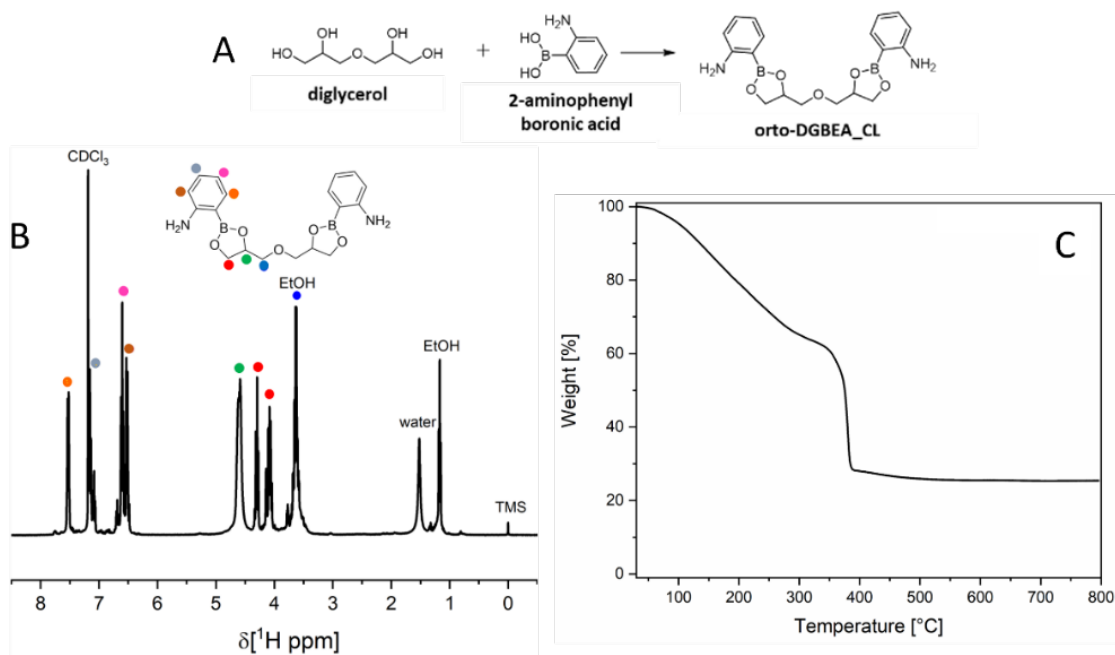


Figure appx. 2.4 Reaction scheme (A); ¹H NMR spectrum (B); TGA (C) of orto-DGBEA.

m-DGBEA

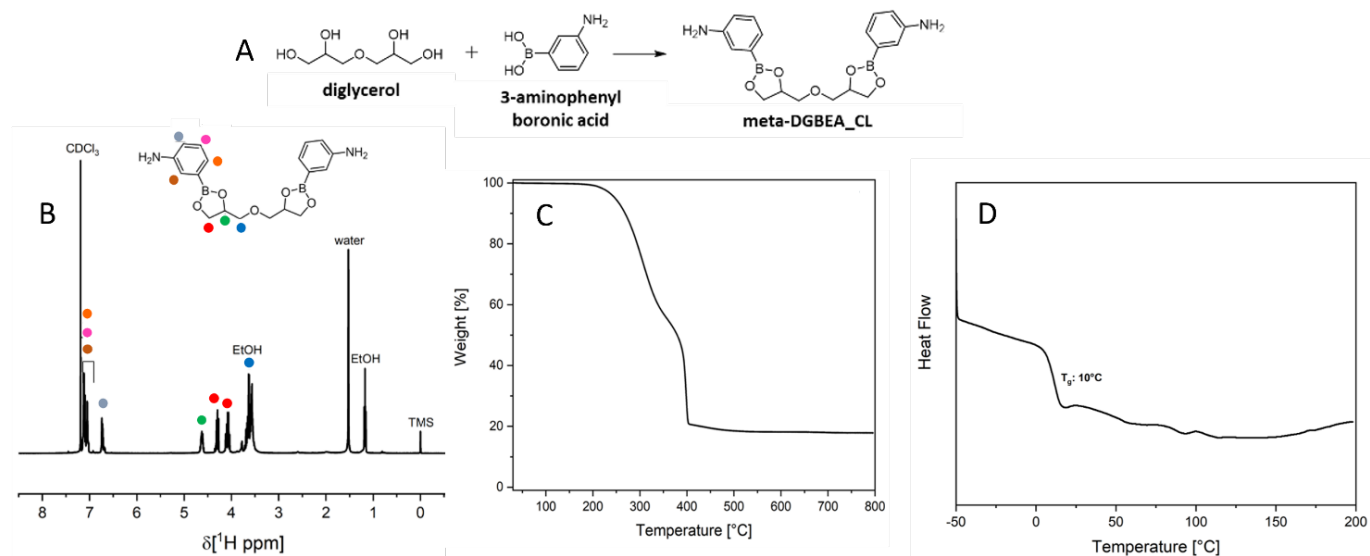


Figure appx. 2.5 Reaction scheme (A); ¹H NMR spectrum (B); TGA (C) and DSC (D) of meta-DGBEA.

p-DGBEA

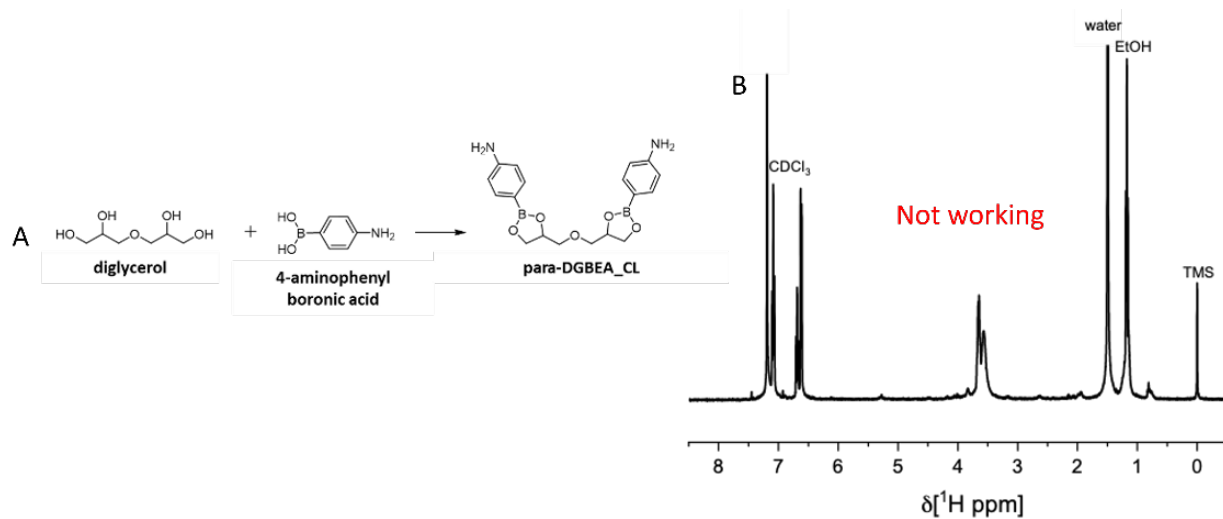


Figure appx. 2.6 Reaction scheme (A) and ¹H NMR spectrum (B) of para-DGBEA.

m-BDBEA

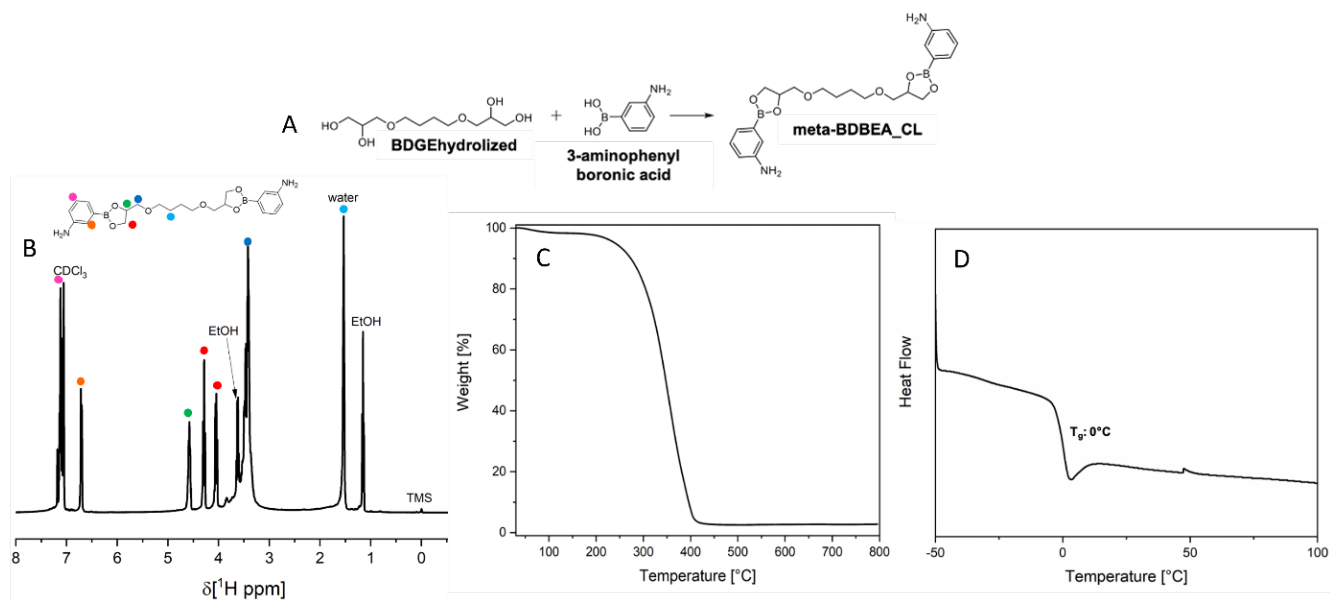


Figure appx. 2.7 Reaction scheme (A); ^1H NMR spectrum (B); TGA (C) and DSC (D) of *meta*-BDBEA.

m-PTBEA

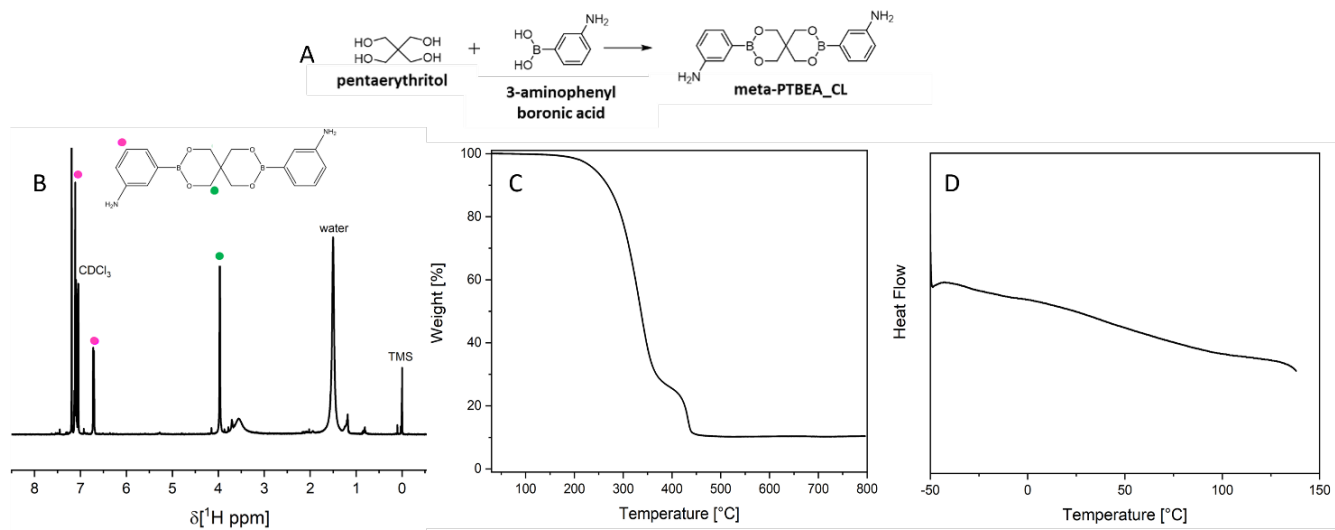


Figure appx. 2.8 Reaction scheme (A); ^1H NMR spectrum (B); TGA (C) and DSC (D) of *meta*-PTBEA.

Dihydroxy diboronic ester cross-linkers

m-HDGBE

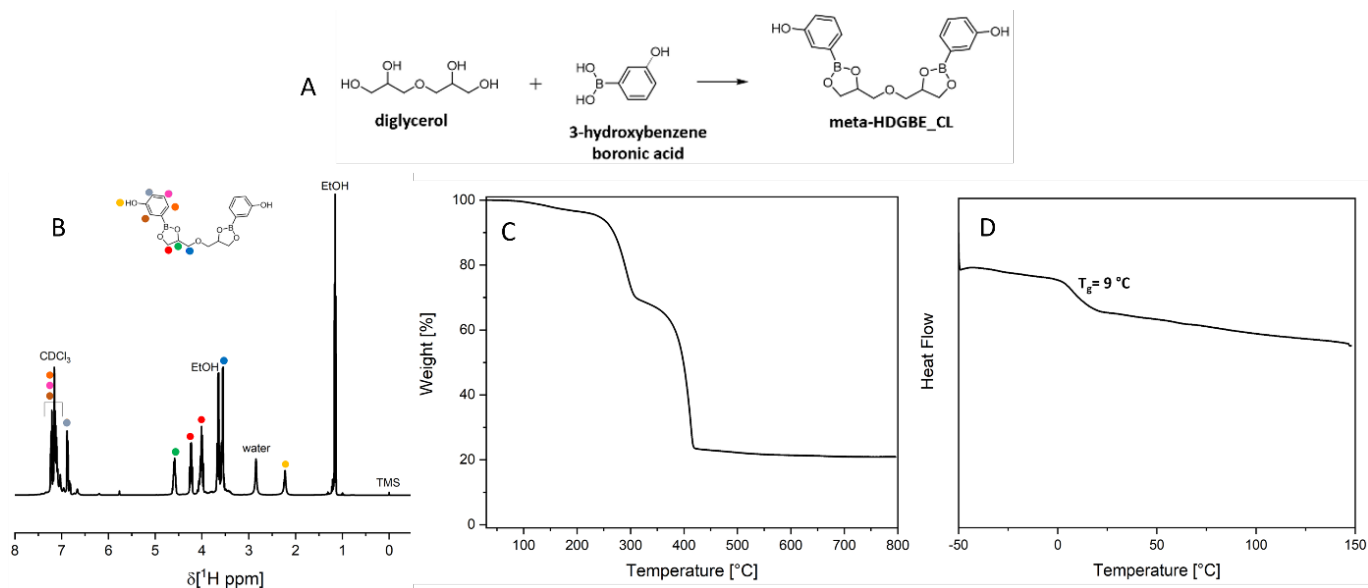


Figure appx. 2.9 Reaction scheme (A); ¹H NMR spectrum (B); TGA (C) and DSC (D) of meta-HDGBE.

m-HDBBE

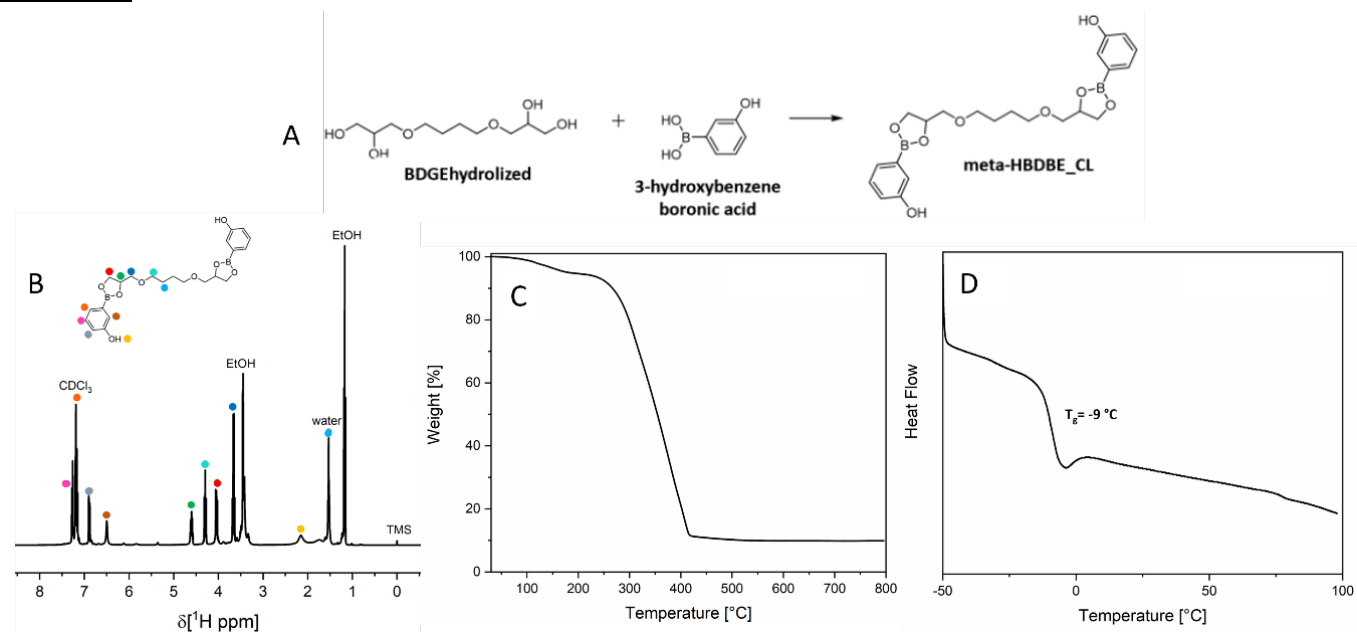


Figure appx. 2.10 Reaction scheme (A); ¹H NMR spectrum (B); TGA (C) and DSC (D) of meta-HDBBE.

Dicarboxy diboronic ester cross-linkers

m-CDGBE

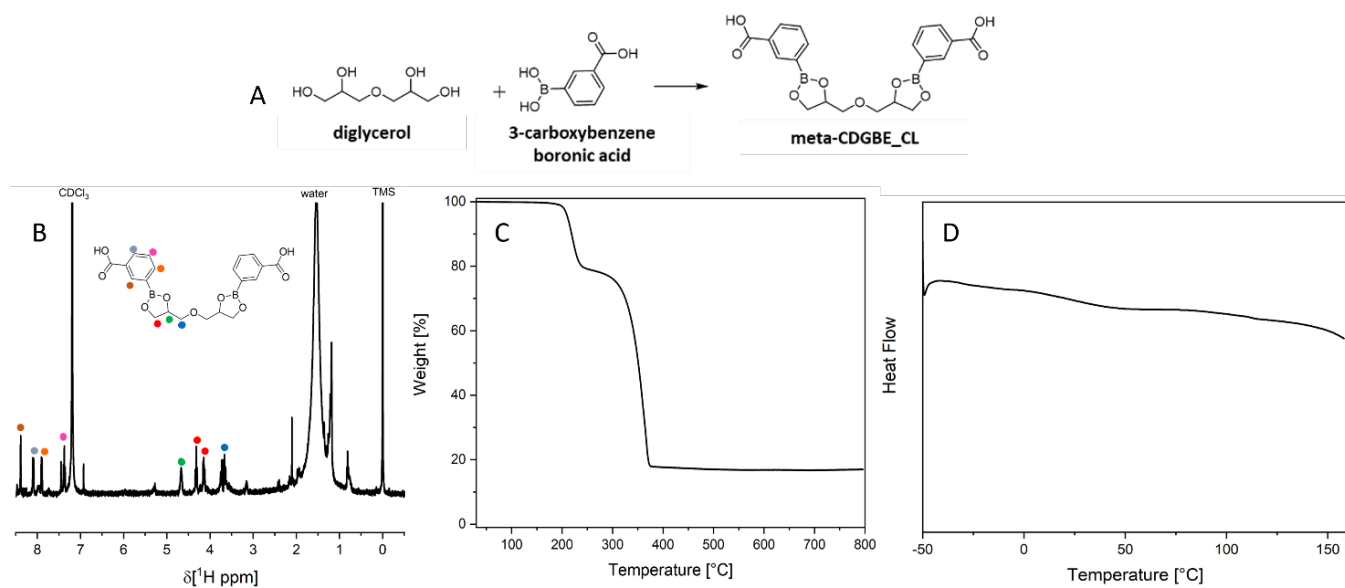


Figure appx. 2.11 Reaction scheme (A); ¹H NMR spectrum (B); TGA (C) and DSC (D) of meta-CDGBE.

m-CBDBE

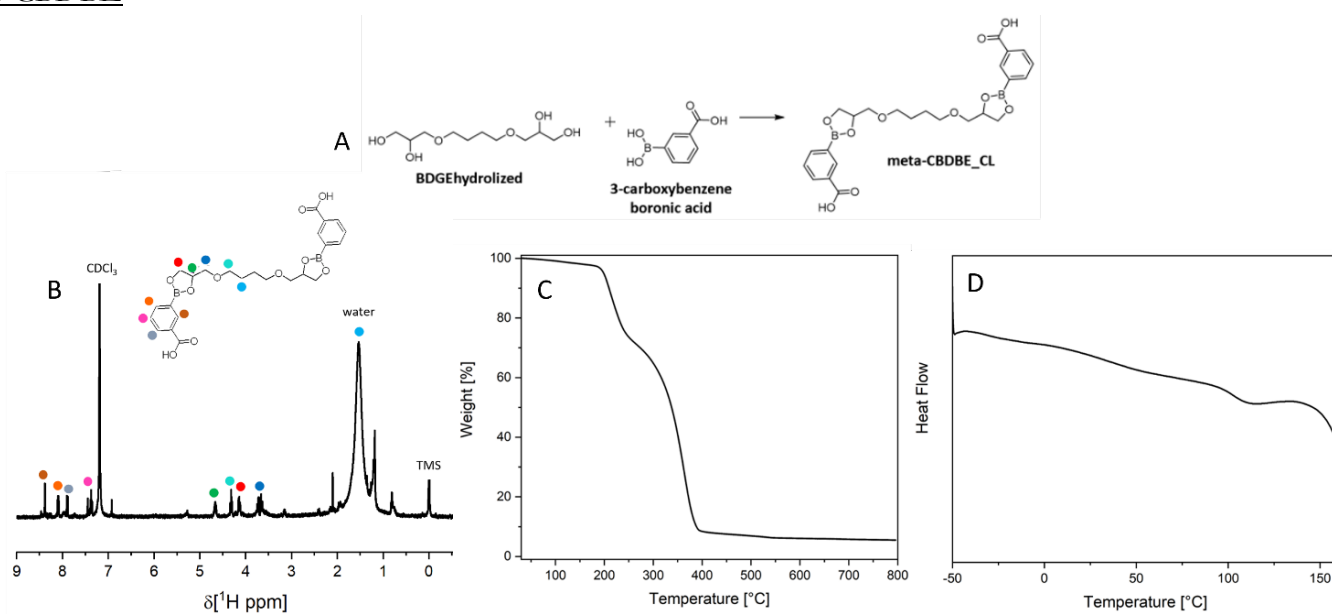


Figure appx. 2.12 Reaction scheme (A); ¹H NMR spectrum (B); TGA (C) and DSC (D) of meta-CBDBE.

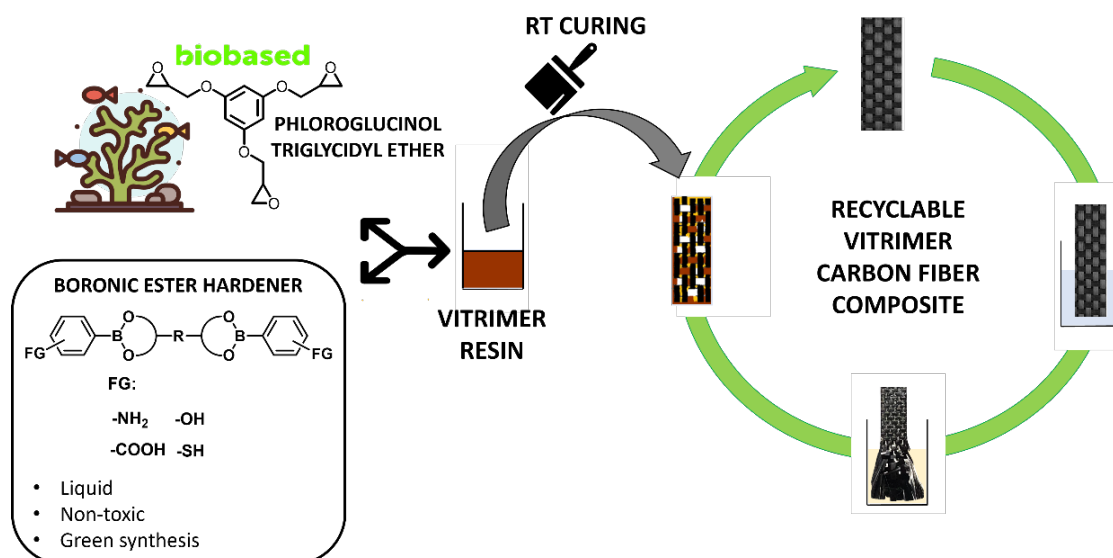
3. Chapter III: Amino-Boronic Ester Vitrimer for Room-temperature Curable Biobased Recyclable Carbon-fibre Composites

Objectives

In this chapter, thanks to the new boronic ester diamine cross-linker, RT curable vitrimers with high mechanical performance and recyclability under green and mild conditions were developed.

They proved to be an excellent matrix in a fibre-reinforced polymer composite (FRPC), overcoming the well-known recycling problems of the traditional thermoset composite and giving the possibility to recover the components of the composite at the end of their lifetime, therefore bringing huge environmental and economic advantages.

In this way the new materials can solve the most relevant challenge behind thermosets polymers which is to find new recyclable materials while maintaining comparable mechanical performance.



3.1 MATERIAL, METHODS, and MEASUREMENTS

3.1.1 Materials

Phloroglucinol triglycidyl ether (PHTE) with an average molecular weight of 294.30 g/mol and average number of epoxy groups per molecule of 3 was purchased from Specific polymers (France). C-Systems 10 10 CFS epoxy resin was purchased from Cecchi, Italy. Diglycerol was kindly provided by Spiga Nord SPA (Italy), 3-amino phenyl boronic acid (95%) was purchased from FluoroChem. Ethanol (EtOH, 96%), ethyl acetate (EtOAc) and deuterated chloroform (CDCl_3) were purchased from Merck. All materials were used as received unless otherwise stated.

Environmentally friendly synthesis of [3,3'-((oxybis(methylene))bis(1,3,2-dioxaborolane-4,2-diyl))dianiline] (DiGlycerol diBoronic Ester diAmino, DGBEA): 3-amino phenyl boronic acid (20.00 g, 146 mmol) and diglycerol (12,13 g, 73 mmol) were dissolved in ethanol (400 mL) and stirred for 24 hours at room temperature (RT). Subsequently ethanol was removed under reduced pressure to obtain the target compound as a viscous light-brown liquid (26,80 g, 99%) (**Figure appx. 3.1**).

3.1.2 Methods

Procedure for PHTE crosslinking: desired amount of PHTE and DGBEA (epoxide to amino ratio of 1:1) were placed in a Teflon mould and heated to 60 °C to decrease the viscosity of both compounds (around 5 min) after that they were mixed with a spatula until homogenization and cured at RT for 24 h, following a post-curing treatment in an oven at 60 °C for 3 h.

Procedure for EPP crosslinking: desired amount of EPP and DGBEA (epoxide to amino ratio of 1:1) were placed in a Teflon mould and heated to 60 °C to decrease the viscosity of both compounds (around 5 min) after that they were mixed with a spatula until homogenization and cured at RT for 24 h, following a post-curing treatment in an oven at 60 °C for 3 h.

Procedure for commercial epoxy resin crosslinking: desired amount of bisphenol A diglycidyl ether (BADGE) based pre-polymer and polyamine hardener (pre-polymer to hardener mass ratio of 2:1) were placed in a Teflon mould and mixed until the mixture became homogenous (around 2 min) and cured at RT for 24 h (**Figure 3.9A**).⁴⁷

Procedure for the fabrication of the composites: carbon fibre-reinforced composites were prepared by overlapping and impregnating three carbon fibre layers with dimensions of $10 \times 10 \text{ cm}^2$ with 30 g of the commercial epoxy resin or the vitrimer resin using a spatula. The impregnated layers were placed between two metal sheets with 9 kg weight on top to ensure the correct adhesion between the fibres and the resin and to remove the excess of the resin. The composites were cured for 24 hours at RT and for the vitrimer resin post-curing at 60 °C for 3 h was applied (**Figure 3.9A**).⁴⁷

3.1.3 Measurements

Infrared spectra were obtained with a single-reflection attenuated total reflection (ATR) accessory (MIRacle ATR, PIKE Technologies) coupled to a Fourier Transform Infrared (FTIR) spectrometer (Bruker Vertex 70V). All spectra were recorded under vacuum in the $4000\text{--}500 \text{ cm}^{-1}$ range with a resolution of 4 cm^{-1} , accumulating 32 scans.

$^1\text{H NMR}$ analysis was carried out at room temperature using 5 mm tubes on an Avance III 400 MHz spectrometer, Bruker, equipped with a Broad Band Inverse probe (BBI).

Chemical shifts are reported in ppm and were determined by reference to tetramethylsilane (TMS).

Gel fraction was determined to confirm the successful of the synthesis. The test was performed by weighing small piece (~200 mg) of a material and placing it in a vial with 10 mL of ethyl acetate for 24 h. Then the ethyl acetate was removed and the remaining undissolved part of the material was washed with ethyl acetate, dried under vacuum at 50 °C for 24 h, and weighed again. Gel fraction was calculated from the mass ratio of the polymer after and before exposing it to ethyl acetate.

Density of the vitrimer, commercial epoxy samples and their carbon fibre composites were evaluated by cutting rectangular pieces for each sample, measuring all the dimensions and weighing in on an analytical balance to measure their mass.

Bending test was performed using a dual column Instron 3365 universal testing machine equipped with 2 KN load cell and a three-point bend fixture with a 10 mm anvil. Rectangular-shaped samples with 6 x 1 cm² and thickness of 1 mm were cut out directly from matrices and composites.

Reprocessability tests were performed by compression moulding under 4 ton of pressure for 5 min at 100 °C using Carver 3853 CE press. The obtained sheets were cut into rectangular and underwent the bending test four times. After the first cycle, all the tested samples and the residual pieces of the vitrimer went through compression moulding again and cut again into rectangular-shape samples and tested at the bending tester again. At least five measurements were carried out for each sample and results were averaged to obtain a mean value. Both Young's modulus values were calculated using the built-in software of the bending tester.

Recyclability of the vitrimer was evaluated by hydrolysis and dissolution of around 200 mg of vitrimer in 90% v/v EtOH for 3 h at 60 °C and subsequent film casting to regenerate the original vitrimer.

Differential scanning calorimetry (DSC) was performed using Discovery DSC 250, TA Instruments. The analysis on the cross-linker were carried out at a heating and cooling rate of 10 °C/min from -50°C to 150°C and the measurements on the vitrimer were carried out at a heating and cooling rate of 10 °C/min from 0°C to 200°C with nitrogen as cell purge gas (50 ml/min). Glass transition temperatures were deduced from the second heating.

Thermogravimetric analysis (TGA) was performed on TGA Q 500, TA Instruments analyser under nitrogen atmosphere (flux: 50 ml/min) from 30 °C to 800 °C at a heating rate of 10 °C/min.

Optical microscopy images were taken with Leica DFC 420 optical microscope with a 10x magnification.

SEM analysis was conducted by JEOL JSM-6490LA scanning electron microscope (SEM), with an acceleration voltage of 10 kV with a 150x magnification.

DMTA/stress relaxation were performed using a DMTA TA Q800 in temperature sweep mode. Samples were tested in temperature sweeps from -50 to 100 °C with a heating rate of 2 °C min⁻¹. Experiments were performed in a single frequency oscillation mode with a frequency of 1 Hz and a displacement amplitude of 0.1% in auto tension offset control.

Rheology analysis were performed using an Ares rheometer, TA instruments. All measurements were carried out in plate-plate geometry (1 mm thickness). Frequency sweeps were carried out from 100 to 0.01 Hz from 80 to 160 °C with a constant strain amplitude of 1%.

Biodegradability was assessed by measuring the biochemical oxygen demand (BOD) with OxiTop-IDS system. The biodegradability was determined by monitoring the oxygen consumption in a closed bottle filled with 432 mL of seawater to mimic a real environmental condition since it contains microorganisms and nutrients needed for their growth. Samples were tested in duplicate and the experiments were conducted at RT inside dark glass bottles hermetically closed with the OxiTop measuring head. Sodium hydroxide was used as a CO₂ scavenger to sequester carbon dioxide produced during biodegradation, and biotic consumption of the oxygen present in the free volume of the system was measured as a function of the decrease in pressure. Raw data of oxygen consumption (mg O₂/L) were corrected by subtracting the mean values of the blanks, obtained by measuring the oxygen consumption of the seawater in the absence of any test material. After this subtraction, values were normalized on the mass of the individual samples and referred to 100 mg of the material (mg O₂/100 mg). Cotton and polypropylene were added as reference samples.⁴⁷

3.2 RESULTS AND DISCUSSION

3.2.1 Design of the vitrimer resin

Since the goal of the thesis was the synthesis of a green material, it was designed a solvent and catalyst-free, vitrimer resin that at the end of its lifetime does not generate any wastes. PHTE was selected as a suitable compound for the synthesis of the vitrimer being that it can be derived from brown algae, so it is biobased. Moreover, it has high amount of epoxy groups that can participate in the crosslinking reaction with the boronic ester diamine cross-linker. (**Table appx. 3.1**). More specifically PHTE has 3 epoxy groups per molecule (calculated based on the ¹HNMR, **Figure appx. 3.2**). PHTE was crosslinked through an amino-epoxy click reaction between the epoxy groups and DGBEA (under the name of vitrimer resin when not cured and vitrimer or PHTE-vitrimer or PHTE-DGBEA when cured) (**Figure 3.1A**), by simply mixing both chemicals stoichiometrically (epoxy to amine ratio of 1) at RT (**Figure 3.1B** and **Table appx. 3.1**). The synthesis did not require a solvent, because DGBEA is a viscous liquid with a T_g of 10 °C which allows easy homogenization with the PHTE warming both components to 60 °C for a few minutes. After curing (24 h, RT) and post-curing (3 h, 60 °C), a transparent, slightly orange and very rigid material was obtained, as shown in **Figure 3.1**.

Commercial epoxy resin based on EPP and a polyamine hardener was used as a reference material (under the name of commercial epoxy resin when not cured and commercial epoxy when cured) for comparison with the vitrimer resin. It was cured following the same procedure for 24 h at room temperature (except for the post-curing treatment) according to manufacturer's specification after which a rigid, transparent, greenish material was obtained. Moreover, to demonstrate the versatility of the cross-linked it was also used to prepare a vitrimer from a commercial EPP resin (under the name of EPP vitrimer or EPP-DGBEA) (**Figure appx. 3.4**). More specifically EPP has 6,3 mmol of epoxy groups/grams of samples (calculated based on the ¹HNMR, **Figure appx. 3.3** and **Figure appx. 3.5**). The synthesis was done following the same procedure to cross-link the PHTE.

As shown in a previous work⁴⁷ the difference between the vitrimer resin and the commercial epoxy resin is that the first contains dynamic crosslinks capable of exchange reactions which allows the network rearrangements, on the other hand the commercial

epoxy resin shows a permanent cross-linked network. Therefore, at service temperatures the vitrimer behaves like a permanently crosslinked polymer, but above the T_g the exchange reactions speed up, making flow possible, but always keeping the number of crosslinks constant (**Figure 3.1C**).

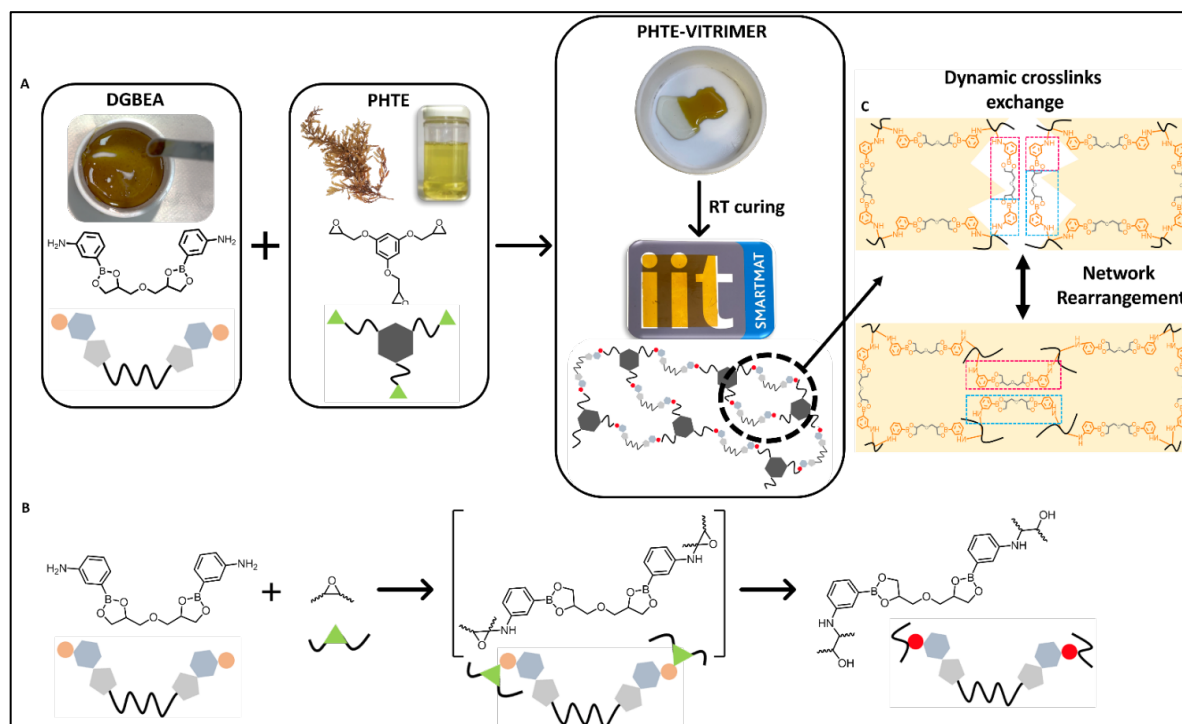


Figure 3.1 .Schematic representation of the PHTE-DGBEA vitrimer synthesis (A), the amino-epoxy “click” reaction (B) and scheme of the network rearrangement by boronic ester exchange (C).

From the kinetics study of the cross-linking and through the gel fraction test at different time points was revealed that the plateau was reached after 20 hours indicating completion of the crosslinking reaction (confirmed also by the FT-IR analysis as shown in **Figure 3.4**). However, following a post-curing cycle at 60 °C for 3 h it was possible to slightly increase the gel fraction even further. (**Table appx. 3.2** and **Figure 3.2**). The vitrimer precursors, PHTE and DGBEA, as well as both components of the commercial epoxy resin, separately show high solubility in ethyl acetate. Instead, once cross-linked both materials were not soluble in ethyl acetate with high gel fractions, 88% after the curing at RT and 99% after the post-curing for the PHTE-vitrimer (**Figure appx. 3.6A**, **Table appx. 3.3** and **Table appx. 3.4**) and 100% for the commercial epoxy (**Figure appx. 3.6C**, **Table appx. 3.2**) proves a successful curing. For what concern the EPP vitrimer it shows a gel fraction of 80% after 24h and 95% after the same post-curing treatment previously mentioned (**Figure 3.4**, **Figure appx. 3.6B** and **Table appx. 3.4**).

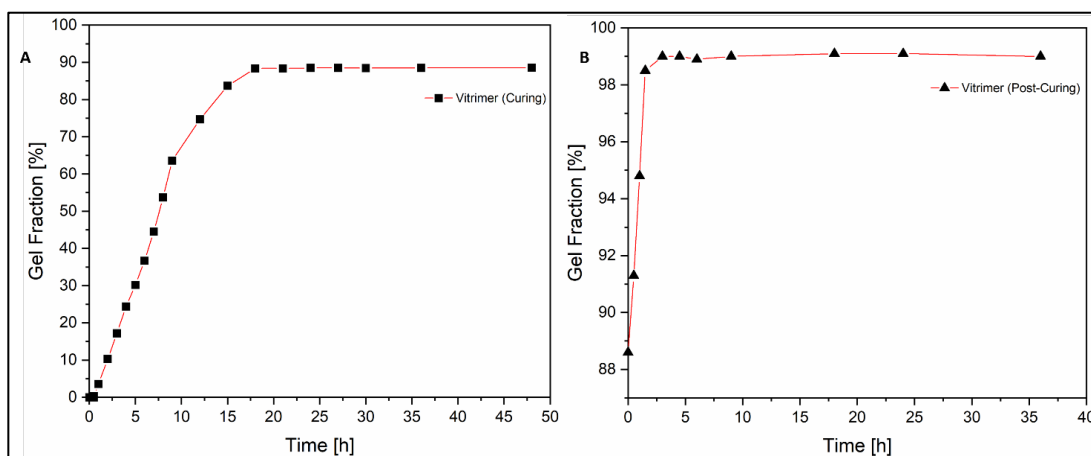


Figure 3.2 Gel fraction of PHTE-vitrimer at different curing times during the curing (A) and post-curing treatment (B).

3.2.2 Vitrimer characterization

Mechanical and thermomechanical performance

Materials were tested in bending mode in order to evaluate the flexural mechanical properties. The typical bending test curves showed an average flexural modulus of 3.9 GPa and a flexural strength of around 29 MPa while the epoxy resin shows an average flexural modulus of 3.6 GPa and a flexural strength of 99 MPa (Figure 3.4A, B and C). It must be pointed out that there is no significant difference from the mechanical point of view between the PHTE-vitrimer that was just cured or also post-cured and the same can be observed for the commercial epoxy as demonstrated in Figure appx. 3.7. Instead, for what concern the EPP-vitrimer the typical bending test curves showed an average flexural modulus of 2,2 GPa and a flexural strength of around 8, indeed the material is very fragile (Figure 3.4A, B and C).

Generally, DMTA shows that the rubbery modulus of a vitrimer is nearly constant due to the constant cross-link density, like in the case of the commercial epoxy resin (reference thermoset). Surprisingly, the rubbery modulus of PHTE-vitrimer appears to slowly decrease since the sample is slightly stretched during the measurement due to the fast stress relaxation (Figure 3.4H and Figure appx. 3.8).

From the frequency sweep it can be noticed that the PHTE-based vitrimer behaves like a solid below 80°C with fairly constant storage modulus (G') that is much higher than the loss modulus (G''), and then, when heated above 80 °C, the boronic ester exchange speeds up enabling flow and processability. The crossover point moves toward shorter timescales (higher frequency) with the increasing temperature, which means that the material relaxes stress and flows faster. The crossover frequency can be used to determine the activation energy ($E_a = 90$ kJ/mol) and topology-freezing transition temperature ($T_v = 10$ °C) of the system. The T_v is only theoretical since it is lower than the glass transition temperature ($T_g \sim 80$ °C), which means that even though the boronic ester exchange reactions could occur, they are frozen below the T_g due to restricted chain mobility. When the material is heated above the T_g , segmental motion is slowly initiated while the exchange reactions are already fast.

Above T_v , exchangeable reactions happen fast and a vitrimer can be reprocessed and recycled easily, instead, below T_v exchangeable reactions are slow and a vitrimer behave like a traditional thermoset.¹³⁷ In case of the vitrimer presented in this work T_v is lower than the T_g which means that even though the exchange reactions could occur at temperature below it, they are frozen due to restricted chain mobility. Instead above the

T_g , segmental motion slowly starts moving while the boronic ester exchange reactions happen fast. Further increasing the temperature, the boronic ester exchange dominates the network rearrangements reflecting in a viscosity decrease even lower, following the Arrhenius law (**Figure 3.3**).^{48, 138, 139} Furthermore, as it is clearly shown in **Figure appx. 3.9** the relaxation rate is increased with temperature, therefore in good agreement with the Arrhenius law, because the relaxation process is essentially controlled by the boronic ester exchange, process that is accelerated at higher temperatures.

In comparison the previous ELO-DBEDT vitrimer (presented in chapter II) the new PHTE-DGBEA vitrimer showed a higher activation energy despite its reprocessability is easier in terms of lower temperature and processing time.

If a boronic ester vitrimer has a higher activation energy compared to another, it means that more energy is required to initiate the chemical reactions necessary for the network rearrangements. Higher activation energy can imply that this material might require more external stimuli (like heat or pressure to trigger its dynamic nature). It is important to consider that the E_a is measured across the entire system, not solely for the boronic ester bonds, consequently, the values are significantly impacted by the specific epoxy molecules utilized. Indeed, the PHTE, characterized by its aromatic ring, exhibits greater rigidity compared to the more flexible ELO, therefore this difference in flexibility likely contributes to the observed higher activation energy.

The typical activation energy for boronic ester vitrimers ranges between 7.7 and 13.8 kJ/mol up to 38.9 kJ/mol.^{94, 151, 152} However, higher values have been observed, particularly when cyclic compounds were used. Reported values in these instances range between 76.7 kJ/mol and 142 kJ/mol.^{35, 153-155} Therefore, the observed value of 90 kJ/mol for the PHTE-based vitrimer aligns well with previously reported values.

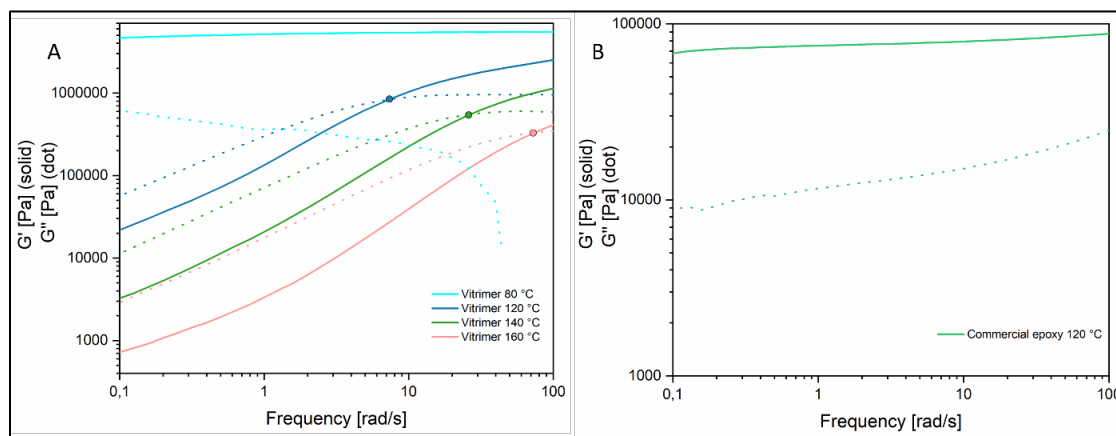


Figure 3.3 Rheology frequency sweep curves of PHTE-vitrimer (A) and commercial epoxy (B).

For what concern the commercial epoxy, the relaxation modulus is fairly constant since it is characterized by a permanent crosslinked network, which does not allow the relaxation of any stress and therefore any rearrangements.

TGA analysis confirmed that the PHTE-based vitrimer is stable and do not decompose to volatile compounds up to around 250 °C even though it is made from a potentially biobased phloroglucinol. Instead, the commercial epoxy starts to lose weight at 150 °C (**Figure 3.4D**), that might be due to the evaporation of some additives present inside the resin that most likely do not participate in the crosslinking such as benzyl alcohol. The DSC measurements show that the above mentioned vitrimer presents a T_g of 74 °C, higher than the commercial epoxy that has a T_g of 63 °C (**Figure 3.4E**), most probably

thanks to the higher content of aromatic rings coming both from the phloroglucinol and the boronic ester diamine crosslinker. Furthermore, the vitrimer has a density of around 1.23 g/cm³ while the commercial epoxy of around 1.13 g/cm³ (Table appx. 3.5).

For what concern the EPP-based vitrimer it shows a good thermal stability and it does not decompose to volatile compounds up to around 250 °C, from the DSC analysis the T_g (55 °C) is lower than that of the PHTE (Figure 3.4D and E). Performing DMA measurements on the EPP-vitrimer wasn't possible due to its brittleness.

Biodegradability

The PHTE-vitrimer starts to biodegrade after just 1 day in seawater and within a month, the BOD reaches values of 5 mg O₂/100 mg material. The biodegradation is not immediate (it starts after 4 days) since the boronic ester linkages need to undergo hydrolysis first. To compare the biodegradability of the synthesized vitrimer with references we report the biodegradability curve of a cotton fabric which is a well-known biobased and biodegradable material and of poly-propylene which is not biodegradable. The cotton fabric (in blue) reached 12,5 mg O₂/100 mg material after 30 days, instead the poly-propylene (in red) remained at 0 mg O₂/100 mg. The DGBEA cross-linker show a high biodegradability thanks to the presence of the diglycerol (Figure 3.4I). To the best of the knowledge, this is one of the first studies about biodegradability of vitrimers and the developed vitrimer itself is one of the first examples of biodegradable vitrimers. Performing an analysis on the EPP-vitrimer is necessary as well.

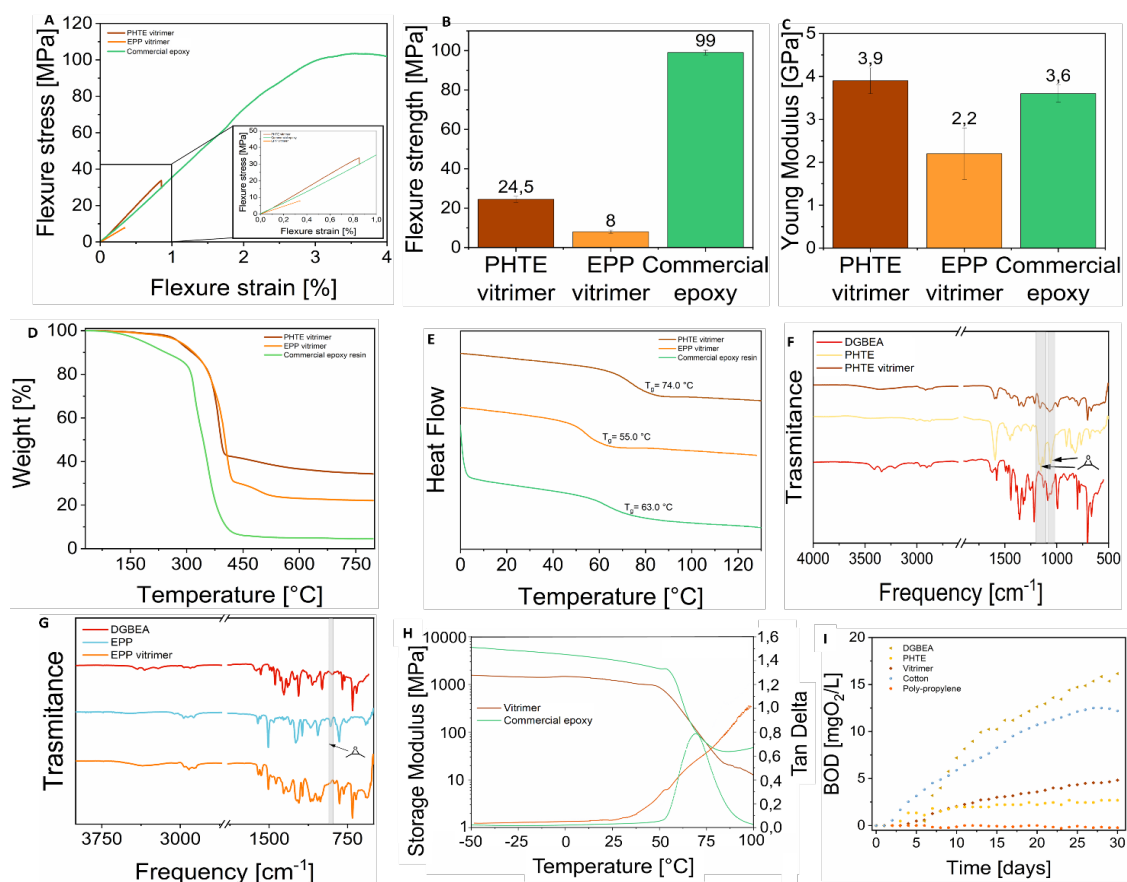


Figure 3.4 Typical flexural curve (A), young modulus (B) and flexural strength (C) of PHTE and EPP vitrimers and commercial epoxy; TGA (D) and DSC (E) curves of vitrimers and commercial epoxy; IR spectrum of the PHTE-vitrimer (F) and EPP-vitrimer before and after curing (G) DMTA curves of the PHTE-vitrimer and commercial epoxy (H); BOD of the DGBEA cross-linker, PHTE, PHTE-vitrimer and cotton fabric and poly-propylene as references (I).

3.2.3 Shape memory effect

Vitrimer characterized by the presence of dynamic boronic ester linkages have the ability to be reshaped, and it is precisely the dynamic nature of these materials which allows the behaviour of shape memory, giving the possibility to change both temporary and permanent shapes of the material. To enable the remodelling of the vitrimer, it has to be heated above its glass transition temperature to make it soft. More specifically, when a low temperature and heating time is used (100 °C for 60 s), the PHTE-based vitrimer does not have enough time to relax all the stress induced by giving to it the new shape, it is frozen in the new state (from rectangular shape - permanent shape n°1 into a “C” shape - temporary shape n°1). Indeed, the new form is only temporary since it is maintained by cooling the vitrimer below its T_g immediately after the reshaping (**Figure 3.5A1-A3**). The original shape can be recovered by reheating the vitrimer to 100 °C for 5 min thanks to presence of the residual stress (**Figure 3.5A4**).¹⁴¹ Since the process is reversible it can be repeated several times changing different temporary shapes. The changing of the temporary shape can be induced also in the epoxy resin.

The difference between a vitrimer and a conventional thermoset is that for the first one it is possible to also change its permanent shape (given during the curing process), Indeed, given enough energy and time, which means warming it up to a higher temperature and for a longer time, it can relax all the stress induced by the reshaping. Increasing the temperature to 120 °C and the heating time to 15 min, the permanent shape could be changed from rectangular to bridge shape (permanent shape n°2). As mentioned before since the changing of the temporary shape can be repeated several times, this new permanent shape could be restored after giving the sample a different temporary shape (“L” shape - temporary shape n°2) by heating it, again, at 100 °C for 60 s (**Figure 3.5A4-A8**).

On the contrary, since the commercial epoxy cannot relax stress due to the covalent network it cannot change the permanent shape. (**Figure 3.5B**). Studying the shape memory effects of the EPP-vitrimer is also necessary.

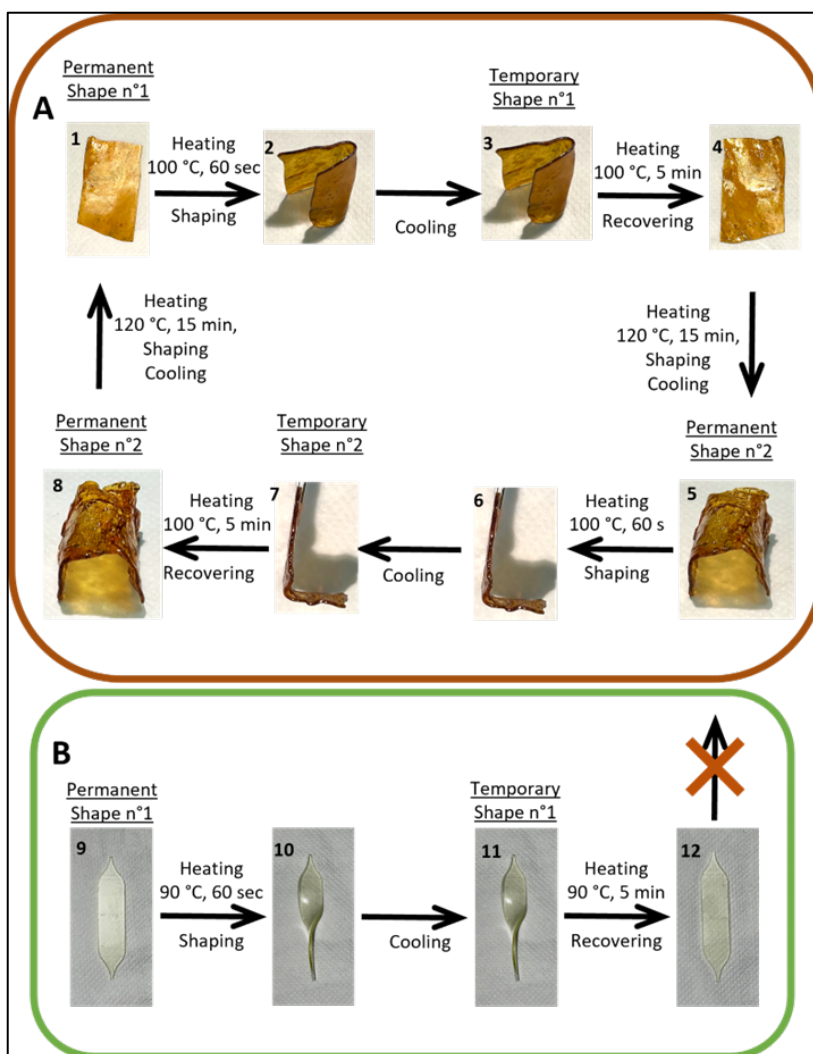


Figure 3.5 Shape memory effect of the PHTE-vitrimer (A) and the commercial epoxy (B)

3.2.4 Vitrimer recycling

The recycling of polymers is divided into three main categories: mechanical, chemical and energy recovering.

Mechanical recycling, as the name implies, consists of recovering the material through mechanical processes such as grinding. Moreover, it allows multiple re-use or recycling since it does not change the chemical structure of the polymer. Through this method, thermoplastic polymers can be reprocessed using typical techniques such as, injection or compression moulding. On the other hand, thermoset materials can be ground into small particles and used only as fillers since the material is not reprocessable anymore after the curing, which is called downcycling.

Chemical recycling instead changes the chemical structure of a polymer, enables the recovery of chemicals and mixtures of monomers which can be used as raw materials for new synthesis of virgin polymers, or low molecular weight gases for energy recovery. Unfortunately, this process is mainly limited to condensation polymers.

Energy recovering consists of burning the plastic in place of fossil fuels for energy production, a process typically performed on thermoset materials.

The proposed dynamic thermoset vitrimer resin offers the possibility to overcome all these issues and allows for both mechanical and chemical recycling, as described below.¹⁴²⁻

145

Mechanical recycling

The PHTE-vitrimer could be recycled mechanically by techniques typically employed for thermoplastic materials. More in details, a two-step process was used, consisting of grinding the matrix and subsequent compression moulding of the pieces to obtain a “second generation” material **Figure 3.7A**).

The reprocessability of the vitrimer was evaluated by compression moulding followed by characterization after each processing cycle (analytically described in the experimental part), like bending tests, DMA, gel fraction, and FT-IR. The vitrimer could be easily processed by compression moulding at 100 °C for 5 min under 3 tons of pressure, into transparent and uniform sheets. After the initial bending test of the virgin material, it was ground and compression moulded, up to four times. After each reprocessing step, bending test, gel fraction and FT-IR were performed to prove that the material did not deteriorate. Even after the fourth reprocessing, no significant changes in mechanical performance (**Figure 3.6A, B and C**), crosslink density (**Table appx. 3.6 and Table appx. 3.7**) or chemical structure (**Figure appx. 3.10 and Figure appx. 3.11 and Figure appx. 3.13**) were observed, demonstrating the reliability of the reprocessability, dynamic nature and robustness of the developed biobased boronic ester vitrimer. Instead, the epoxy resin it was not possible to reprocess it due to the static covalent network. Indeed, when it was compression moulded it just broke to small pieces that did not fuse together under the tested conditions. (**Figure 3.7A**), as already shown in the previous paper.⁴⁷

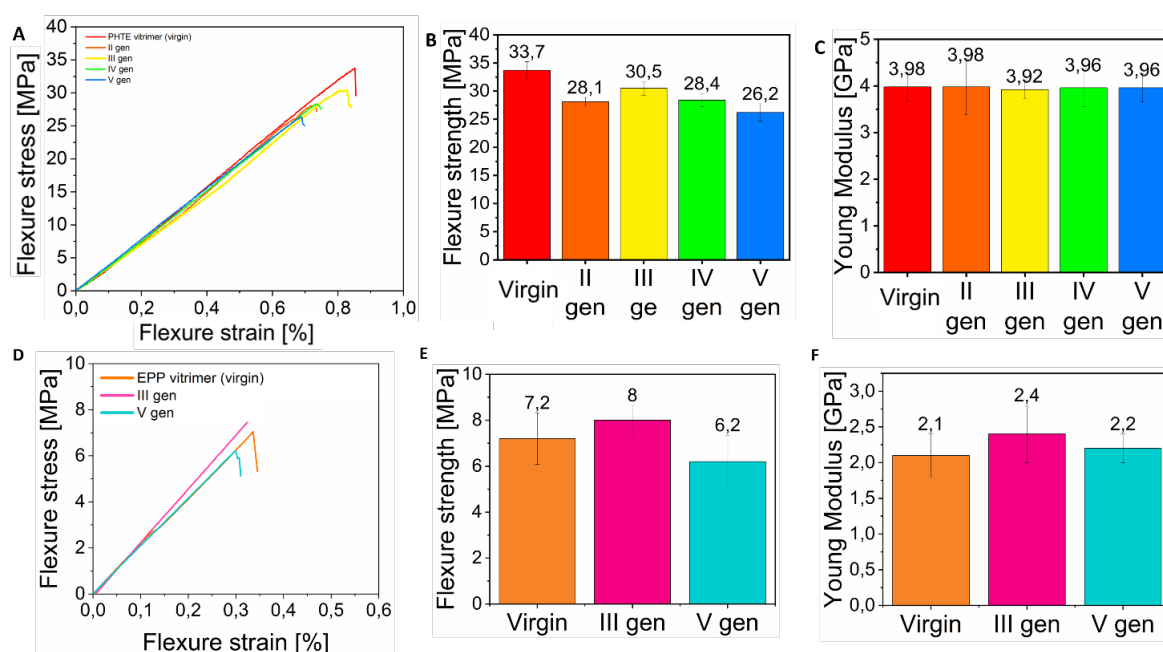


Figure 3.6 Typical bending curve (A), flexural strength (B) and young modulus (C) of the virgin (I gen) and the reprocessed (II-V gen) PHTE-vitrimer and bending curve (D), flexural strength (E) and young modulus (F) of the virgin and the reprocessed EPP-vitrimer

For what concern EPP-vitrimer it was reprocessable as the PHTE-vitrimer following the same method and parameters (**Figure 3.7A B**), moreover, even after subjecting the material to four reprocessing cycles, there were no notable alterations in mechanical performance crosslink density or chemical structure were observed. This demonstrates the efficiency of mechanical recycling (**Figure 3.6D, E and F, Figure appx. 3.10 and Figure appx. 3.13**).

DMTA analysis on the four times reprocessed PHTE-vitrimer gave another evidence of the effectiveness of the recycling, concluding that the material keeps the thermomechanical properties constant for, at least, 4 reprocessing cycles. Indeed, the DMTA curves of the virgin and reprocessed materials are overlapped (**Figure appx. 3.12**). TGA confirmed that the recycled vitrimer is stable up to around 250 °C, indeed there is no difference in the TGA analysis between the virgin and the recycled vitrimer (both chemically and mechanically) (**Figure appx. 3.10**) which is another proof about the solidity of the vitrimer.

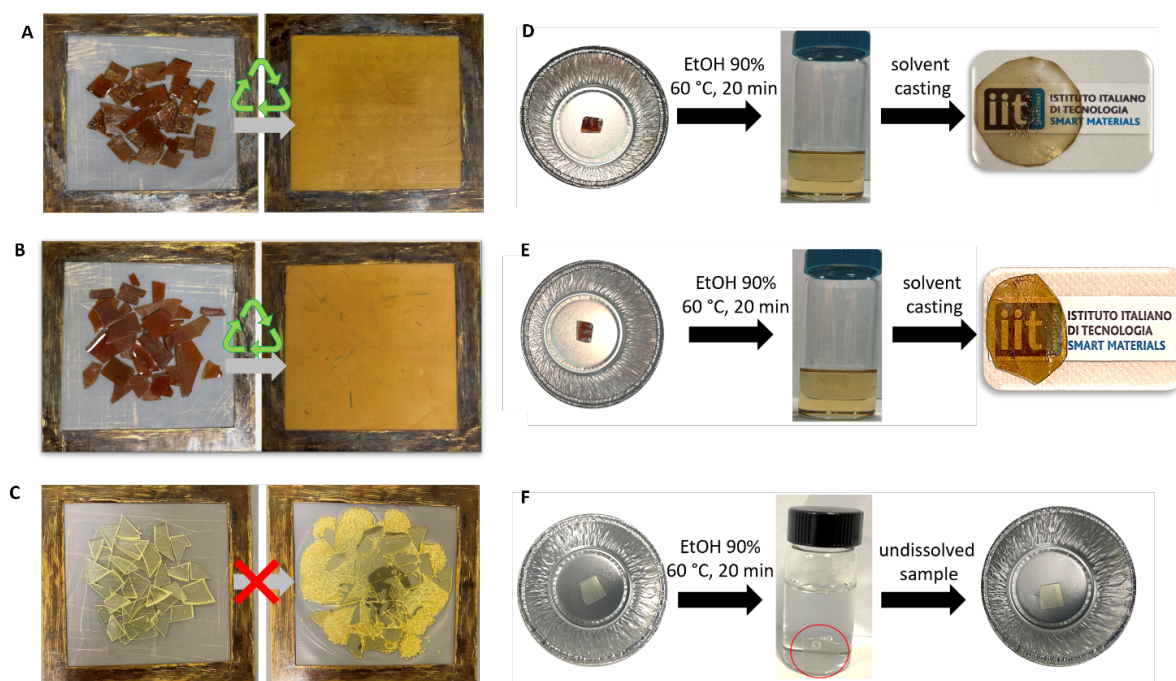


Figure 3.7 Mechanically recycled PHTE-vitrimer (A), EPP-vitrimer (B) and unsuccessful attempt to mechanically recycle the commercial epoxy (C) under 5 ton of pressure for 10 min at 100 °C; Chemical recycling of the vitrimers by hydrolysis and dissolution in 90% v/v ethanol at 60 °C for 20 minutes and subsequent solvent casting to regenerate the vitrimer as a thin, transparent film (D and E) and unsuccessful attempt to chemically recycle commercial epoxy (F).

Chemical recycling

The PHTE-vitrimer resin showed good resistance to different organic solvents such as THF, isopropanol and acetone, in the same way as the epoxy matrix. Nevertheless, since the vitrimer is characterized by the boronic ester motifs, hydrolysis of these linkages can occur. Taking advantage of this behaviour it is possible to subject the vitrimer to the chemical recycling in 90% v/v ethanol, a green solvent.^{146, 147} The dissolution of the vitrimer took place at RT but proceeded very slowly. On the other hand, by heating the mixture to 60 °C the dissolution was much faster and it took just 20 minutes to completely dissolve the material. Indeed, heating the material near the T_g makes it softer and much easier to dissolve. It was possible to dissolve 1 g of the material in 15 ml of the solvent and FT-IR measurements confirmed that it was possible to fully recover the original solid material by a simple casting of the hydrolysed solution (**Figure 3.7D** and **Figure appx. 3.13**).

The EPP-based vitrimer also exhibited a good chemical recyclability, in fact it was feasible to hydrolyse it following the same process used for the PHTE-based vitrimer (**Figure 3.7E**).

Besides, to confirm that the hydrolysis of the boronic ester bonds were responsible for the dissolution of the PHTE-based vitrimer it a ^1H NMR of the vitrimer dissolved in aqueous DMSO- d_6 was recorded, indeed -OH groups and diglycerol were detected (**Figure 3.8**). In addition to that, the epoxy signals of the PHTE disappeared as proof of the successful crosslinking. The same experiment was conducted on the EPP-based vitrimer (**Figure appx. 3.14**).

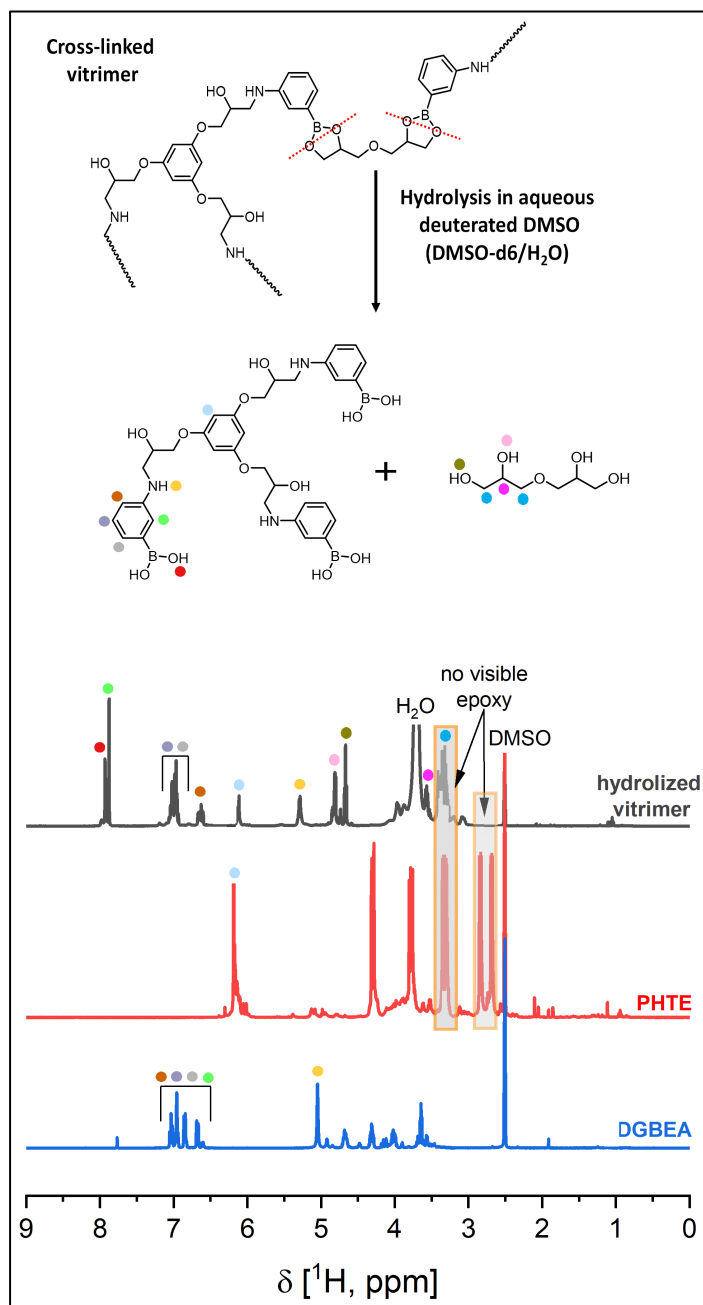


Figure 3.8 ^1H NMR spectra of PHTE (DMSO- d_6), DGBEA (DMSO- d_6) and PHTE-DGBEA vitrimer hydrolysed in aqueous DMSO- d_6 .

On the contrary, as already observed, the commercial epoxy cannot be chemical recycled under the same conditions (**Figure 3.7F**).

The recycling is much more efficient in comparison to the previous work⁴⁷, since it requires a less temperature and time to be completely hydrolysed. Making a fibre reinforced composite with the new PHTE-based vitrimer, as a matrix, the recycling will

be easier and faster as well as, the separation, purification, regeneration and reusing of both the matrix and reinforcements, a process that is not possible for traditional thermosets, like epoxy resins.

3.2.5 Carbon fibre composite preparation and characterization

In few recent years, researchers have been studying new approaches to overcome the difficulty of recycling thermoset polymers by modifying the matrix introducing linkers, which makes the materials much easier to break down under certain conditions while retaining their mechanical properties. More in details, one of this strategy is, indeed, cross-linking the matrix with dynamic bonds, such as boronic ester linkages.

To prove that, a composite with three carbon fibre layers using the new biobased PHTE-vitrimer resin was prepared by hand layup and compared to an epoxy composite, as described in the experimental section. The vitrimer composite showed an average elastic modulus of 25 GPa and a flexure strength of 396 MPa while the commercial epoxy composite had an average elastic modulus of 23 GPa and a flexural strength of 290 MPa (**Figure 3.9N, M and N**). The composites showed very similar mechanical performances, in particular the young modules for both the composites were almost identical, since the carbon fibres bears the greatest part of the load, indeed the function of the resin is to transfer the load to the reinforcement and to keep the composite together.

In order to evaluate the quality of the vitrimer composite in terms of impregnation capability of the resin, SEM and optical microscopy were employed. Images of the top and inner layers (**Figure 3.9B and D**) and of the cross-section (**Figure 3.9C and E**) revealed an excellent interfacial bonding between the carbon fibres and the matrices. Indeed, the vitrimer, as well as the commercial epoxy resin impregnated the carbon fibres very well, ensuring a good adhesion between the layers without exfoliation or slippage between the carbon layers and that is reflected in the high flexural strength for both composites. The TGA analysis showed that for the commercial epoxy composite the percentage of the matrix was (epoxy resin) 40% and the reinforcement (carbon fibres) 60% (**Figure appx. 3.15 and Figure appx. 3.16**). On the other hand, for the vitrimer composite was 40% reinforcements and 60% (**Figure appx. 3.17**) matrix which are the same values of obtained for the composite made with ELO discussed in chapter II. In comparison to the ELO-based composite, the PHTE-based composite showed higher mechanical performance most probably thanks to the better performance showed by the PHTE vitrimer matrix. The densities of both composites are very similar since the densities of both the matrices (vitrimer and commercial epoxy) are quite close (**Table appx. 3.5**).

Developing a fibre-reinforced composite using, also, the EPP-vitrimer as the matrix is crucial for a more thorough characterization of the matrix (EPP-vitrimer) and its behaviour.

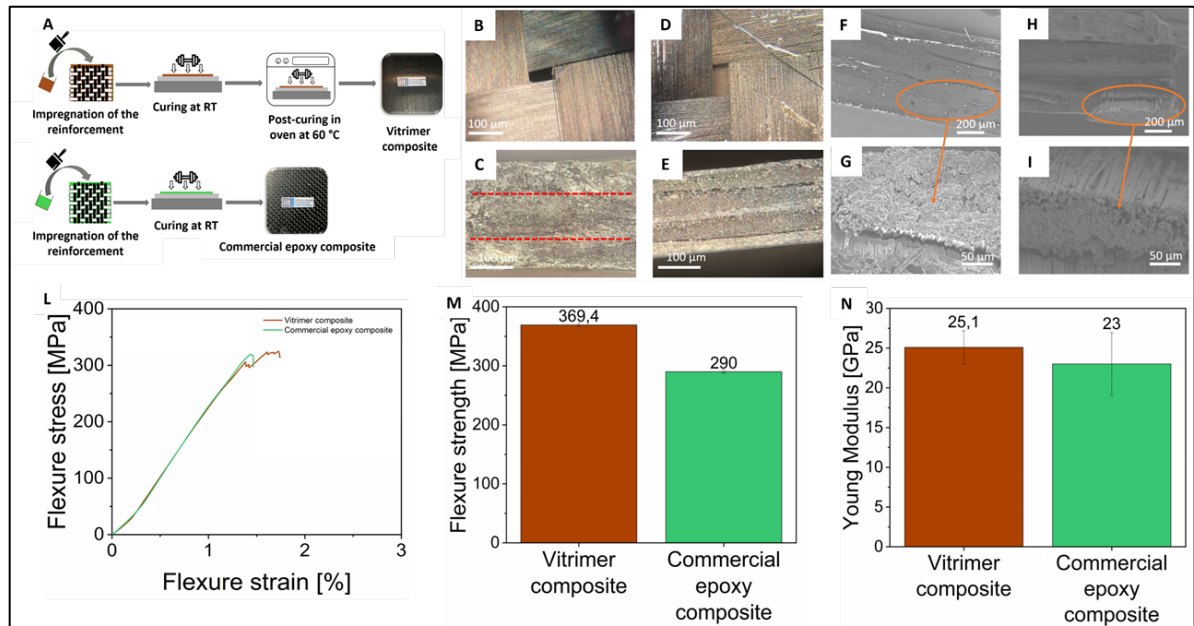


Figure 3.9 Fabrication of the carbon fibre-reinforced composites (A); Optical microscope images of the top surface and the cross-section of the PHTE-vitrimer composite (B-C) and commercial epoxy composite (D-E); SEM images of the cross-section of the PHTE-vitrimer composite (F-G) and the commercial epoxy composite (H-I); Typical flexural curve (L), flexural strength (M) and Young Modulus (N) of the PHTE-vitrimer composite and the commercial epoxy composite.

3.2.6 Composites recycling

The high potential and unique characteristics possessed by carbon fibres have led to a significant increment in their market demands in the last decades, however this has brought the problem of recycling. Indeed, when incorporated into a thermoset polymer matrix they became hardly recyclable due to the difficulty of recycling reinforced thermoset materials, as previously described. Indeed, the impossibility of removing the matrix without damaging the reinforcements is the biggest problem concerning the recycling of the above-mentioned materials. 148, 156

Since the PHTE-vitrimer resin was easily soluble in 90% v/v ethanol, a recyclability attempt was conducted on the vitrimer composite (Figure 3.10A).

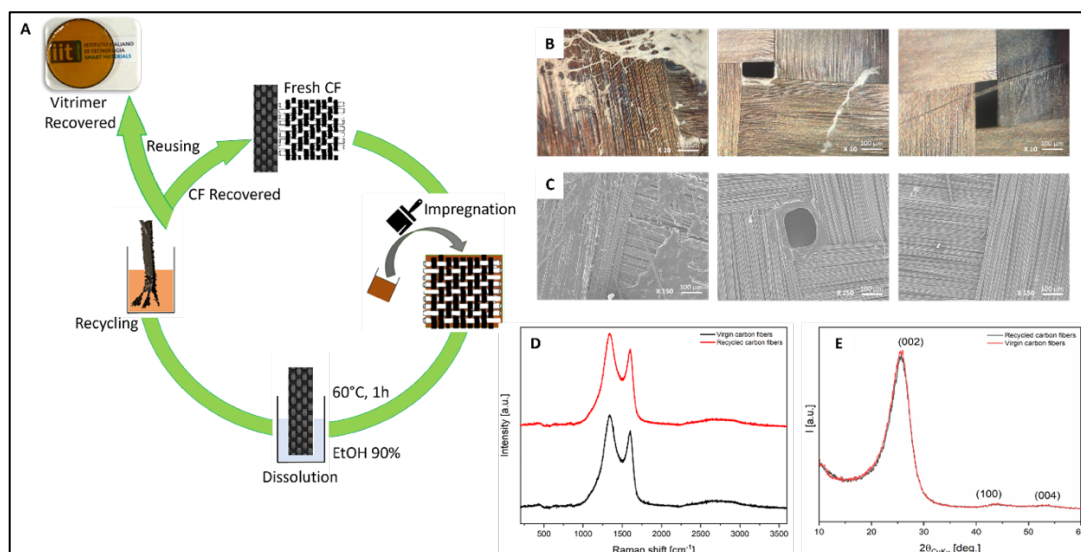


Figure 3.10 Recyclability scheme of the PHTE-vitrimer composite (A); Optical (B) and SEM (C) images of recycled carbon fibre at different time of the process at 0h, 1.5h and 3h.; Raman spectra of the virgin and recycled carbon fibres (D); XRD patterns of the virgin and recycled carbon fibres (E).

On the other hand, as mentioned before, since the commercial epoxy did not dissolve in EtOH 90% v/v due to its thermosetting nature it was not possible to recycle the composite and recover the carbon fibres under the previously mentioned conditions (**Figure appx. 3.18**).

On the contrary, thanks to the hydrolysis of the boronic ester linkages of the PHTE-vitrimer resin, it was possible to efficiently recycle the vitrimer composite under very mild conditions. The vitrimer composite was placed in EtOH 90% v/v solution at 60 °C and kept for 3h, instead of 20 minutes to be completely sure that all the residues of resin on the carbon fibres are dissolved.

At the end of the process, the three carbon fibre layers could be easily separated, washed with fresh EtOH 90% v/v and dried under ambient conditions. The vitrimer itself could be regenerated as well by simple evaporation of the solvent. Employing the chemical recycling more than 99% of the carbon fibre and vitrimer matrix were recovered (**Table appx. 3.8**).

After the recovering of the carbon fibres, surface morphology and mechanical properties were further determined by optical microscopy, SEM, XRD and Raman spectroscopy. The SEM analysis showed that the morphology of the recovered carbon fibres was indistinguishable from the pristine ones, proving the effectiveness of the recycling process. In addition, from the optical microscopy and SEM analysis it was notable that the recycled carbon fibres did not have any vitrimer residues attached (**Figure 3.10B and C**).

Furthermore, the XRD and Raman spectroscopy performed on the recycled carbon fibres showed no change in comparison to the virgin ones (**Figure 3.10E and F**). To prove that the recycled carbon fibres have not been damaged a new composite was prepared using a new vitrimer resin. The flexural stress-strain curves (**Figure appx. 3.19**) of the pristine vitrimer composite and the recycled vitrimer composite were almost the same, a proof that the recycling method not only allows for the recycling of the reinforcements, but ensure also to preserve fibres' structure and any their mechanical properties. Since CF has high costs, the recycling of CF without sacrificing performance characteristics could bring huge benefits from the economic point of view.

3.3 CONCLUSIONS

It was utilized an environmentally friendly and catalyst and solvent-free process to synthesize a new biobased vitrimer (PHTE-DGBEA) which has chemistry similarities with epoxy resins, specifically involving amino-epoxy coupling. This novelty is based on the reaction between a new amino-boronic crosslinker and the phloroglucinol triglycidyl ether. Additionally, it demonstrates the ability of the new crosslinkers to engage with a commercial epoxy pre-polymer, commonly employed in epoxy resin preparation. A significant advancement lies in its room temperature (RT) curing capability, marking this material as the first amino-boronic vitrimer curable under ambient conditions.

The bending test on the vitrimer showed a brittle behaviour similar to a commercial epoxy resin. Moreover, thanks to the dynamic nature of the material it exhibits a shape memory effect with the possibility of changing not only the temporary, but also the permanent shape, behaviour not possible for a traditional thermoset.

The vitrimer displays an excellent recyclability both mechanically and chemically, it was reprocessable through techniques typically employed for thermoplastics and easily subjected to hydrolysis in aqueous ethanol following a solvent casting to regenerate the original material. Besides, both the cross-linker and the vitrimer were found to be biodegradable in sea water meaning that in case it accidentally ends up in the marine environment a waste accumulation will be prevented.

Since the vitrimer has shown a good recyclability, it can be used to build carbon fibre composites, indeed at the end of its life it can be recycled fully recovering both the matrix and the reinforcement layers. In addition, the vitrimer composite has a very similar mechanical performance and density to the traditional one made with commercial epoxy resin.

In summary, the presented composite can solve most problems concerning traditional thermoset composites, since it is made from biobased resources and allows for a fast and easy recovery of the reinforcement under very mild conditions. Besides that, the matrix can be prepared following the same curing method of a commercial epoxy resin with the advantages of being able to be repaired, reused and recycled multiple times, keeping the same mechanical performance.

3.4 APPENDIX

Design of the vitrimer resin

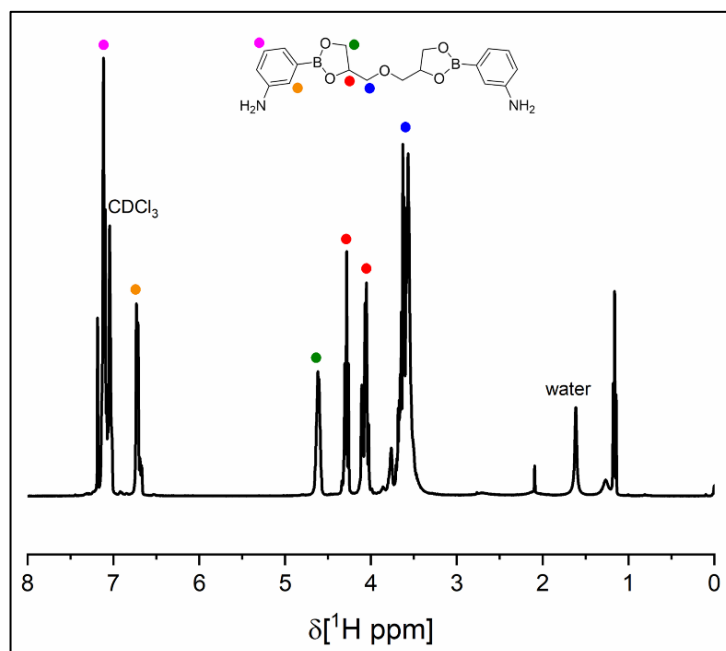


Figure appx. 3.1 ¹H NMR spectra of DGBEA in CDCl₃.

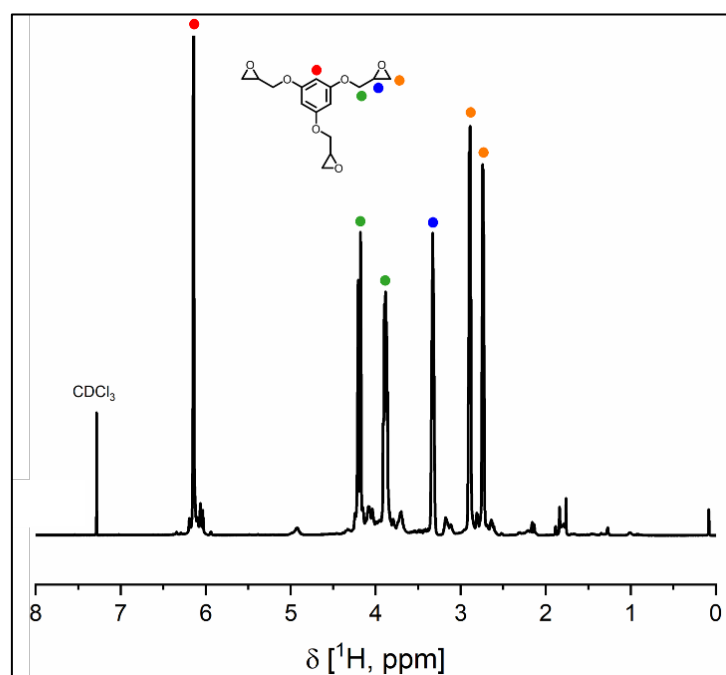


Figure appx. 3.2. ¹H NMR spectra of PHTE in CDCl₃.

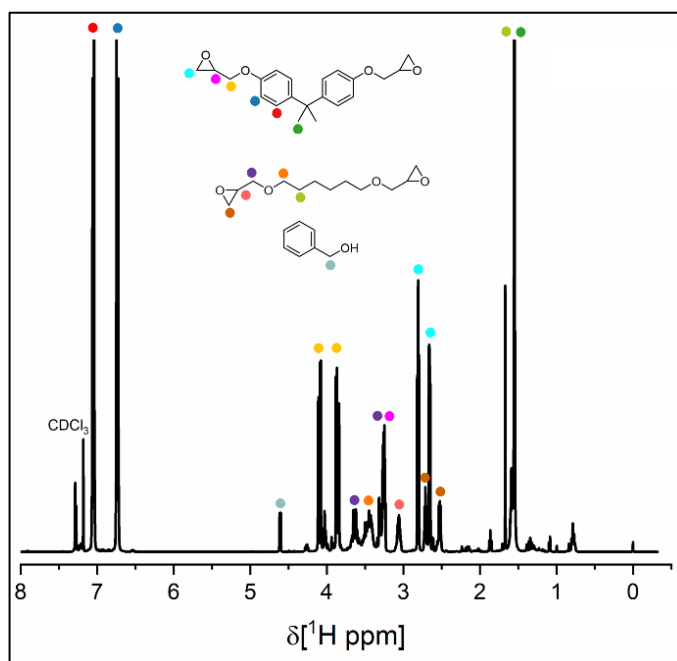


Figure appx. 3.3 ^1H NMR spectra of EPP in CDCl_3 .

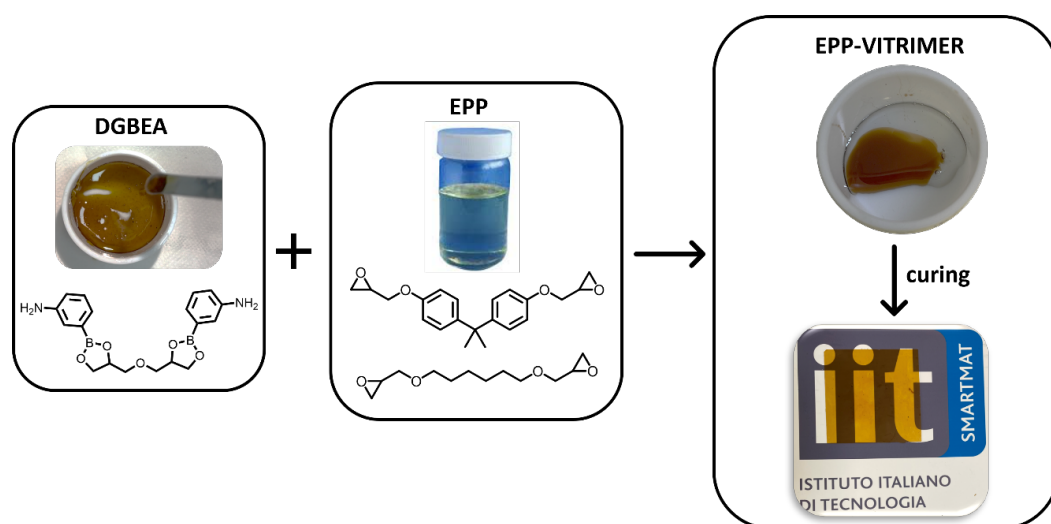


Figure appx. 3.4 Schematic representation of the EPP-DGBEA vitrimer synthesis.

From the ^1H NMR analysis was found that the commercial epoxy resin (according to the data sheet) was made of: 79% mol bisphenol A diglycidyl ether (BADGE), 18% mol 1,4-butanediol diglycidyl ether (BDDGE) and 2,7% mol benzyl alcohol

The molecular weight of the BADGE is 340,42 g/mol \rightarrow 3658,4 g is the weight of the BADGE

The molecular weight of the BDDGE is 202,25 g/mol \rightarrow 26936,5 g is the weight of the BDDGE

The molecular weight of the benzyl alcohol is 108,14 g/mol \rightarrow 301,1 g is the weight of the benzyl alcohol

In total the weight of the sample is: 30895,9 g

The epoxy mols are: (79 mol + 19 mol) $\cdot 2 = 194,4$ mol (since each molecule has 2 epoxy groups)

Therefore, taking as weight 100g, the mol of epoxy groups are: 0,63 mol (or 6,3 mmol of epoxy groups/grams of sample)

Figure appx. 3.5 Epoxy content calculation for the commercial epoxy sample

Table appx. 3.1 Composition, gel fraction after post-curing and glass transition temperature of the vitrimer resins and the commercial epoxy resin

Material	Component A [g]	Component B [g]	Gel Fraction [%]	T_g (DSC) ^b [°C]
PHTE-vitrimer	PHTE	DGBEA		
	3,25	6,74	99	74.0
EPP-vitrimer	BADGE based epoxy resin (EPP)	DGBEA		
	4,59	5,41	95	55.0
Thermoset	BADGE based epoxy resin (EPP)	Polyamine hardener		
	6,66	3,33	99,6	63.0

^b β transition temperatures (T_β) were determined by DSC from the second heating scan.

Table appx. 3.2 Gel fraction of the PHTE-vitrimer (curing) at different curing times.

Material (vitrimer)	Before [mg]	After [mg]	Gel fraction [%]
1	200,3	7,200	3,60
2	202,0	20,80	10,3
3	201,3	34,60	17,2
4	201,2	49,10	24,4
5	204,2	61,70	30,2
6	205,1	75,30	36,7
7	204,2	90,80	44,5
8	200,6	107,7	53,7
9	205,2	130,5	63,6
12	199,3	148,9	74,7
15	200,4	167,7	83,7
18	201,6	178,2	88,4
21	202,4	178,9	88,4
24	199,1	176,2	88,5
27	200,2	177,1	88,5

30	198,4	175,4	88,4
36	199,1	176,2	88,5

Table appx. 3.3 Gel fraction of the PHTE-vitrimer (post-curing) at different curing times.

Material (vitrimer)	Before [mg]	After [mg]	Gel fraction [%]
1	202,3	191,8	94,8
1,5	203,5	200,4	98,5
3	205,3	203,2	99
4,5	202,7	200,7	99
6	199,6	197,4	98,9
9	203,1	201,1	99
18	201,3	199,5	99,1
24	206,6	204,7	99,1
36	201,1	199,1	99

Table appx. 3.4 Gel fraction of the vitrimers and the commercial epoxy.

Material	Before [mg]	After [mg]	Gel Fraction [%]
PHTE-vitrimer (curing)	201,6	181,4	88,0
PHTE-vitrimer (post-curing)	204,3	202,3	99,0
EPP-vitrimer (curing)	202,3	161,8	80,0
EPP-vitrimer (post- curing)	201,6	181,4	95,0
Thermoset Commercial epoxy	201,3	200,5	99,6

Table appx. 3.5 Density of the PHTE-vitrimer, the commercial epoxy and the composites.

Material	Gel Fraction [g/cm ³]	Standard Deviation
Vitrimer	1,22	0,013
Commercial epoxy	1,13	0,017
Vitrimer composite	1,34	0,036
Commercial epoxy composite	1,31	0,040

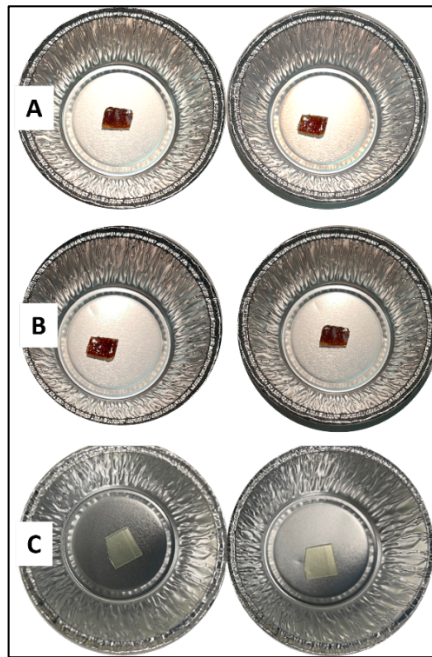


Figure appx. 3.6 Samples of the PHTE-vitrimer (A), EPP-vitrimer and the commercial epoxy (B) before (left) and after (right) the gel fraction test.

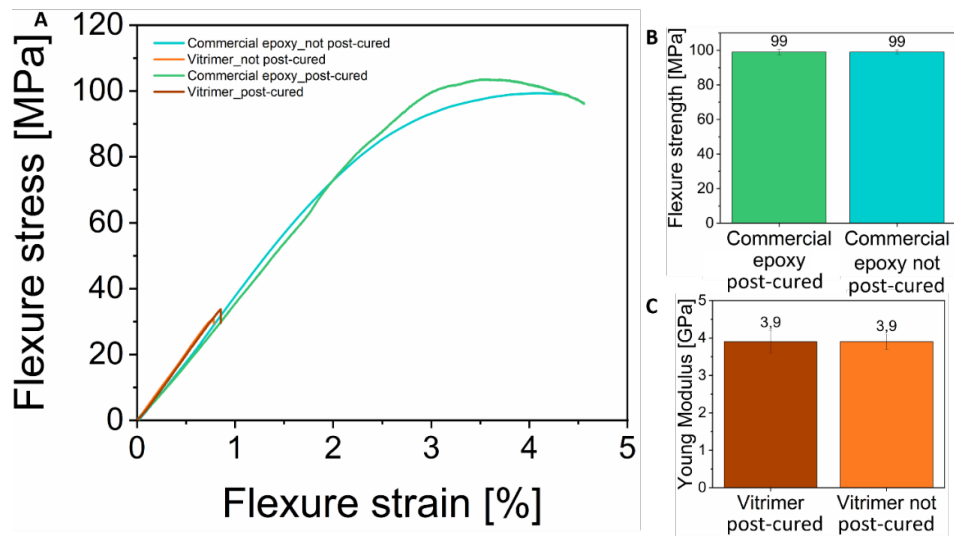


Figure appx. 3.7 Typical flexural curve (A), young modulus (B) and flexural strength (C) of PHTE-vitrimer and epoxy resin cured and post-cured.



Figure appx. 3.8 PHTE-vitrimer sample before (A) after the DMA measurement (B).

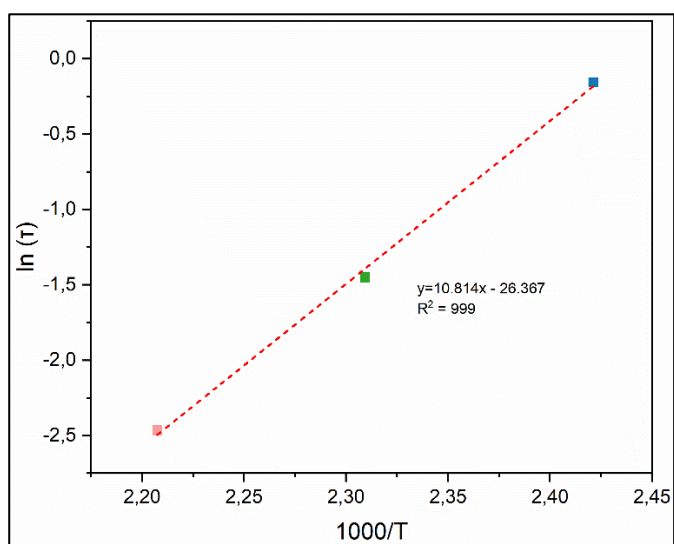


Figure appx. 3.9 Arrhenius plot of relaxation times of the PHTE-vitrimer.

Vitrimer recycling

Reprocessability (mechanically recycling)

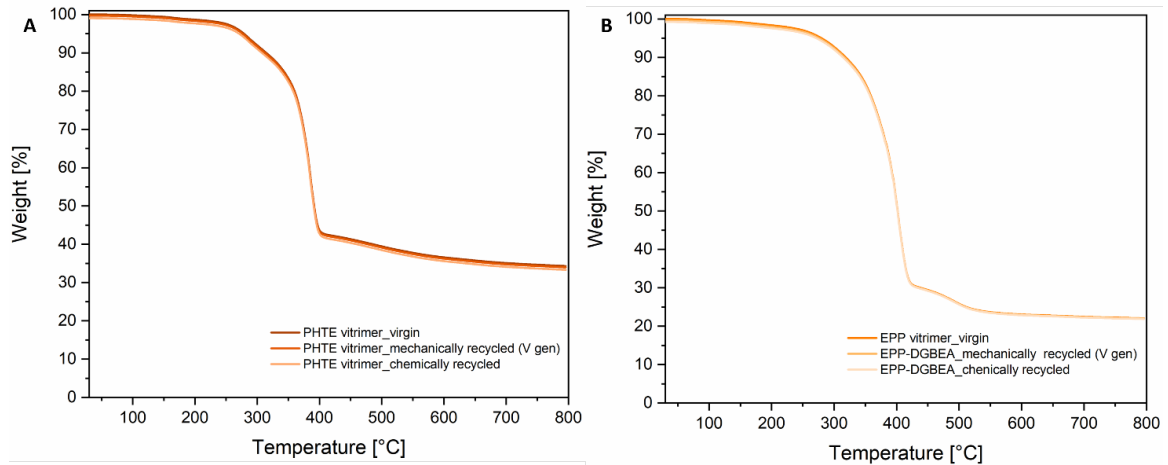


Figure appx. 3.10 TGA curves of virgin, mechanically and chemically recycled PHTE-vitrimer (A) and EPP-vitrimer (B).

Table appx. 3.6 Gel fraction, thermal stability and mechanical performance of the virgin and the reprocessed PHTE-vitrimer.

Material (vitrimer)	Gel Fraction [%]	T_g (DSC) [°C]	Young Modulus (Bending test) [GPa]
I Gen (Virgin Material)	99,0	74,0	3,98
II Gen	99,0	74,0	3,98
III Gen	98,9	74,0	3,92
IV Gen	99,1	74,0	3,96
V Gen	99,0	74,0	3,96

Table appx. 3.7 Gel fraction of the virgin PHTE-vitrimer and reprocessed up to 4 times.

Material (vitrimer)	Before [mg]	After [mg]	Gel fraction [%]
I Gen (Virgin Material)	201,6	202,2	99,0
II Gen	202,5	200,6	99,1
III Gen	201,3	199,0	98,9
IV Gen	200,4	198,4	99,0
V Gen	201,6	199,6	99,0

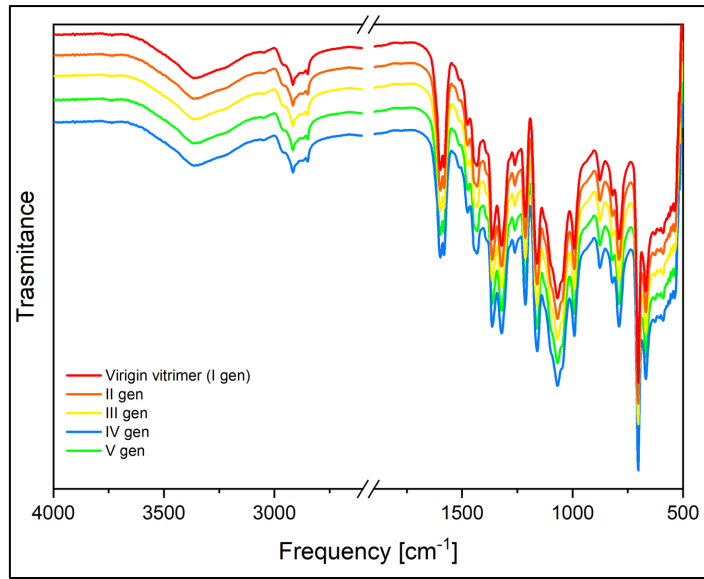


Figure appx. 3.11 FT-IR spectra of the virgin PHTE-vitrimer and reprocessed up to 4 times.

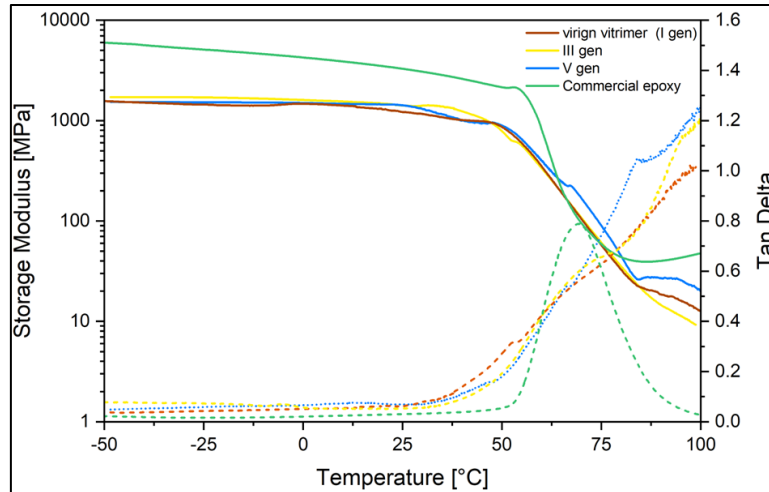


Figure appx. 3.12 DMTA curves of virgin (I gen) and reprocessed (III-V gen) PHTE-vitrimer and commercial resin.

Recycling (chemical recycling)

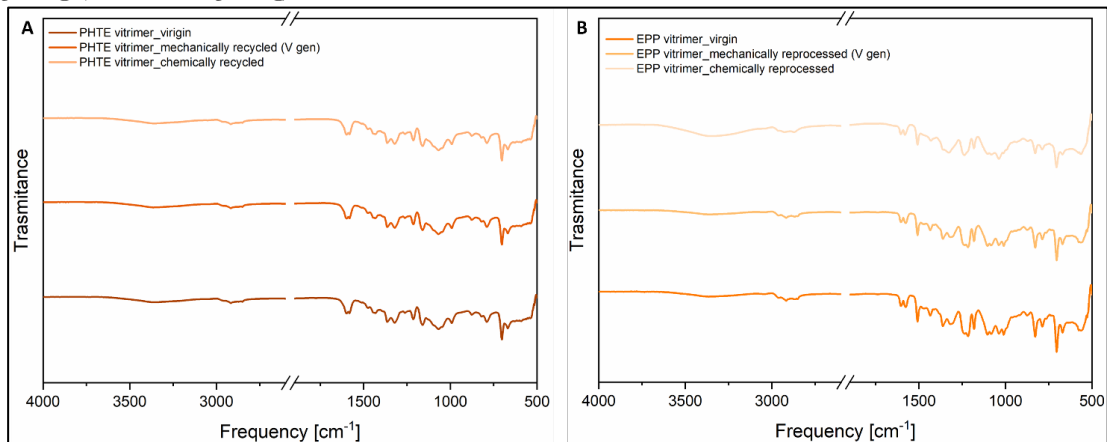


Figure appx. 3.13 FT-IR spectra of vitrimer as synthesized and after chemical and mechanical recycling (A); recovered material after hydrolysis in 90% v/v EtOH and casting (chemical recycling)

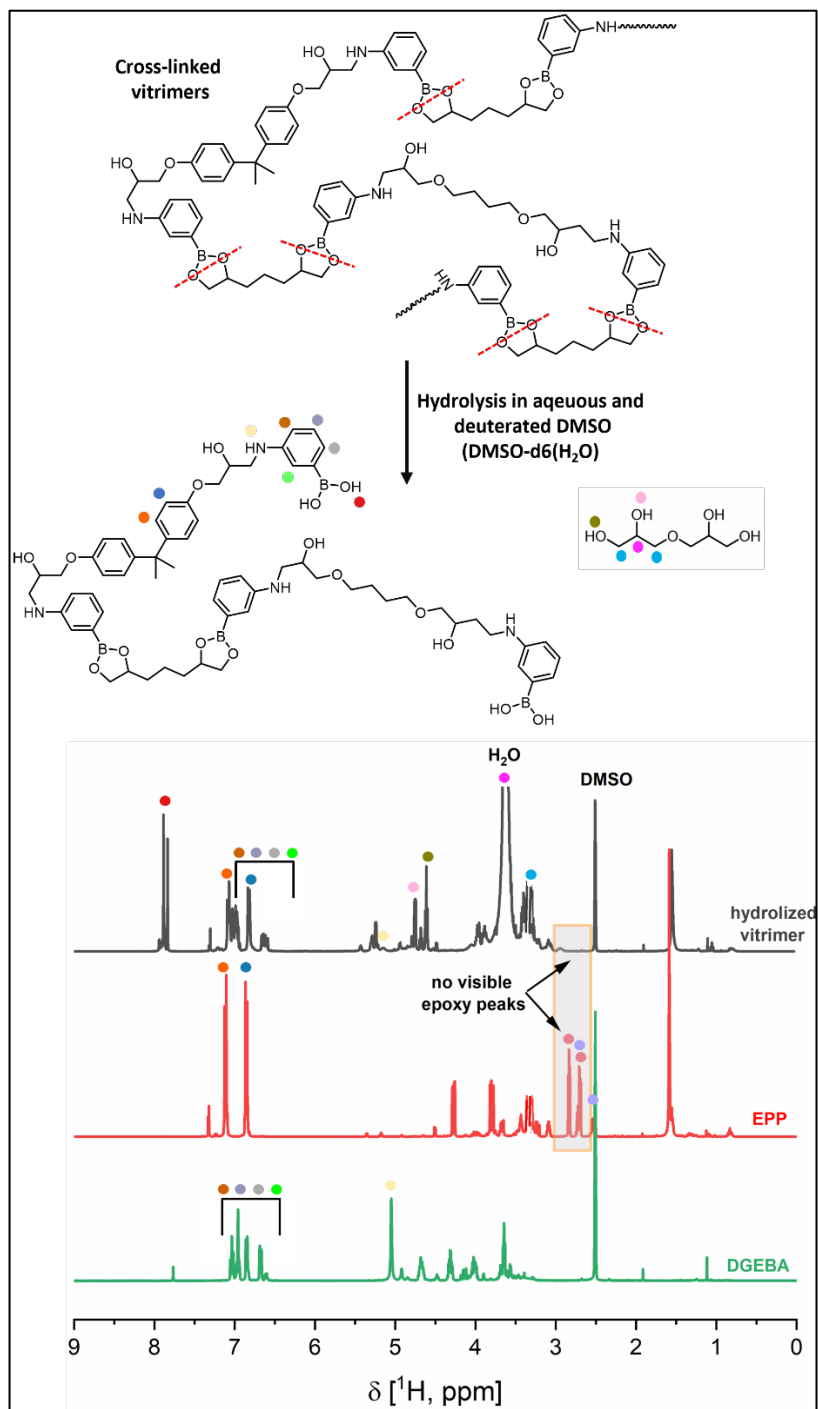


Figure appx. 3.14 ¹H NMR spectra of EPP (DMSO-d₆), DGEBA (DMSO-d₆) and EPP-DGEBA vitrimer hydrolysed in aqueous DMSO-d₆.

Composites Recycling

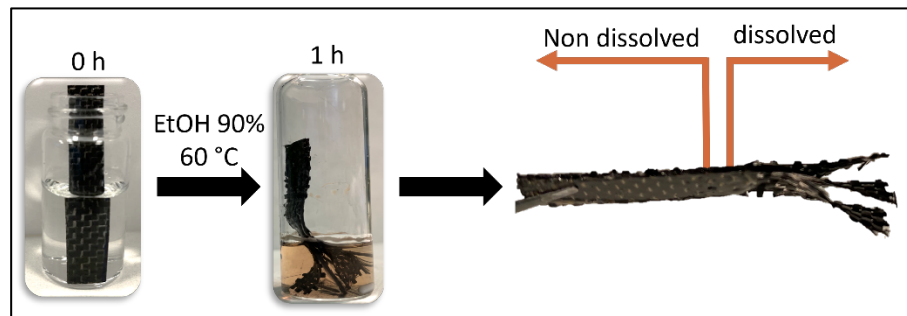


Figure appx. 3.15 Partial dissolution of the PHTE-vitrimer matrix in 90% EtOH solution (left part) and carbon fibres in contact with the solution were separated from the resin (right part)

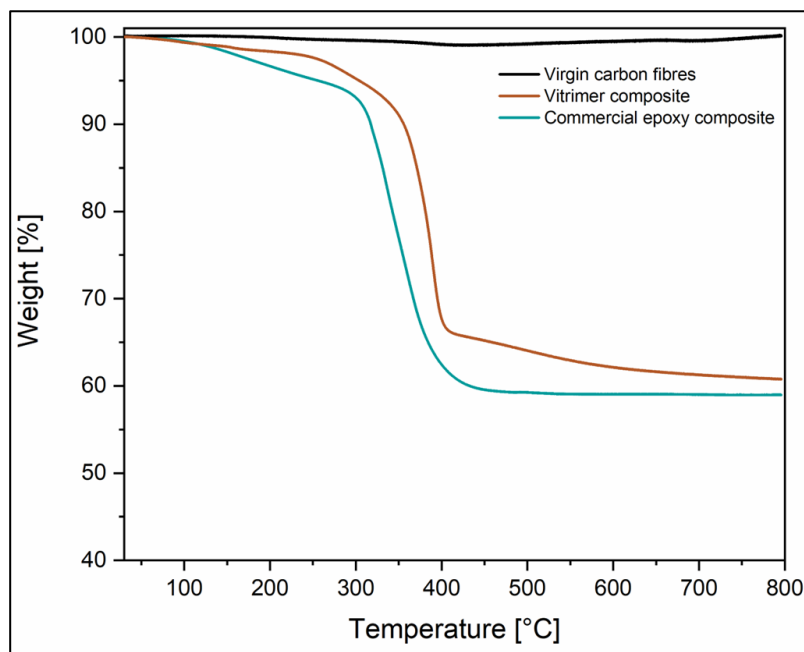


Figure appx. 3.16 TGA curves of the virgin carbon fibres (black), PHTE-vitrimer composite (brown) and commercial epoxy composite (aqua green).

Reinforcement: 100%
 Vitrimer residue: 35%
 Vitrimer composite residue: 60%

Vitrimer composite $0,6 = x \cdot 0,35 + (1 - x) \cdot 1 \rightarrow 0,6 = 0,35x - 1x + 1 \rightarrow 0,65x = 0,4 \rightarrow x \sim 0,6 \rightarrow 60\% \text{ matrix}$

Figure appx. 3.17 Matrix and reinforcement content

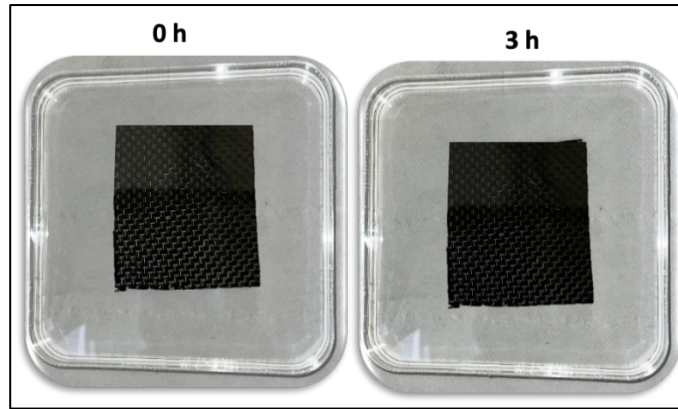


Figure appx. 3.18 Unsuccessful attempt to recycle carbon fibre-reinforced commercial epoxy composite in 90% EtOH solution.

Table appx. 3.8 Chemical Recyclability of the PHTE-vitrimer, commercial epoxy, commercial epoxy composite and PHTE-vitrimer composite.

Material (vitrimer)	Material Recycled [%]	Material dissolved [%]	Material undissolved [%]
Vitrimer matrix	99,7	100	-
Vitrimer composite	99,0	60% (vitrimer matrix)	40% (CF)
Commercial epoxy matrix	-	-	98,5
Commercial epoxy composite	-	-	99,4

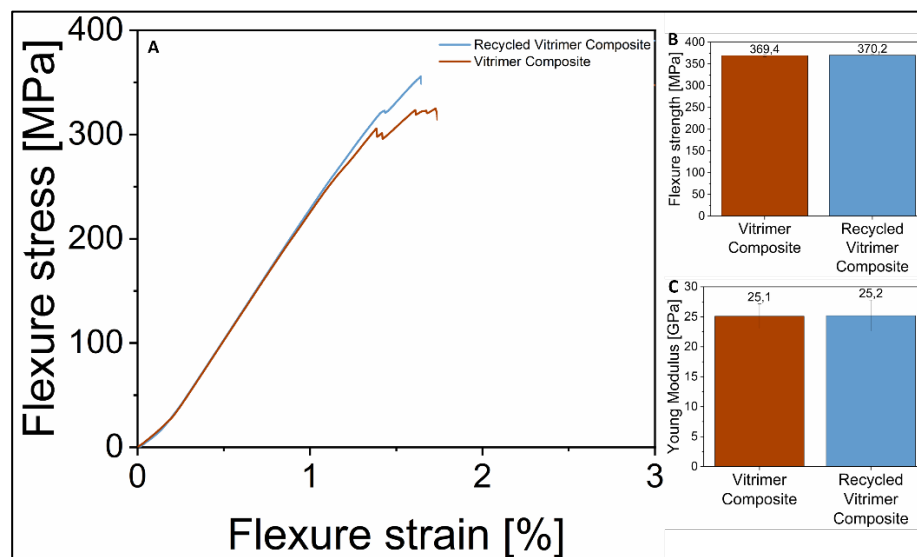


Figure appx. 3.19 Typical bending curve (A), flexural strength (B) and young modulus (C) of the virgin and recycled PHTE-vitrimer composite

Conclusions and outlook

The objective of this thesis was to explore the possibility of replacing epoxy resins, typically used to prepare high performance fibre-reinforced composites, by a new class of material characterized by a dynamic behaviour - vitrimers. The ideal candidate material should be, firstly biobased, and secondly reprocessable and recyclable.

As first example a diboronic ester dithiol cross-linker was used, through a catalyst and solvent free synthesis, to prepare the ELO-DBEDT vitrimer. The material was found reprocessable, recyclable and biodegradable. The mechanical performance was satisfying and it was possible to prepare a carbon reinforced composites and compare it with the one prepared with a commercial epoxy resin. Satisfyingly, both the composites showed equal mechanical performance.

Then, since the aim of the project was to replace epoxy resins which are typically comprised of two liquid components: an epoxy resins and a polyamine hardener, the focus was placed on the cross-linker.

The DBEDT hardener had two main drawbacks, indeed it was solid, therefore, to synthesize the vitrimer it was necessary to warm up the reaction mixture until the melting point of the crosslinker and then the curing required high temperature. Instead, generally epoxy resin are prepared from viscous liquid reagents and cured at room temperature. Secondly thioglycerol, a toxic compound with a very unpleasant smell had to be used for the synthesis in order to introduce the thiol functional groups.

Therefore, the synthesis was re-drawn, following the green chemistry principles, using safe chemicals and replacing thiol groups with alternative functional groups including amino groups.

Many variants were prepared and the most promising one, the DGBEA, was used to produce a new vitrimer using an epoxy molecule from brown algae (PHTE). Finally, the curing was possible at RT and the material showed better mechanical performance than the ELO-based vitrimer. Moreover, the recycling and reprocessing of the PHTE based vitrimer were easier and it showed a comparable biodegradability to the ELO-vitrimer. Furthermore, the versatility of this new boronic acid diamine crosslinker was demonstrated by using it to cure a commercial epoxy resin instead of the standard polyamine hardener producing a recyclable, dynamic material (EPP-based vitrimer) which, yet, requires further analysis to be completely characterized.

Carbon reinforced composite fabricated using the PHTE-DGBEA resin showed the highest performance, even higher than the composite prepared with the commercial epoxy resin.

The synthesized vitrimers have great potential to solve the most relevant problems facing thermosetting materials and could be a good alternative to epoxy resins.

Some potential improvements could be: assess production costs for large-scale manufacturing of these vitrimers, indeed, identifying cost-effective raw materials and scalable synthesis methods can make these materials more commercially viable.

Despite achieving satisfying mechanical properties, continuous research is necessary to improve the strength, durability, and stability of vitrimers could broaden their applications and competitiveness. Though the boronic ester vitrimers show promise in biodegradability, striving for even higher eco-friendliness could be an area for future research. Exploring additives or modifications to accelerate decomposition without compromising performance is valuable.

Since the most of the raw material are biobased, assessing the availability and sustainability of raw materials, especially biobased ones, on a large scale is vital for mass production.

Addressing these improvements and challenges could pave the way for wider adoption of vitrimers as a viable alternative to epoxy resins, offering enhanced performance and eco-friendly characteristics.

Focusing on the synthesized cross-linkers, further research might focus on enhancing the stability of liquid cross-linkers, especially those prone to degradation at low temperatures, like *o*-DGBEA. Strategies to improve their thermal resilience without compromising their liquid state could be explored.

Moreover, the investigation of a wider range of flexible tetraols and their impact on the resulting material's properties could offer insights into achieving desired melting points and structural characteristics. This includes exploring variations in molecular weight or branching in these tetraols.

Delving deeper into the influence of different functional groups (amino, hydroxyl, carboxyl) within the phenyl ring of the boronic acid on the material properties could be beneficial. Understanding the interplay between these groups and their impact on crystallinity and melting points would enrich the understanding of molecular interactions. But also, exploring how the positioning of functional groups in the aromatic ring affects both the thermal stability of the resulting product and the ease of obtaining a pure, well-defined compound could provide insights into optimizing synthesis pathways. In fact, investigating the specific interactions (such as hydrogen bonding) between different functional groups within the cross-linker molecules could provide a deeper understanding of their influence on material properties. But also, exploring the compatibility of these cross-linkers with different molecules (pre-polymers) or blends might open avenues for designing customizable materials with specific properties suited for diverse applications. In additions, assessing the feasibility of scaling up the synthesis methods for these cross-linkers and evaluating their potential applications in industrial settings could pave the way for practical implementation.

In conclusion, by delving deeper into the molecular interactions, exploring a wider range of tetraols, and assessing their applicability in real-world scenarios, further advancements can be made towards tailoring cross-linkers and designing materials with specific properties for various industries and applications.

List of publications and patents

Peer-reviewed journal publications:

Sangaletti, D.; Ceseracciu, L.; Marini, L.; Athanassiou, A.; Zych, A., Biobased boronic ester vitrimer resin from epoxidized linseed oil for recyclable carbon fiber composites. *Resources, Conservation and Recycling* 2023, 198, 107205. <https://doi.org/10.1016/j.resconrec.2023.107205>

Patent applications:

Sangaletti, D.; Athanassiou, A.; Zych, Low melting and liquid boronic ester cross-linkers for preparation of vitrimers (currently under submission)

References

1. wordsense.eu <https://www.wordsense.eu/plastica/>.
2. statista.com <https://www.statista.com/search/?q=polymers&Search=&p=1>.
3. plasticseurope.org <https://plasticseurope.org>.
4. Baur, E.; Osswald, T. A.; Rudolph, N., 2 - Introduction. In *Plastics Handbook*, Baur, E.; Osswald, T. A.; Rudolph, N., Eds. Hanser: 2019; pp 13-43.
5. op.europa.eu <https://op.europa.eu/en/publication-detail/-/publication/e69ac5e8-9337-481f-b9ab-3fa7497ebb6c>.
6. ourworldindata.org <https://ourworldindata.org/grapher/mean-product-lifetime-plastic>.
7. Siddique, R.; Khatib, J.; Kaur, I., Use of recycled plastic in concrete: a review. *Waste Manag* **2008**, *28* (10), 1835-52.
8. Wilcox, C.; Van Sebille, E.; Hardesty, B. D., Threat of plastic pollution to seabirds is global, pervasive, and increasing. *Proceedings of the National Academy of Sciences* **2015**, *112* (38), 11899-11904.
9. Schuyler, Q.; Hardesty, B. D.; Wilcox, C.; Townsend, K., Global analysis of anthropogenic debris ingestion by sea turtles. *Conserv Biol* **2014**, *28* (1), 129-39.
10. Ellenmacarthurfoundation.org <https://www.ellenmacarthurfoundation.org/the-new-plastics-economy-rethinking-the-future-of-plastics-and-catalysing>.
11. Geyer, R.; Jambeck, J. R.; Law, K. L., Production, use, and fate of all plastics ever made. *Sci Adv* **2017**, *3* (7), e1700782.
12. www.eea.europa.eu <https://www.eea.europa.eu/publications/european-marine-litter-assessment/mismanaged-waste-a-key-source>.
13. oceanservice.noaa.gov <https://oceanservice.noaa.gov/facts/microplastics.html>.
14. iucn.org <https://www.iucn.org/our-work/region/mediterranean/our-work/marine-biodiversity-and-blue-economy/plastics-mediterranean>.
15. european-bioplastics.org <https://www.european-bioplastics.org/bioplastics/>.
16. plasticsrecyclers.eu <https://www.plasticsrecyclers.eu>.
17. Lee, A.; Liew, M. S., Tertiary recycling of plastics waste: an analysis of feedstock, chemical and biological degradation methods. *Journal of Material Cycles and Waste Management* **2021**, *23* (1), 32-43.
18. Rahimi, A.; García, J. M., Chemical recycling of waste plastics for new materials production. *Nature Reviews Chemistry* **2017**, *1* (6), 0046.
19. Coates, G. W.; Getzler, Y. D. Y. L., Chemical recycling to monomer for an ideal, circular polymer economy. *Nature Reviews Materials* **2020**, *5* (7), 501-516.
20. Singh, N.; Hui, D.; Singh, R.; Ahuja, I. P. S.; Feo, L.; Fraternali, F., Recycling of plastic solid waste: A state of art review and future applications. *Composites Part B: Engineering* **2017**, *115*, 409-422.
21. Lazarevic, D.; Aoustin, E.; Buclet, N.; Brandt, N., Plastic waste management in the context of a European recycling society: Comparing results and uncertainties in a life cycle perspective. *Resources, Conservation and Recycling* **2010**, *55* (2), 246-259.
22. Hopewell, J.; Dvorak, R.; Kosior, E., Plastics recycling: challenges and opportunities. *Philos Trans R Soc Lond B Biol Sci* **2009**, *364* (1526), 2115-26.
23. iso.org <https://www.iso.org/obp/ui/en/#iso:std:iso:15270:ed-2:v1:en>.

24. Schyns, Z. O. G.; Shaver, M. P., Mechanical Recycling of Packaging Plastics: A Review. *Macromolecular Rapid Communications* **2021**, *42* (3), 2000415.
25. 2022, p. o.-t. f. <https://plasticseurope.org/knowledge-hub/plastics-the-facts-2022-2/>.
26. Stern, M. D.; Tobolsky, A. V., Stress-Time-Temperature Relations in Polysulfide Rubbers. *The Journal of Chemical Physics* **2004**, *14* (2), 93-100.
27. Osthoff, R. C.; Bueche, A. M.; Grubb, W. T., Chemical Stress-Relaxation of Polydimethylsiloxane Elastomers¹. *Journal of the American Chemical Society* **1954**, *76* (18), 4659-4663.
28. Tobolsky, A. V.; Carlson, D.; Indictor, N., Viscoelastic properties of plasticized polymers. *Journal of Applied Polymer Science* **1963**, *7* (1), 393-397.
29. Chen, X.; Dam, M. A.; Ono, K.; Mal, A.; Shen, H.; Nutt, S. R.; Sheran, K.; Wudl, F., A thermally re-mendable cross-linked polymeric material. *Science* **2002**, *295* (5560), 1698-702.
30. Bowman, C. N.; Kloxin, C. J., Covalent Adaptable Networks: Reversible Bond Structures Incorporated in Polymer Networks. *Angewandte Chemie International Edition* **2012**, *51* (18), 4272-4274.
31. Kloxin, C. J.; Bowman, C. N., Covalent adaptable networks: smart, reconfigurable and responsive network systems. *Chemical Society reviews* **2013**, *42* (17), 7161-73.
32. Montarnal, D.; Capelot, M.; Tournilhac, F.; Leibler, L., Silica-like malleable materials from permanent organic networks. *Science* **2011**, *334* (6058), 965-8.
33. Denissen, W.; Winne, J. M.; Du Prez, F. E., Vitrimers: permanent organic networks with glass-like fluidity. *Chemical Science* **2016**, *7* (1), 30-38.
34. Lucherelli, M. A.; Duval, A.; Avérous, L., Biobased vitrimers: Towards sustainable and adaptable performing polymer materials. *Progress in Polymer Science* **2022**, *127*, 101515.
35. Röttger, M.; Domenech, T.; van der Weegen, R.; Breuillac, A.; Nicolay, R.; Leibler, L., High-performance vitrimers from commodity thermoplastics through dioxaborolane metathesis. *Science* **2017**, *356* (6333), 62-65.
36. Winne, J. M.; Leibler, L.; Du Prez, F. E., Dynamic covalent chemistry in polymer networks: a mechanistic perspective. *Polymer Chemistry* **2019**, *10* (45), 6091-6108.
37. Zou, W.; Dong, J.; Luo, Y.; Zhao, Q.; Xie, T., Dynamic Covalent Polymer Networks: from Old Chemistry to Modern Day Innovations. *Advanced Materials* **2017**, *29* (14), 1606100.
38. Kloxin, C. J.; Bowman, C. N., Covalent adaptable networks: smart, reconfigurable and responsive network systems. *Chemical Society Reviews* **2013**, *42* (17), 7161-7173.
39. Chakma, P.; Konkolewicz, D., Dynamic Covalent Bonds in Polymeric Materials. *Angewandte Chemie International Edition* **2019**, *58* (29), 9682-9695.
40. Froidevaux, V.; Borne, M.; Laborbe, E.; Auvergne, R.; Gandini, A.; Boutevin, B., Study of the Diels–Alder and retro-Diels–Alder reaction between furan derivatives and maleimide for the creation of new materials. *RSC Advances* **2015**, *5* (47), 37742-37754.

41. Yu, K.; Taynton, P.; Zhang, W.; Dunn, M. L.; Qi, H. J., Reprocessing and recycling of thermosetting polymers based on bond exchange reactions. *RSC Advances* **2014**, *4* (20), 10108-10117.
42. Lei, Z. Q.; Xiang, H. P.; Yuan, Y. J.; Rong, M. Z.; Zhang, M. Q., Room-Temperature Self-Healable and Remoldable Cross-linked Polymer Based on the Dynamic Exchange of Disulfide Bonds. *Chemistry of Materials* **2014**, *26* (6), 2038-2046.
43. Taynton, P.; Ni, H.; Zhu, C.; Yu, K.; Loob, S.; Jin, Y.; Qi, H. J.; Zhang, W., Repairable Woven Carbon Fiber Composites with Full Recyclability Enabled by Malleable Polyimine Networks. *Adv Mater* **2016**, *28* (15), 2904-9.
44. Hassib, H. B.; Abdel-Kader, N. S.; Issa, Y. M., Kinetic Study of the Hydrolysis of Schiff Bases Derived from 2-Aminothiophenol. *Journal of Solution Chemistry* **2012**, *41* (11), 2036-2046.
45. Ying, H.; Zhang, Y.; Cheng, J., Dynamic urea bond for the design of reversible and self-healing polymers. *Nature Communications* **2014**, *5* (1), 3218.
46. Matsuura, H., Secondary Stress Relaxation Mechanism in Ion-Containing Polymers I. A New Analytical Method. *Polymer Journal* **1986**, *18* (12), 1027-1035.
47. Sangaletti, D.; Ceseracciu, L.; Marini, L.; Athanassiou, A.; Zych, A., Biobased boronic ester vitrimer resin from epoxidized linseed oil for recyclable carbon fiber composites. *Resources, Conservation and Recycling* **2023**, *198*, 107205.
48. Zych, A.; Tellers, J.; Bertolacci, L.; Ceseracciu, L.; Marini, L.; Mancini, G.; Athanassiou, A., Biobased, Biodegradable, Self-Healing Boronic Ester Vitrimers from Epoxidized Soybean Oil Acrylate. *ACS Applied Polymer Materials* **2021**, *3* (2), 1135-1144.
49. Sharma, H.; Krishnakumar, B.; Dickens, T. J.; Yun, G. J.; Kumar, A.; Rana, S., A bibliometric survey of research trends in vitrimer. *Heliyon* **2023**, *9* (6), e17350.
50. Lu, L.; Fan, J.; Li, G., Intrinsic healable and recyclable thermoset epoxy based on shape memory effect and transesterification reaction. *Polymer* **2016**, *105*, 10-18.
51. Montarnal, D.; Capelot, M.; Tournilhac, F.; Leibler, L., Silica-Like Malleable Materials from Permanent Organic Networks. *Science* **2011**, *334* (6058), 965-968.
52. Liu, T.; Zhao, B.; Zhang, J., Recent development of repairable, malleable and recyclable thermosetting polymers through dynamic transesterification. *Polymer* **2020**, *194*, 122392.
53. Capelot, M.; Unterlass, M. M.; Tournilhac, F.; Leibler, L., Catalytic Control of the Vitrimer Glass Transition. *ACS Macro Letters* **2012**, *1* (7), 789-792.
54. Denissen, W.; Rivero, G.; Nicolaÿ, R.; Leibler, L.; Winne, J. M.; Du Prez, F. E., Vinylogous Urethane Vitrimers. *Advanced Functional Materials* **2015**, *25* (16), 2451-2457.
55. Guerre, M.; Taplan, C.; Nicolaÿ, R.; Winne, J. M.; Du Prez, F. E., Fluorinated Vitrimer Elastomers with a Dual Temperature Response. *Journal of the American Chemical Society* **2018**, *140* (41), 13272-13284.
56. Cromwell, O. R.; Chung, J.; Guan, Z., Malleable and Self-Healing Covalent Polymer Networks through Tunable Dynamic Boronic Ester Bonds. *Journal of the American Chemical Society* **2015**, *137* (20), 6492-6495.
57. Brutman, J. P.; Fortman, D. J.; De Hoe, G. X.; Dichtel, W. R.; Hillmyer, M. A., Mechanistic Study of Stress Relaxation in Urethane-Containing Polymer Networks. *The Journal of Physical Chemistry B* **2019**, *123* (6), 1432-1441.

58. Fortman, D. J.; Sheppard, D. T.; Dichtel, W. R., Reprocessing Cross-Linked Polyurethanes by Catalyzing Carbamate Exchange. *Macromolecules* **2019**, *52* (16), 6330-6335.
59. Zheng, N.; Fang, Z.; Zou, W.; Zhao, Q.; Xie, T., Thermoset Shape-Memory Polyurethane with Intrinsic Plasticity Enabled by Transcarbamoylation. *Angewandte Chemie International Edition* **2016**, *55* (38), 11421-11425.
60. Fortman, D. J.; Brutman, J. P.; Cramer, C. J.; Hillmyer, M. A.; Dichtel, W. R., Mechanically Activated, Catalyst-Free Polyhydroxyurethane Vitrimers. *Journal of the American Chemical Society* **2015**, *137* (44), 14019-14022.
61. Hu, S.; Chen, X.; Torkelson, J. M., Biobased Reprocessable Polyhydroxyurethane Networks: Full Recovery of Crosslink Density with Three Concurrent Dynamic Chemistries. *ACS Sustainable Chemistry & Engineering* **2019**, *7* (11), 10025-10034.
62. Chen, X.; Li, L.; Jin, K.; Torkelson, J. M., Reprocessable polyhydroxyurethane networks exhibiting full property recovery and concurrent associative and dissociative dynamic chemistry via transcarbamoylation and reversible cyclic carbonate aminolysis. *Polymer Chemistry* **2017**, *8* (41), 6349-6355.
63. Taynton, P.; Yu, K.; Shoemaker, R. K.; Jin, Y.; Qi, H. J.; Zhang, W., Heat- or Water-Driven Malleability in a Highly Recyclable Covalent Network Polymer. *Advanced Materials* **2014**, *26* (23), 3938-3942.
64. Taynton, P.; Zhu, C.; Loob, S.; Shoemaker, R.; Pritchard, J.; Jin, Y.; Zhang, W., Re-healable polyimine thermosets: polymer composition and moisture sensitivity. *Polymer Chemistry* **2016**, *7* (46), 7052-7056.
65. Giuseppone, N.; Schmitt, J.-L.; Schwartz, E.; Lehn, J.-M., Scandium(III) Catalysis of Transimination Reactions. Independent and Constitutionally Coupled Reversible Processes. *Journal of the American Chemical Society* **2005**, *127* (15), 5528-5539.
66. Kovaříček, P.; Lehn, J.-M., Merging Constitutional and Motional Covalent Dynamics in Reversible Imine Formation and Exchange Processes. *Journal of the American Chemical Society* **2012**, *134* (22), 9446-9455.
67. Ciaccia, M.; Cacciapaglia, R.; Mencarelli, P.; Mandolini, L.; Di Stefano, S., Fast transimination in organic solvents in the absence of proton and metal catalysts. A key to imine metathesis catalyzed by primary amines under mild conditions. *Chemical Science* **2013**, *4* (5), 2253-2261.
68. Roy, C. D.; Brown, H. C., Stability of boronic esters – Structural effects on the relative rates of transesterification of 2-(phenyl)-1,3,2-dioxaborolane. *Journal of Organometallic Chemistry* **2007**, *692* (4), 784-790.
69. Lorand, J. P.; Edwards, J. O., Polyol Complexes and Structure of the Benzeneboronate Ion. *The Journal of Organic Chemistry* **1959**, *24* (6), 769-774.
70. Yoon, J.; Czarnik, A. W., Fluorescent chemosensors of carbohydrates. A means of chemically communicating the binding of polyols in water based on chelation-enhanced quenching. *Journal of the American Chemical Society* **1992**, *114* (14), 5874-5875.
71. Barker, S. A.; Hatt, B. W.; Somers, P. J.; Woodbury, R. R., The use of poly(4-vinylbenzeneboronic acid) resins in the fractionation and interconversion of carbohydrates. *Carbohydrate Research* **1973**, *26* (1), 55-64.
72. Wang, X.; Xia, N.; Liu, L., Boronic Acid-Based Approach for Separation and Immobilization of Glycoproteins and Its Application in Sensing. *International Journal of Molecular Sciences* **2013**, *14* (10), 20890-20912.

73. Kaupp, G.; Naimi-Jamal, M. R.; Stepanenko, V., Waste-Free and Facile Solid-State Protection of Diamines, Anthranilic Acid, Diols, and Polyols with Phenylboronic Acid. *Chemistry – A European Journal* **2003**, *9* (17), 4156-4161.
74. Gosecki, M.; Kazmierski, S.; Gosecka, M., Diffusion-Controllable Biomineralization Conducted In Situ in Hydrogels Based on Reversibly Cross-Linked Hyperbranched Polyglycidol. *Biomacromolecules* **2017**, *18* (10), 3418-3431.
75. Gosecka, M.; Gosecki, M.; Urbaniak, M., Composite Dynamic Hydrogels Constructed on Boronic Ester Cross-Links with NIR-Enhanced Diffusivity. *Biomacromolecules* **2022**, *23* (3), 948-959.
76. Marco-Dufort, B.; Tibbitt, M. W., Design of moldable hydrogels for biomedical applications using dynamic covalent boronic esters. *Materials Today Chemistry* **2019**, *12*, 16-33.
77. Guan, Y.; Zhang, Y., Boronic acid-containing hydrogels: synthesis and their applications. *Chemical Society Reviews* **2013**, *42* (20), 8106-8121.
78. Yang, P.; Zhu, F.; Zhang, Z.; Cheng, Y.; Wang, Z.; Li, Y., Stimuli-responsive polydopamine-based smart materials. *Chemical Society Reviews* **2021**, *50* (14), 8319-8343.
79. Hong, S. H.; Kim, S.; Park, J. P.; Shin, M.; Kim, K.; Ryu, J. H.; Lee, H., Dynamic Bonds between Boronic Acid and Alginate: Hydrogels with Stretchable, Self-Healing, Stimuli-Responsive, Remoldable, and Adhesive Properties. *Biomacromolecules* **2018**, *19* (6), 2053-2061.
80. Springsteen, G.; Wang, B., A detailed examination of boronic acid–diol complexation. *Tetrahedron* **2002**, *58* (26), 5291-5300.
81. Gamoh, K.; Brooks, C. J. W., Stability and Reversed-Phase Liquid Chromatographic Studies of Cyclic Boronates. *Analytical Sciences* **1993**, *9* (4), 549-552.
82. Sheepwash, E.; Luisier, N.; Krause, M. R.; Noé, S.; Kubik, S.; Severin, K., Supramolecular polymers based on dative boron–nitrogen bonds. *Chemical Communications* **2012**, *48* (63), 7808-7810.
83. Ono, K.; Shimo, S.; Takahashi, K.; Yasuda, N.; Uekusa, H.; Iwasawa, N., Dynamic Interconversion between Boroxine Cages Based on Pyridine Ligation. *Angewandte Chemie International Edition* **2018**, *57* (12), 3113-3117.
84. Campillo-Alvarado, G.; Vargas-Olvera, E. C.; Höpfl, H.; Herrera-España, A. D.; Sánchez-Guadarrama, O.; Morales-Rojas, H.; MacGillivray, L. R.; Rodríguez-Molina, B.; Farfán, N., Self-Assembly of Fluorinated Boronic Esters and 4,4'-Bipyridine into 2:1 N→B Adducts and Inclusion of Aromatic Guest Molecules in the Solid State: Application for the Separation of o,m,p-Xylene. *Crystal Growth & Design* **2018**, *18* (5), 2726-2743.
85. Höpfl, H., The tetrahedral character of the boron atom newly defined—a useful tool to evaluate the N→B bond. *Journal of Organometallic Chemistry* **1999**, *581* (1), 129-149.
86. Brus, J.; Czernek, J.; Urbanova, M.; Kobera, L.; Jegorov, A., An efficient 2D 11B–11B solid-state NMR spectroscopy strategy for monitoring covalent self-assembly of boronic acid-derived compounds: the transformation and unique architecture of bortezomib molecules in the solid state. *Physical Chemistry Chemical Physics* **2017**, *19* (1), 487-495.
87. Yang, X.; Lee, M. C.; Sartain, F.; Pan, X.; Lowe, C. R., Designed boronate ligands for glucose-selective holographic sensors. *Chemistry* **2006**, *12* (33), 8491-7.

88. Brooks, W. L. A.; Sumerlin, B. S., Synthesis and Applications of Boronic Acid-Containing Polymers: From Materials to Medicine. *Chemical Reviews* **2016**, *116* (3), 1375-1397.
89. Wulff, G.; Lauer, M.; Böhnke, H., Rapid Proton Transfer as Cause of an Unusually Large Neighboring Group Effect. *Angewandte Chemie International Edition in English* **1984**, *23* (9), 741-742.
90. Gosecki, M.; Gosecka, M., Boronic Acid Esters and Anhydrates as Dynamic Cross-Links in Vitrimers. *Polymers* **2022**, *14* (4), 842.
91. Yang, Y.; Du, F.-S.; Li, Z.-C., Thermally healable and reprocessable polymethacrylate networks based on diol-mediated metathesis of 6-membered boronic esters. *Polymer Chemistry* **2020**, *11* (11), 1860-1870.
92. Brunet, J.; Collas, F.; Humbert, M.; Perrin, L.; Brunel, F.; Lacôte, E.; Montarnal, D.; Raynaud, J., High Glass-Transition Temperature Polymer Networks Harnessing the Dynamic Ring Opening of Pinacol Boronates. *Angewandte Chemie International Edition* **2019**, *58* (35), 12216-12222.
93. Chen, Y.; Tang, Z.; Zhang, X.; Liu, Y.; Wu, S.; Guo, B., Covalently Cross-Linked Elastomers with Self-Healing and Malleable Abilities Enabled by Boronic Ester Bonds. *ACS Appl Mater Interfaces* **2018**, *10* (28), 24224-24231.
94. Breuillac, A.; Kassalias, A.; Nicolaÿ, R., Polybutadiene Vitrimers Based on Dioxaborolane Chemistry and Dual Networks with Static and Dynamic Cross-links. *Macromolecules* **2019**, *52* (18), 7102-7113.
95. Wang, S.; Xing, X.; Zhang, X.; Wang, X.; Jing, X., Room-temperature fully recyclable carbon fibre reinforced phenolic composites through dynamic covalent boronic ester bonds. *Journal of Materials Chemistry A* **2018**, *6* (23), 10868-10878.
96. Xie, L.; Wang, Y.; Chen, G.; Feng, H.; Zheng, N.; Ren, H.; Zhao, Q.; Xie, T., A thermadap epoxy based on borate ester crosslinking and its carbon fiber composite as rapidly processable prepreg. *Composites Communications* **2021**, *28*, 100979.
97. Chong, K. L.; Lai, J. C.; Rahman, R. A.; Adrus, N.; Al-Saffar, Z. H.; Hassan, A.; Lim, T. H.; Wahit, M. U., A review on recent approaches to sustainable bio-based epoxy vitrimer from epoxidized vegetable oils. *Industrial Crops and Products* **2022**, *189*, 115857.
98. Sahoo, S. K.; Mohanty, S.; Nayak, S. K., Toughened bio-based epoxy blend network modified with transesterified epoxidized soybean oil: synthesis and characterization. *RSC Advances* **2015**, *5* (18), 13674-13691.
99. Ma, Z.; Wang, Y.; Zhu, J.; Yu, J.; Hu, Z., Bio-based epoxy vitrimers: Reprocessability, controllable shape memory, and degradability. *Journal of Polymer Science Part A: Polymer Chemistry* **2017**, *55* (10), 1790-1799.
100. Łukaszczyk, J.; Janicki, B.; Kaczmarek, M., Synthesis and properties of isosorbide based epoxy resin. *European Polymer Journal* **2011**, *47* (8), 1601-1606.
101. Xue, B.; Tang, R.; Xue, D.; Guan, Y.; Sun, Y.; Zhao, W.; Tan, J.; Li, X., Sustainable alternative for bisphenol A epoxy resin high-performance and recyclable lignin-based epoxy vitrimers. *Industrial Crops and Products* **2021**, *168*, 113583.
102. Zhao, S.; Abu-Omar, M. M., Renewable Epoxy Networks Derived from Lignin-Based Monomers: Effect of Cross-Linking Density. *ACS Sustainable Chemistry & Engineering* **2016**, *4* (11), 6082-6089.

103. Yang, W.; Yi, Q.; Liu, F.; Pan, X.; Zeng, Y., Fabrication of malleable, repairable, weldable, recyclable and robust epoxy vitrimers from itaconic acid for recycled adhesion. *European Polymer Journal* **2023**, *196*, 112278.
104. Memon, H.; Wei, Y.; Zhu, C., Correlating the thermomechanical properties of a novel bio-based epoxy vitrimer with its crosslink density. *Materials Today Communications* **2021**, *29*, 102814.
105. Tao, Y.; Fang, L.; Dai, M.; Wang, C.; Sun, J.; Fang, Q., Sustainable alternative to bisphenol A epoxy resin: high-performance recyclable epoxy vitrimers derived from protocatechuic acid. *Polymer Chemistry* **2020**, *11* (27), 4500-4506.
106. Zeng, Y.; Li, J.; Liu, S.; Yang, B., Rosin-Based Epoxy Vitrimers with Dynamic Boronic Ester Bonds. *Polymers* **2021**, *13* (19), 3386.
107. Krishnakumar, B.; Pucci, A.; Wadgaonkar, P. P.; Kumar, I.; Binder, W. H.; Rana, S., Vitrimers based on bio-derived chemicals: Overview and future prospects. *Chemical Engineering Journal* **2022**, *433*, 133261.
108. Auvergne, R.; Caillol, S.; David, G.; Boutevin, B.; Pascault, J. P., Biobased thermosetting epoxy: present and future. *Chem Rev* **2014**, *114* (2), 1082-115.
109. Bisphenol A diglycidyl ether [MAK Value Documentation, 2003]. In *The MAK-Collection for Occupational Health and Safety*, pp 44-78.
110. Goodman, S. H., 1 - Introduction. In *Handbook of Thermoset Plastics (Second Edition)*, Goodman, S. H., Ed. William Andrew Publishing: Westwood, NJ, 1998; pp 1-22.
111. Ibeh, C. C., 2 - Phenol-Formaldehyde Resins. In *Handbook of Thermoset Plastics (Second Edition)*, Goodman, S. H., Ed. William Andrew Publishing: Westwood, NJ, 1998; pp 23-71.
112. Zaske, O. C.; Goodman, S. H., 4 - Unsaturated Polyester and Vinyl Ester Resins. In *Handbook of Thermoset Plastics (Second Edition)*, Goodman, S. H., Ed. William Andrew Publishing: Westwood, NJ, 1998; pp 97-168.
113. Goodman, S. H., 6 - Epoxy Resins. In *Handbook of Thermoset Plastics (Second Edition)*, Goodman, S. H., Ed. William Andrew Publishing: Westwood, NJ, 1998; pp 193-268.
114. Campbell, F. C., Chapter 3 - Thermoset Resins: The Glue That Holds the Strings Together. In *Manufacturing Processes for Advanced Composites*, Campbell, F. C., Ed. Elsevier Science: Amsterdam, 2004; pp 63-101.
115. Landis, A. L.; Lau, K. S. Y., 8 - High-Performance Polyimides and Related Thermoset Polymers: Past and Present Development, and Future Research Directions. In *Handbook of Thermoset Plastics (Second Edition)*, Goodman, S. H., Ed. William Andrew Publishing: Westwood, NJ, 1998; pp 302-467.
116. Gusakova, K.; Saiter, J.-M.; Grigoryeva, O.; Gouanve, F.; Fainleib, A.; Starostenko, O.; Grande, D., Annealing behavior and thermal stability of nanoporous polymer films based on high-performance Cyanate Ester Resins. *Polym. Degrad. Stab.* **2015**, *120*, 402-409.
117. Mirdehghan, S. A., 1 - Fibrous polymeric composites. In *Engineered Polymeric Fibrous Materials*, Latifi, M., Ed. Woodhead Publishing: 2021; pp 1-58.
118. Weidmann, S.; Volk, P.; Mitschang, P.; Markaide, N., Investigations on thermoforming of carbon fiber reinforced epoxy vitrimer composites. *Composites Part A: Applied Science and Manufacturing* **2022**, *154*, 106791.

119. Zhang, J.; Chevali, V. S.; Wang, H.; Wang, C.-H., Current status of carbon fibre and carbon fibre composites recycling. *Composites Part B: Engineering* **2020**, *193*, 108053.
120. Boulanghien, M.; R'Mili, M.; Bernhart, G.; Berthet, F.; Soudais, Y., Mechanical Characterization of Carbon Fibres Recycled by Steam Thermolysis: A Statistical Approach. *Advances in Materials Science and Engineering* **2018**, *2018*, 8630232.
121. Utekar, S.; V K, S.; More, N.; Rao, A. R., Comprehensive study of recycling of thermosetting polymer composites – Driving force, challenges and methods. *Composites Part B-engineering* **2021**, *207*, 108596.
122. Huang, J.; Zhang, L.; Tang, Z.; Guo, B., Bioinspired engineering of sacrificial bonds into rubber networks towards high-performance and functional elastomers. *Composites Communications* **2018**, *8*, 65-73.
123. Zhang, Z. P.; Rong, M. Z.; Zhang, M. Q.; Yuan, C. e., Alkoxyamine with reduced homolysis temperature and its application in repeated autonomous self-healing of stiff polymers. *Polymer Chemistry* **2013**, *4* (17), 4648-4654.
124. Capelot, M.; Montarnal, D.; Tournilhac, F.; Leibler, L., Metal-catalyzed transesterification for healing and assembling of thermosets. *J Am Chem Soc* **2012**, *134* (18), 7664-7.
125. Tellers, J.; Pinalli, R.; Soliman, M.; Vachon, J.; Dalcanale, E., Reprocessable vinylogous urethane cross-linked polyethylene via reactive extrusion. *Polymer Chemistry* **2019**, *10* (40), 5534-5542.
126. Obadia, M. M.; Mudraboyina, B. P.; Serghei, A.; Montarnal, D.; Drockenmuller, E., Reprocessing and Recycling of Highly Cross-Linked Ion-Conducting Networks through Transalkylation Exchanges of C-N Bonds. *J Am Chem Soc* **2015**, *137* (18), 6078-83.
127. Alabiso, W.; Schlögl, S., The Impact of Vitrimers on the Industry of the Future: Chemistry, Properties and Sustainable Forward-Looking Applications. *Polymers (Basel)* **2020**, *12* (8).
128. Wang, S.; Ma, S.; Li, Q.; Xu, X.; Wang, B.; Yuan, W.; Zhou, S.; You, S.; Zhu, J., Facile in situ preparation of high-performance epoxy vitrimer from renewable resources and its application in nondestructive recyclable carbon fiber composite. *Green Chemistry* **2019**, *21* (6), 1484-1497.
129. Otsuka, H.; Ohishi, T., Dynamic Covalent PN (Polymer Nanomaterials). In *Encyclopedia of Polymeric Nanomaterials*, Kobayashi, S.; Müllen, K., Eds. Springer Berlin Heidelberg: Berlin, Heidelberg, 2021; pp 1-7.
130. Krishnakumar, B.; Sanka, R. V. S. P.; Binder, W. H.; Parthasarthy, V.; Rana, S.; Karak, N., Vitrimers: Associative dynamic covalent adaptive networks in thermoset polymers. *Chemical Engineering Journal* **2020**, *385*, 123820.
131. Sharma, H.; Rana, S.; Singh, P.; Hayashi, M.; Binder, W. H.; Rossegger, E.; Kumar, A.; Schlögl, S., Self-healable fiber-reinforced vitrimer composites: overview and future prospects. *RSC Advances* **2022**, *12* (50), 32569-32582.
132. Liu, Y.; Wang, B.; Ma, S.; Yu, T.; Xu, X.; Li, Q.; Wang, S.; Han, Y.; Yu, Z.; Zhu, J., Catalyst-free malleable, degradable, bio-based epoxy thermosets and its application in recyclable carbon fiber composites. *Compos. B. Eng.* **2021**, *211*, 108654.
133. Li, W.; Xiao, L.; Huang, J.; Wang, Y.; Nie, X.; Chen, J., Bio-based epoxy vitrimer for recyclable and carbon fiber reinforced materials: Synthesis and structure-property relationship. *Composites Science and Technology* **2022**, *227*, 109575.

134. Leguillon, D.; Martin, É.; Lafarie-Frenot, M.-C., Flexural vs. tensile strength in brittle materials. *Compt. Rendus Mec.* **2015**, *343* (4), 275-281.
135. Röttger, M.; Domenech, T.; Weegen, R. v. d.; Breuillac, A.; Nicolaj, R.; Leibler, L., High-performance vitrimers from commodity thermoplastics through dioxaborolane metathesis. *Science* **2017**, *356* (6333), 62-65.
136. Liu, Y.; Tang, Z.; Wang, D.; Wu, S.; Guo, B., Biomimetic design of elastomeric vitrimers with unparalleled mechanical properties, improved creep resistance and retained malleability by metal–ligand coordination. *J. Mater. Chem. A* **2019**, *7* (47), 26867-26876.
137. Yang, Y.; Zhang, S.; Zhang, X.; Gao, L.; Wei, Y.; Ji, Y., Detecting topology freezing transition temperature of vitrimers by AIE luminogens. *Nat. Commun.* **2019**, *10* (1), 3165.
138. Nishimura, Y.; Chung, J.; Muradyan, H.; Guan, Z., Silyl Ether as a Robust and Thermally Stable Dynamic Covalent Motif for Malleable Polymer Design. *J. Am. Chem. Soc.* **2017**, *139* (42), 14881-14884.
139. Denissen, W.; Winne, J. M.; Du Prez, F. E., Vitrimers: permanent organic networks with glass-like fluidity. *Chem. Sci.* **2016**, *7* (1), 30-38.
140. Chen, Y.; Tang, Z.; Zhang, X.; Liu, Y.; Wu, S.; Guo, B., Covalently Cross-Linked Elastomers with Self-Healing and Malleable Abilities Enabled by Boronic Ester Bonds. *ACS Appl. Mater. Interfaces* **2018**, *10* (28), 24224-24231.
141. Wu, X.; Huang, W. M.; Zhao, Y.; Ding, Z.; Tang, C.; Zhang, J., Mechanisms of the Shape Memory Effect in Polymeric Materials. *Polymers* **2013**, *5* (4).
142. Leszczyński, S.; Brzychczyk, B., Waste management of half-finished products and thermosetting wastes. *Polish J. Chem. Technol.* **2007**, *9* (3), 122-126.
143. Xue, X.; Liu, S.-Y.; Zhang, Z.-Y.; Wang, Q.-Z.; Xiao, C.-Z., A technology review of recycling methods for fiber-reinforced thermosets. *J. Reinf. Plast. Compos.* **2022**, *41* (11-12), 459-480.
144. Hamad, K.; Kaseem, M.; Deri, F., Recycling of waste from polymer materials: An overview of the recent works. *Polym. Degrad. Stab.* **2013**, *98* (12), 2801-2812.
145. Utekar, S.; V K, S.; More, N.; Rao, A., Comprehensive study of recycling of thermosetting polymer composites – Driving force, challenges and methods. *Compos. B. Eng.* **2021**, *207*, 108596.
146. Cash, J. J.; Kubo, T.; Bapat, A. P.; Sumerlin, B. S., Room-Temperature Self-Healing Polymers Based on Dynamic-Covalent Boronic Esters. *Macromolecules* **2015**, *48* (7), 2098-2106.
147. Kim, C.; Ejima, H.; Yoshie, N., Non-swellable self-healing polymer with long-term stability under seawater. *RSC Adv.* **2017**, *7* (31), 19288-19295.
148. Yu, K.; Taynton, P.; Zhang, W.; Dunn, M. L.; Qi, H. J., Influence of stoichiometry on the glass transition and bond exchange reactions in epoxy thermoset polymers. *RSC Adv.* **2014**, *4* (89), 48682-48690.
149. Tang, S. K.; Davey, R. J.; Sacchi, P.; Cruz-Cabeza, A. J., Can molecular flexibility control crystallization? The case of para substituted benzoic acids. *Chemical Science* **2021**, *12* (3), 993-1000.
150. chem.libretexts.org
https://chem.libretexts.org/Courses/Mount_Royal_University/Chem_1201/Unit_5/%3A_Intermolecular_Forces/5.2%3A_Intermolecular_Forces%20ref.

151. Chen, Y.; Tang, Z.; Liu, Y.; Wu, S.; Guo, B., Mechanically Robust, Self-Healable, and Reprocessable Elastomers Enabled by Dynamic Dual Cross-Links. *Macromolecules* **2019**, *52* (10), 3805-3812.
152. Shi, Y.; Hong, Y.; Hong, J.; Yu, A.; Lee, M. W.; Lee, J.; Goh, M., Bio-based boronic ester vitrimer for realizing sustainable and highly thermally conducting nanocomposites. *Composites Part B: Engineering* **2022**, *244*, 110181.
153. van Hurne, S.; Kisters, M.; Smulders, M. M. J., Covalent adaptable networks using boronate linkages by incorporating TetraAzaADamantanes. *Frontiers in Chemistry* **2023**, *11*.
154. Gosecki, M.; Gosecka, M., Boronic Acid Esters and Anhydrates as Dynamic Cross-Links in Vitrimers. *Polymers (Basel)* **2022**, *14* (4).
155. Lei, Y.; Zhang, A.; Lin, Y., Reprocessability of dynamic polydioxaborolane networks activated by heat, moisture and mechanical force. *Polymer* **2020**, *209*, 123037.
156. Isa, A.; Nosbi, N.; Che Ismail, M.; Md Akil, H.; Wan Ali, W. F. F.; Omar, M. F., A Review on Recycling of Carbon Fibres: Methods to Reinforce and Expected Fibre Composite Degradations. *Materials (Basel)* **2022**, *15* (14).